NUREG-0978

Mark III LOCA-Related Hydrodynamic Load Definition

Generic Technical Activity B-10
Final Report

U.S. Nuclear Regulatory Commission

Office of Nuclear Reactor Regulation

M. B. Fields, J. A. Kudrick

NOTICE

Availability of Reference Materials Cited in NRC Publications

Most documents cited in NRC publications will be available from one of the following sources:

1. The NRC Public Document Room, 1717 H Street, N.W.
   Washington, DC 20555
2. The NRC/GPO Sales Program, U.S. Nuclear Regulatory Commission,
   Washington, DC 20555
3. The National Technical Information Service, Springfield, VA 22161

Although the listing that follows represents the majority of documents cited in NRC publications, it is not intended to be exhaustive.

Referenced documents available for inspection and copying for a fee from the NRC Public Document Room include NRC correspondence and internal NRC memoranda; NRC Office of Inspection and Enforcement bulletins, circulars, information notices, inspection and investigation notices; Licensee Event Reports; vendor reports and correspondence; Commission papers; and applicant and licensee documents and correspondence.

The following documents in the NUREG series are available for purchase from the NRC/GPO Sales Program: formal NRC staff and contractor reports, NRC-sponsored conference proceedings, and NRC booklets and brochures. Also available are Regulatory Guides, NRC regulations in the *Code of Federal Regulations,* and *Nuclear Regulatory Commission Issuances.*

Documents available from the National Technical Information Service include NUREG series reports and technical reports prepared by other federal agencies and reports prepared by the Atomic Energy Commission, forerunner agency to the Nuclear Regulatory Commission.

Documents available from public and special technical libraries include all open literature items, such as books, journal and periodical articles, and transactions. *Federal Register* notices, federal and state legislation, and congressional reports can usually be obtained from these libraries.

Documents such as theses, dissertations, foreign reports and translations, and non-NRC conference proceedings are available for purchase from the organization sponsoring the publication cited.

Single copies of NRC draft reports are available free, to the extent of supply, upon written request to the Division of Technical Information and Document Control, U.S. Nuclear Regulatory Commission, Washington, DC 20555.

Copies of industry codes and standards used in a substantive manner in the NRC regulatory process are maintained at the NRC Library, 7920 Norfolk Avenue, Bethesda, Maryland, and are available there for reference use by the public. Codes and standards are usually copyrighted and may be purchased from the originating organization or, if they are American National Standards, from the American National Standards Institute, 1430 Broadway, New York, NY 10018.

GPO Printed copy price: $4.75

NUREG-0978

Mark III LOCA-Related Hydrodynamic Load Definition

Generic Technical Activity B-10
Final Report

Manuscript Completed: August 1984
Date Published: August 1984

M. B. Fields, J. A. Kudrick

Division of Systems Integration
Office of Nuclear Reactor Regulation
U.S. Nuclear Regulatory Commission
Washington, D.C. 20555

Abstract

This report, prepared by the staff of the Office of Nuclear Reactor Regulation and its consultants at the Brookhaven National Laboratory, provides a discussion of LOCA-related suppression pool hydrodynamic loads in boiling water reactor (BWR) facilities with the Mark III pressure-suppression containment design. Its issuance completes NRC Generic Technical Activity B-10, "Behavior of BWR Mark III Containment."

On the basis of certain large-scale tests conducted between 1973 and 1979, the General Electric Company developed LOCA-related hydrodynamic load definitions for use in the design of the standard Mark III containment. The staff and its consultants have reviewed these load definitions and their bases and conclude that, with a few specified changes, the proposed load definitions provide conservative loading conditions.

The staff approved acceptance criteria for LOCA-related hydrodynamic loads are provided in Appendix C of this report.

Table of Contents

Table of Contents (Continued)

Appendices

Appendices (Continued)

List of Illustrations

List of Illustrations (Continued)

List of Tables

ACKNOWLEDGEMENTS

The review of the Mark III containment LOCA-related hydrodynamic loads definitions, developed by General Electric, was accomplished with substantial assistance from the Brookhaven National Laboratory and their consultants. The authors wish to acknowledge the following individuals that have contributed substantially to this report:

Brookhaven National Laboratory

C. Economos - Coordinator
G. Maise
J. Ranlet

Princeton University

G. Bienkowski

Massachusetts Institute of Technology

A. A. Sonin
R. Kamm

1 INTRODUCTION

There are 10 BWR facilities with the Mark III containment system in various stages of the licensing process in the United States. The first of the domestic facilities with the Mark III containments, the Grand Gulf Nuclear Station, Unit 1, was issued a low power operating license in June 1982. The Kuosheng facilities in Taiwan are currently at power. A listing of the domestic BWR facilities with the Mark III containment system is provided in Table 1-1.

The Mark III containment system design is the most recent generation of pressure suppression containment designs and was developed by General Electric (GE) in early 1970. As in the case of the Mark I and II designs, small scale tests were conducted in 1971 to provide a data base for the development of analytical models. Investigation of the vent clearing phenomena was emphasized in this program since the major differences between the Mark III design and the earlier pressure suppression containments are the vent configuration and the way the vents are cleared.

A large scale test program was initiated in the fall of 1973[1] to confirm the analytical models[2] used in the Mark III design. The Pressure Suppression Test Facility (PSTF) located in San Jose, California was constructed by GE and used to conduct the various test series. This facility was initially tested with an 8-degree sector of a full-scale Mark III suppression pool with a single column of horizontal vents.[3] Later testing phases included one-third scale, three vent tests and one-ninth scale, nine vent tests.

The primary objective of the test program was to confirm the conservatism in the analytical models used to predict the Mark III containment pressure response. In the first test series, it was observed that wetwell internal structures located above the suppression pool could be subjected to significant hydrodynamic loads during the pool swell process. Therefore, additional test series were conducted to determine the loads for the design of the affected structures.

In addition to the information obtained from the PSTF data, other LOCA-related dynamic load information was obtained from foreign testing programs[4] for similar pressure suppression containments. It was from these foreign tests that oscillatory condensation loads on the suppression pool boundaries during the later stages of steam vent flow were identified.

The Mark III LOCA-related pool dynamic loads were first reviewed at the PDA stage for GESSAR-238NI.[5] The Staff concluded the information available was sufficient to adequately define the pool dynamic loads for those nuclear plants undergoing Construction Permit (CP) reviews. Since the issuance of the GESSAR-238NI Safety Evaluation Report (SER), GE has conducted further tests and analyses to confirm and refine the original load definitions. These tests and analyses investigated the effect of chugging, steam condensation, and multivent interaction on the original pool dynamic load definition. To keep

Table 1-1 Plants Utilizing the Mark III Containment Design

Plant Name	Licensing Status
Grand Gulf, 1, 2	OR
Perry 1, 2	OL
River Bend 1, 2	OL
Clinton 1, 2	OL
Hartsville A1, A2	Post-CP-Indefinitely Deferred

the NRC and Mark III applicants apprised of the current status of these tests, GE issued an Interim Containment Loads Report (22A4365) in April 1978 and revised this report several times before the docketing of the GESSAR-II application in March of 1980. The GESSAR-II application is GE's Final Design Approval (FDA) submittal for their standard Balance of Plant (BOP) design and is to be referenced by Mark III OL applicants. Appendix 3B of GESSAR-II[33] provides the finalized pool dynamic load definition for Mark III containments, and was the basic document used for review by the Staff and its consultants.

The NRC's program for reviewing the Mark III LOCA-related hydrodynamic load definition was identified as Task Action Plan (TAP) B-10, "Behavior of BWR Mark III Containment." Technical assistance for the review of the proposed load definitions was obtained from the Brookhaven National Laboratory (BNL) under NRC contract FIN A3320. BNL was instrumental in the staff's earlier CP stage review of the Mark III hydrodynamic loads and was used extensively by the NRC staff in the review of Mark I and II hydrodynamic loads.

Based on the reviews by the staff and its consultants of the test data and analyses, the staff has developed appropriate acceptance criteria suitable for use by owners of plants that utilize the Mark III containment design. The staff intends to assess the acceptability of the Mark III designs using these criteria which are given in Appendix C to this report. The basic design features and concepts found in GESSAR-II that affect LOCA-related hydrodynamic loads are utilized by all applicants with Mark III containment designs. The staff will review each Mark III containment application for possible design differences that might invalidate the acceptance criteria provided in Appendix C to this report. Applicants with design differences from the standard Mark III containment concept as detailed in GESSAR-II will be required to demonstrate that the LOCA-related hydrodynamic load definitions contained in Appendix 3B to GESSAR-II, as modified by the staff's acceptance criteria, are applicable to their plant.

2 BACKGROUND

2.1 Mark III Containment System Description

The function of the Mark III containment system is to condense the steam released during a postulated LOCA event, to limit the release of fission products associated with an accident and to serve as a source of water for the Emergency Core Cooling System (ECCS). Figure 2-1 shows the principal features of the standard Mark III containment concept (GESSAR-II). The containment system is divided into two major subvolumes, a drywell enclosing the reactor system, and the primary containment surrounding the drywell and containing the suppression pool. The containment and the drywell volumes are connected, through the suppression pool, by an array of horizontal vents in the drywell wall.

The primary containment in the standard plant design is a steel structure consisting of a vertical cylinder, domed top, and a flat base. The region outside and around the suppression pool area is filled with concrete to mitigate the effects of SRV actuation. The net free volume of the primary containment, excluding the drywell, is 1.139×10^6 ft^3 and the design pressure is 15 psig. An alternate primary containment design that is being used by Grand Gulf, Units 1 & 2, and Clinton, Units 1 & 2 is a steel-lined concrete structure.

An additional structure called the shield building surrounds the primary containment. Its purpose, in conjunction with the fuel building and part of the auxiliary building, is to provide a secondary containment volume in which fission product leakage from the primary containment following a postulated LOCA, can be diluted and held up prior to release to the environment.

The drywell is an unlined concrete structure, enclosing a net free volume of 274,960 ft^3 and designed for a differential pressure of 30 psid.

The suppression pool is a 360-degree annular pool located in the bottom of the containment and retained between the containment wall and the drywall weir wall. The weir wall is a 360-degree, reinforced concrete wall located inside the drywell and 30 inches from the drywell wall. Located in the vertical section of the drywell wall and below the suppression pool water level are 120 horizontal vent holes which are 27.5 inches in diameter and arranged in 40 circumferential columns of three vents. In the event of a LOCA, the pressure will rise in the drywell due to the release of reactor coolant, and force the level of water downward within the weir annulus. When the water level has been depressed to the level of the first row of vents, the differential pressure will cause air, steam, and entrained water to flow thru the vents from the drywell into the suppression pool. The steam will be condensed in the pool and the air driven from the drywell will be compressed in the primary containment. Noncondensible gases and fission products would be collected and contained in the primary containment air space. At the end of the blowdown, subcooled ECCS water from the postulated pipe break would rapidly quench the steam within the drywell reducing the drywell pressure. The air in the primary

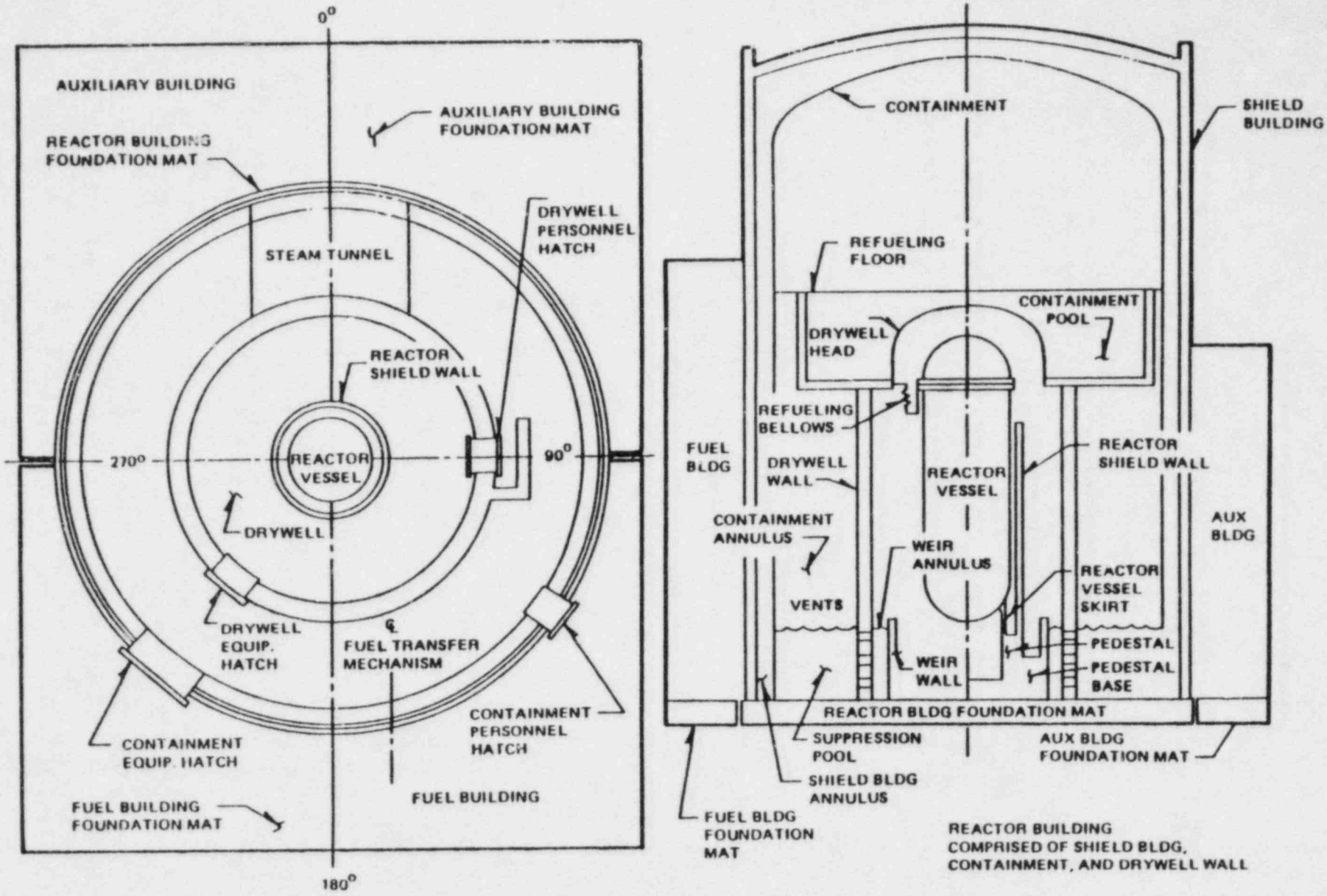

Figure 2-1 Mark III containment

containment space would then be vented back to the drywell through installed vacuum breakers and also through the vents if the pressure differential is great enough, to equalize the pressures between the two volumes. The ECCS will cool the reactor core and transport the energy to the water in the suppression chamber. Cooling systems are provided to remove heat from the water in the suppression chamber, thus providing continuous removal of decay heat from the primary containment under accident conditions following the initial deposition of energy to the suppression pool from the blowdown.

In addition to the suppression function under postulated LOCA conditions, the Mark III containment provides a similar pressure suppression function for safety/relief valve discharge which may occassionally occur to control pressure in the reactor vessel. The safety/relief valve, which relieve the reactor vessel pressure, discharge into pipes which are routed to the suppression pool and terminate below the pool water surface. The mechanism of this pressure suppression function is similar to that for the postulated LOCA event.

2.2 Description of LOCA-Related Hydrodynamic Phenomena

The following is a qualitative description of the various phenomena that would occur during the course of a postulated design basis LOCA in a BWR with the Mark III containment system and a description of the hydrodynamic loads which these phenomena could impose upon the suppression chamber and related structures.

Figure 2-2 shows the sequence of events following a postulated LOCA and the potential loading conditions associated with these events.

Assuming the instantaneous rupture of a steam or recirculation line, a sonic wave will develop in the broken primary system pipe and expand into the drywell atmosphere. This wave rapidly attenuates as a front expanding spherically outward into the drywell. The wave then enters the vent system, progressing into the pool.

Since there would be a very rapid drywell pressure increase associated with the postulated LOCA, a compressive wave could be formed in the weir annulus water. Prior to the clearing of this water through the horizontal vents, this compressive wave could propagate through the suppression pool and result in a dynamic loading on the suppression chamber and structures within the suppression pool.

As the drywell pressure increases, the water initially standing in the vent system will accelerate into the pool and the vents will be cleared of water. During this vent-clearing process, the water leaving the horizontal vents will form jets in the suppression pool and cause water jet impingement loads on the structures within the suppression pool and on the containment wall opposite the vents. During the vent-clearing transient, the drywell is subjected to a pressure differential and the weir wall will experience a vent-clearing reaction force. Immediately following vent-clearing, an air and steam bubble will form at the exit of each vent. The bubble pressure initially is assumed equal to the current drywell pressure (peak calculated is 21.8 psig). This bubble theoretically transmits a pressure wave through the suppression pool water and results in a loading on the suppression pool boundaries and on equipment located in the suppression pool.

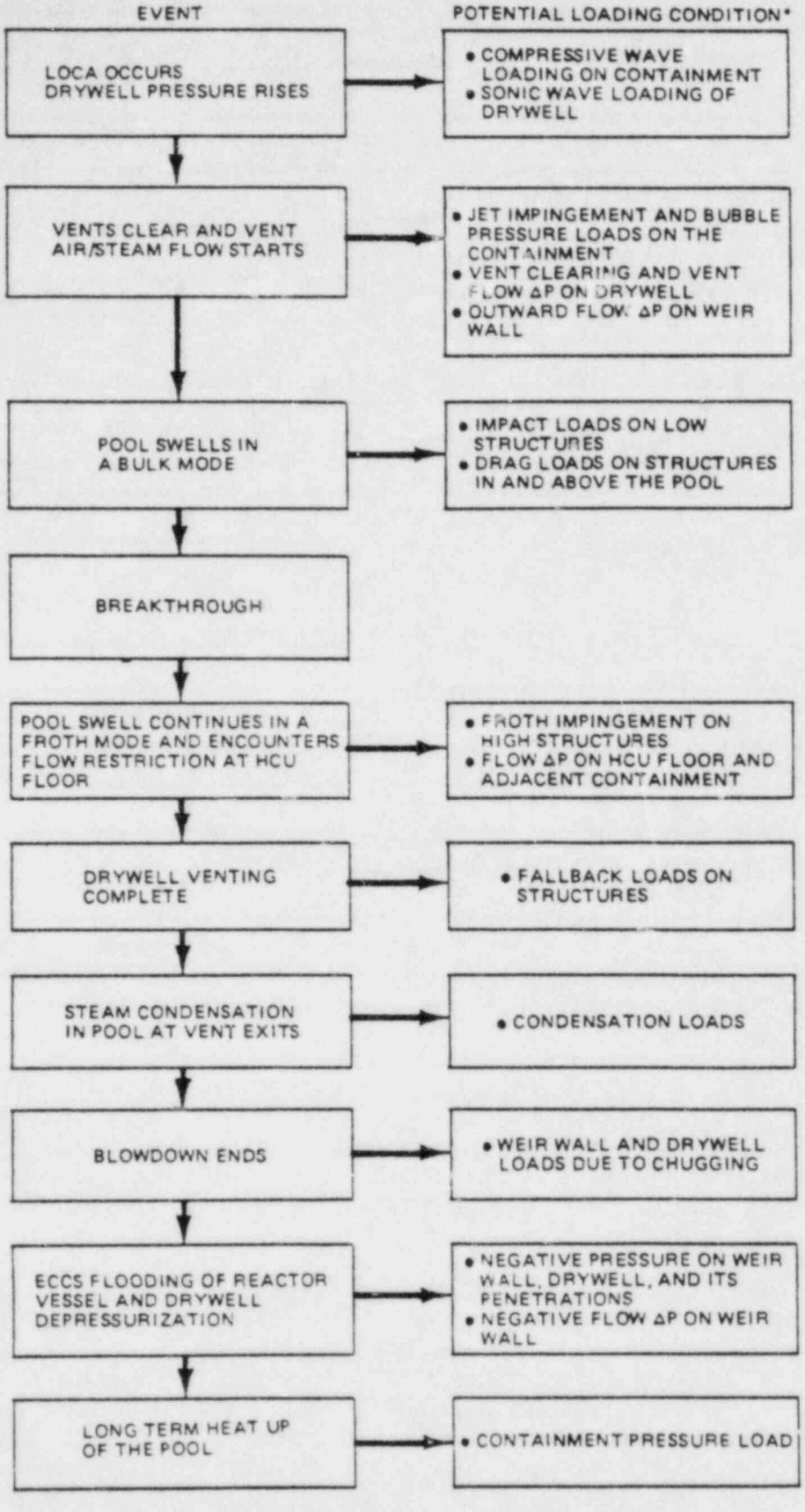

Figure 2-2 Loss-of-Coolant Accident Chronology (Design Basis Accident)

As the air and steam flow from the drywell becomes established in the vent system, the initial vent exit bubble will expand to the suppression pool hydrostatic pressure. The steam fraction of the flow will be condensed but continued injection of drywell air and expansion of the air bubble will result in a rise in the suppression pool surface. During the early stages of this process, the pool swells in a bulk mode (i.e., a slug of water is accelerated upward by the air). During this phase of pool swell, structures close to the pool surface will experience loads as the rising pool surface impacts the lower surfaces of the structures. In addition to these initial impact loads, these same structures will experience drag loads as water flows past them. Equipment and piping in the suppression pool will also experience drag loads. The rising water ligament thins until the air bubble breaks through, signaling the end of the pool swell proper and the beginning of froth formation and froth loads.

Continued injection of drywell air into the suppression pool will result in a period of froth pool swell. This froth swell will impinge on structures it encounters but the two-phase nature of the fluid will result in loads that are much less than the impact loads associated with bulk pool swell.

When the froth reaches the elevation of the floors on which the hydraulic control units for the control rod drives are located (approximately 20 feet above pool level), the froth encounters a flow restriction; at this elevation, there is approximately 25% open area. The froth pool swell will experience a two-phase pressure drop as it is forced to flow through the available open area. This pressure differential represents a load on both the floor structure and on the adjacent containment and drywell. The result is a discontinuous pressure loading at this elevation.

As the drywell air flow through the horizontal vent system decreases and the air/water suppression pool mixture experiences gravity-induced phase separation, pool upward movement will stop and fallback process will start. During this process, floors and other flat structures will experience downward loading.

The pool-swell transient associated with drywell air venting to the pool typically lasts 3 to 5 seconds. Following, will be a long period of high steam flow rate through the top vents; data indicate that this steam will be entirely condensed in a region right at the vent exits. For the Design Basis Accident (DBA) reactor blowdown, steady steam condensation lasts for a period up to 1.5 minutes. Potential structural loadings during the steam condensation phase of the accident have been observed and are included in the containment loading specifications. As the blowdown steam flow decreases to low values, the water in the top row of vents will start to oscillate back and forth causing what has become known as vent chugging. This action results in dynamic loads on the top vents and on the weir wall opposite the upper row of vents. In addition, an oscillatory pressure loading condition can occur on the drywell and containment. Since this phenomenon is steam mass-flux dependent, it is present for all break sizes.

Shortly after onset of the postulated LOCA, the ECCS pumps will automatically start and pump condensate water and/or suppression pool water into the reactor pressure vessel. This water will flood the reactor core and then start to cascade into the drywell from the break (the time at which this occurs depends

upon break size and location). Because the drywell will be full of steam at the time of vessel flooding, the sudden introduction of cool water causes rapid steam condensation and drywell depressurization. When the drywell pressure falls below the containment pressure, the drywell vacuum relief system will be activated and air from the containment will enter the drywell. Eventually sufficient air returns to equalize the drywell and containment pressures; however, during this drywell depressurization transient, there will be a period of negative pressure on the drywell structure which results in a negative-load condition for drywell design and possible hydrodynamic loads on structures within the drywell due to reverse flow through the vents.

Following vessel flooding and drywell/containment pressure equalization, suppression pool water will be continuously recirculated through the core by the ECCS pumps. The energy associated with the core decay heat results in a slow heat up of the suppression pool. To control suppression pool temperature, operators will activate the residual heat removal (RHR) system. After several hours, the RHR heat exchangers will control and limit the suppression pool temperature increase.

The magnitude and timing of LOCA pool swell and steam condensation pool dynamic loads depends on the break size. A spectrum of LOCA break sizes was considered in order to establish the limiting design conditions for the Mark III containments. The LOCA conditions which were considered include the following accident conditions:

1. Design Basis Accident (DBA), a double-ended break of a recirculation line or main steam line;

2. Intermediate Break Accident (IBA), a break that is less than the DBA but is of sufficient magnitude to automatically depressurize the primary system due to loss of fluid and/or automatic initiation of the ECCS. In practice, this means liquid breaks greater than 0.05 ft^2 and steam breaks greater than 0.4 ft^2 (determined by analysis); and

3. Small-Break Accident (SBA), a break that will not result in reactor derpressurization due either to loss of reactor fluid or automatic operation of the ECCS.

The DBA is the design limiting case for the pool swell-related pool dynamic loads including jet, drag, impact and fallback loads. The IBA and SBA cases have a much lower rate of drywell pressurization. Therefore, for these cases the IBA and SBA pool swell loads are correspondingly lower. However, LOCA related steam loads at design values can occur over a wider spectrum of breaks since the maximum condensation loads will occur at low vent mass flux. Condensation oscillation and chugging will occur over an extended period of time for small breaks as a result of the reduced reactor vessel depressurization rate compared to a DBA.

Also, the IBA and SBA cases must be considered in developing the design thermal stratification loads for the suppression pool. In the event of the postulated LOCA, the suppression pool water in the immediate vicinity of the vents will be heated due to the energy release during the steam condensation portion of the transient. For the Mark III horizontal vent configuration, the majority

of the mass and energy will be transferred to the pool through the top vents. Consequently, the upper portion of the suppression pool will be heated more than the lower portion. The vertical temperature gradient resulting from this effect is defined as thermal stratification.

3 HYDRODYNAMIC LOAD EVALUATION

3.1 Introduction

In this section the staff's evaluation of the methodology will be described. The methodology will be employed by the Mark III utilities to define the suppression pool hydrodynamic loads associated with postulated LOCA events. These dynamic loads, in combination with certain other loads which have already been reviewed and evaluated by the staff,[6,7] are used for design evaluation of the various structures and equipment which form the containment system of the standard Mark III plants.

Each of the dynamic LOCA loads identified for the Mark III containment is evaluated separately in the subsections that follow. The evaluation includes the data bases and analytical tools that were used to establish the individual load specifications. Further description of the analyses and test programs which serve as the bases for the load specifications are given in Appendices A and B, respectively.

The phenomena and dynamic loads that occur following onset of the postulated LOCA in a Mark III containment were previously identified (Section 2.2). These loads have been reviewed to determine which were significant based either on their magnitude relative to nonhydrodynamic loads or in terms of the structural response of the containment system. Such loads are designated as "primary" loads and have been given a detailed evaluation. The remaining loads are considered to be of secondary importance either because they are intrinsically small or because they are bounded by other design loads. An evaluation of these secondary loads is provided in Section 3.8.

The primary loads on the Mark III containment are considered to be the following:

- pressure loads on the containment boundaries during the air clearing and pool swell phase of the LOCA blowdown;
- pressure loads on submerged boundaries during condensation oscillation;
- pressure loads on submerged boundaries and the top vents during chugging;
- thermal loads on submerged boundaries and top vents during chugging;
- drag loads on structures located below the initial suppression pool surface during pool swell, condensation oscillation and chugging;
- impact and drag loads on structures located above the initial pool surface during pool swell and above the weir annulus during drywell depressurization; and

- drag loads on structures located between the bottom vent elevation and the HCU floor during fallback.

The following loads are considered to be secondary loads:

- Sonic Wave Loads;
- Compressive Wave Loads;
- Water Jet Loads During Vent Clearing;
- Impact Loads During Fallback;
- Fallback Loads on Containment Boundaries;
- Post-Pool Swell Wave Loads;
- Asymmetric Chugging Loads; and
- Seismic Slosh Loads.

The load evaluations were based on the standard Mark III containment design (GESSAR-II). Plant-unique features that may affect the generic load definition will be reviewed on an individual plant basis. An example of a plant-unique feature is possible encroachment over the suppression pool, such as the Traversing Incore Probe (TIP) Station. Because the design of the TIP Station and other encroachments varies from plant to plant, the staff will review the effects of these encroachments on the hydrodynamic phenomena for each individual plant design. These plant-unique reviews will be reported in the individual Safety Evaluation Reports.

3.2 Loads During Pool Swell

Following onset of a DBA LOCA, the drywell will be pressurized by the escaping steam, and the air initially in the drywell will be forced through the weir annulus and the vents into the wetwell, displacing the water as it advances. In the wetwell, the drywell air will form a large, rapidly expanding bubble which will lift the water ligament above it ("pool swell") at a considerable speed. The rising water ligament will thin until the bubble breaks through, signaling the end of the pool swell proper and the beginning of froth formation and froth loads. The flow field induced by these motions produce loads on all initially submerged structures and boundaries as well as those structures subsequently engulfed by the rising pool.

3.2.1 Pool Swell Velocity

The pool swell velocity controls the impact and drag loads on the structures between the pool rest elevation and the breakthrough elevation.

The design value for the pool swell velocity proposed by GE is 40 ft/s, the same value being used for all elevations between the pool rest elevation and the breakthrough elevation. This was derived primarily from a full-scale PSTF air test 5705-4,[8] which showed a maximum pool swell velocity of 34 ft/s, or 38 ft/s if one discounts an apparent loss of ligament acceleration in the last

few feet of rise in the test; and supported by references to the 1/3 and 1/9 area-scaled (distorted-geometry) pool swell tests, [9,10] which indicated lower velocities (see page 3B0.3.2.1-9 of GESSAR-II[33]. The staff has reviewed the basis for the proposed 40 ft/s pool swell velocity [11,12,13] and found that there were shortcomings in how the tests, which form the basis of this specification, simulated Mark III DBA conditions. To account for these shortcomings, the staff will require that a maximum pool swell velocity of 50 ft/s be used for design purposes. For calculating impacts loads on structures within 10 ft of the pool's rest elevation, a lower speed can be used, consistent with the equation

$$V = 5\ H\ (2.6 - 0.506\ \sqrt{H}) \qquad (3\text{-}1)$$

where V is the pool swell velocity in ft/s, and H is the elevation, in ft, above the pool surface's rest elevation.

To understand the staff's position, it is necessary to briefly review the Mark III pool swell data base. That data base allows three types of predictions of the pool swell velocity, (1) based on full-scale tests, (2) based on distorted geometry tests where the cross-sectional areas were reduced by either a factor of 3 or 9, while the flow-wise dimensions were full-scale, and (3) based on the 1/3 area-scaled distorted geometry tests interpreted as approximately geometrically scaled tests, using the so-called "Modified Froude Scaling" laws to simulate dynamic conditions.

The full-scale test (5705-4) on which the 40 ft/s velocity primarily rested had full-scale in both pool area and break area for the three-vent sector which it was supposed to simulate. However, only two vents were operative, not three as in the Mark III design.

GE has shown elsewhere[14] that with the same submergence and break area, a one-vent test produced only half the pool swell velocity of a two-vent test. There is some reason to suspect, therefore, that the two-vent test may have underestimated the Mark III three-vent pool swell. Secondly, the drywell was only half the correct size for the system, and the drywell pressure was considerably below the value represenative of Mark III DBA conditions in the period following vent clearing, which controls pool swell. This is shown on page 3B0.3.2.3-16 of GESSAR-II (note that the breakthrough point is indicated as occurring at 1.6 times the initial submergence, or 12 ft; the staff puts the breakthrough at 18 ft). The lower post-vent-clearing drywell pressure reduces the driving force for pool swell. This is a second reason why test 5705-4 may have underestimated the Mark III swell for DBA conditions. Since test 5705-4 was the closest of all the available "full-scale" tests to full-scale conditions, we are left with an inadequate full-scale simulation of Mark III pool swell, and a strong suspicion that 40 ft/s may not represent an adequately conservative pool swell velocity.

A second source of pool swell data is available from GE's distorted geometry tests, where all flow areas were scaled down by a factor, while flow-wise dimensions were retained full scale. GE used both 1/3 and 1/9 area-scaled systems. The implicit assumption which was made in interpreting these tests was that pool swell is not significantly affected by the scaledown in

cross-sectional areas, and that full-scale pool swell velocities should be obtained if the system is driven by full-scale drywell pressures at full-scale submergence (7.5 ft). In other words, it was assumed that pool swell is a quasi-one-dimensional process.

Since the drywell was properly scaled in relation to the pool and vent areas in the distorted geometry systems, the drywell pressure history can be characterized by a single parameter, the peak drywell pressure. In other words, if the peak drywell pressure is properly simulated, so is the entire drywell pressure history. The peak drywell pressure predicted by the containment analytical model for GESSAR-238 Standard Plant, prior to bubble breakthrough, is 20 psig (see p. 3B0.3.2.3-8 and the figure on p. 3B0.3.2.3-16 of GESSAR-II). Although the containment model is somewhat conservative (a similar model stripped of all conservatisms gave 16 psig for the 238 Standard Plant, and agreed with GE's PSTF data), the staff feels that the containment analytical model should be used for the design basis drywell pressure for pool swell, consistent with the approach taken with the Mark I and Mark II containments.

Figure 3-1 shows the peak swell velocities obtained in the 1/3 and 1/9 area-scaled systems as a function of peak drywell pressure. The data are for steam blowdowns, which the staff accepts as being representative of the DBA LOCA. At 20 psig, the 1/9 area-scaled system gives a velocity of about 25 ft/s, plus or minus about 2 ft/s; the 1/3 area-scaled system, on the other hand, gives a considerably higher velocity, about 42 ft/s (the corresponding figures quoted by GE are 26 and 33 ft/s, respectively; these are, however, based on an effective peak drywell pressure of 16 psig).

The problem with the distorted geometry data is that the underlying assumption, that area reductions do not affect the pool swell, is unjustified. Ruggieri and Sonin[15] have shown explicitly that three-dimensional effects tend to decrease the pool swell velocity in a Mark III-like geometry as the cross-sectional area of the system is reduced. The same effect is apparent in GE's 1/9 and 1/3 area-scaled results. If the 1/9 area scaled system gives 25 ft/s, and the 1/3 scale system 42 ft/s, what is the proper velocity for a full scale system?

There is yet a third way of deriving a full-scale pool swell velocity from the data. All of the tests which form the basis of Mark III pool swell were done before the Mark I[16] and Mark II[17] programs got underway, and hence they derived no benefit from what was learned in those programs. However, after the small-scale modelling laws were developed and confirmed during the Mark I program, GE noted that their 1/3 area-scaled distorted geometry system with a 5 ft submergence was rather like a 5/7.5 scale true geometric replica of a full-scale system with 7.5 ft submergence, with the exception that (1) the vents were too long by a factor of 1.5, (2) the separation between the vents was too large by a factor of 1.5, (3) the pool was slightly too narrow (the dimension from the drywell wall to the containment wall was 11 ft., whereas it should have been 12.7 ft). In any case, if one were to consider these differences to be minor, one could use Moody's dynamic scaling laws[18] to derive full-scale velocities from the 1/3 area-scaled system with 5 ft submergence.

Now, Moody's scaling laws require that the small-scale tests be done with both absolute and gage pressures scaled down in proportion to system size, and with

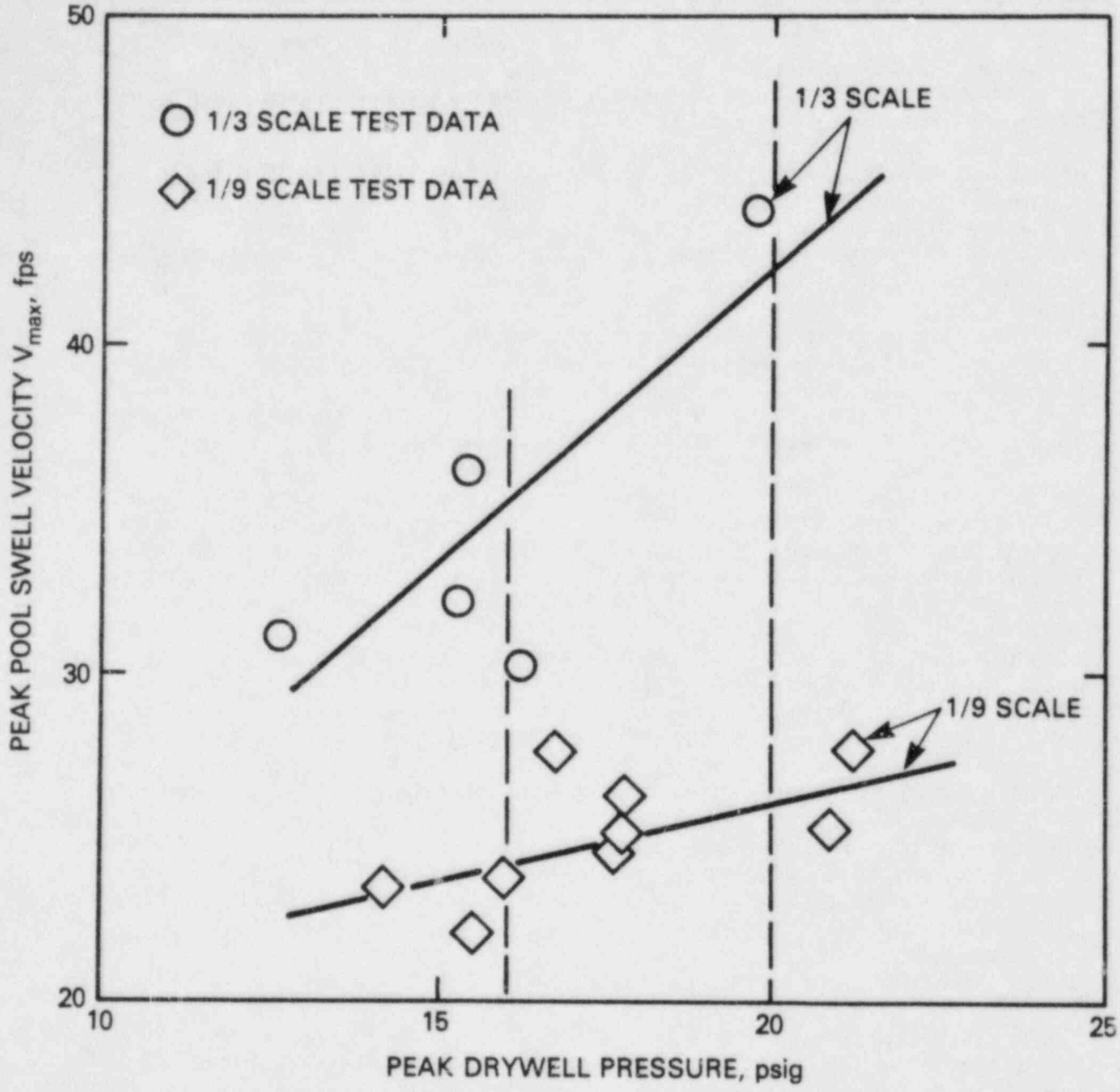

Figure 3-1 Effect of Flow Cross-Section on Pool Swell Velocity in Distorted Geometry Tests. (Scale refers to the ratio of the cross-sectional areas to those in the full-scale system)

flow resistances installed in the vents so that enthalpy flux through the vents becomes scaled with the 7/2 power of system size. Under these conditions the velocities should scale as the square root of the system size. In the 1/3 area-scaled tests, the absolute pressures were not scaled down (i.e., they were too high by a factor of 7.5/5 = 1.5). Also, there were no orifices in the vents, so the enthalpy flux through the vents tended to be too large at a given drywell gage pressure. These two dynamic scaling errors tend to some extent to compensate for each other, with the net effect on pool swell velocity being a conservatism (overestimation) of perhaps as much as 10%,[11,19] although the precise figure cannot be given with confidence. Since this 10% may well be counterbalanced by possible nonconservatisms of the excessively large vent separations and the somewhat too narrow pool, the staff does not feel that any net conservatisms should be claimed for this type of interpretation of the data.

At a peak drywell gage pressure which is equivalent to 20 psig at full scale by linear scaling with system size, and a 5 ft submergence, the 1/3 area-scale system shows a peak pool swell velocity of 39 ft/s, which scales to 48 ft/s at full-scale conditions (Figure 3-2). GE's equivalent figure is 44 ft/s, because they take a 10% conservatism on the actual measured value.

The staff concludes that the approximately Moody-scaled (sometimes referred to as Froude-scaled) value of 48 ft/s is the most reliable one available for system design. However, because of the several approximations made in both the geometric and the dynamic scaling, the staff recommends a somewhat higher value of 50 ft/s for actual use. Although the 2 ft/s difference does not seem like much of a conservatism, given the cited uncertainties, there is actually a larger margin for error because of the staff's adoption of the containment analytical model's peak drywell pressure of 20 psig. As mentioned above, GE's more realistic code puts this pressure at 16 psig, which would correspond to a peak pool swell velocity of 42 ft/s (see Figure 3.2).

The 50 ft/s is to be applied to all elevations higher than 10 ft above the pool rest-level, and below the breakthrough point. The previously given formula for the velocity below the 10 ft level - to be used for calculations of impact load on structures below the 10 ft level - simply represents an analytical fit of the experimental data summarized on p. 3B0.3.2.33-11 of GESSAR-II.

3.2.2 Breakthrough Elevation

The breakthrough elevation is the height above the initial pool surface where the air bubble penetrates the rising pool surface. All structures below the breakthrough elevation are hit by solid water as the surface strikes them. Above the breakthrough point the water ligament is turned into froth. The design value for the breakthrough elevation is 18 ft above the pool rest-surface (p. 3B0.3.2.1-11/12 of GESSAR-II).

The staff finds this specification satisfactory. Although the full-scale test, No. 7705-4, does not properly simulate Mark III pool swell conditions, and the 1/3 area-scaled distorted geometry tests results (p. 3B0.3.2.1-16 of GESSAR-II) do not conclusively make the case for an 18 ft breakthrough point (a linear extrapolation is not necessarily justified), there is sufficient

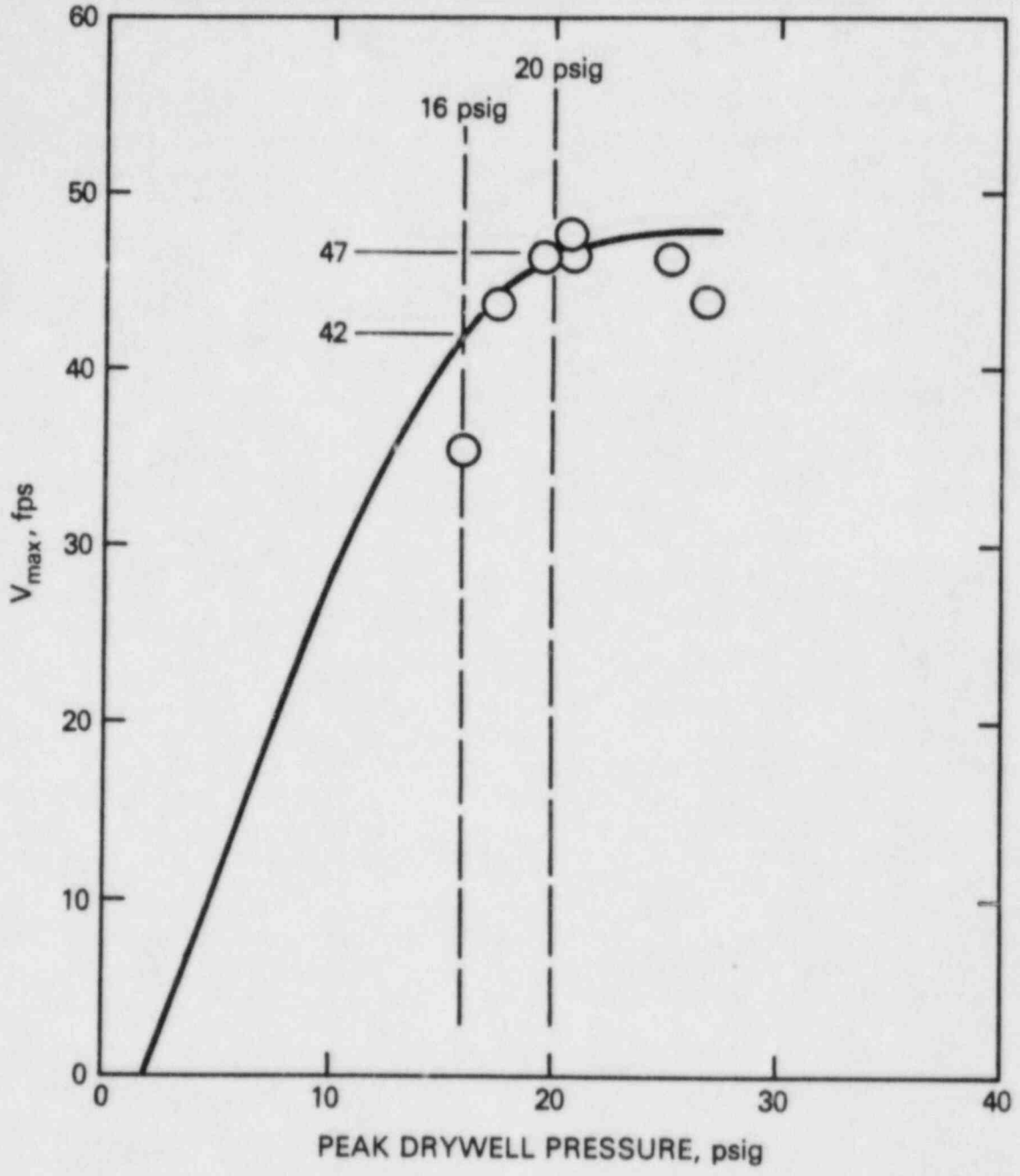

Figure 3-2 Mark III Pool Swell Velocity Derived from 1/3-Scale Tests Based on Approximate Moody Scaling. Indicated Velocities and Pressures Have Been Scaled up to Full Scale ($V \propto \sqrt{L}$; $P \propto L$)

evidence that the 1/3 area-scaled data should overestimate the breakthrough point,[15] and sufficient evidence from the approximately Moody-scaled tests in the 1/3 area-scaled system, which the staff believes to be most representative of the available data, that the breakthrough will occur below 18 ft.[11].

3.2.3 Loads on Submerged Wetwell Boundaries

During pool swell the dynamic pressure of the air bubble is transmitted to the wetwell boundaries, the transmission being strongest at the drywell wall, which is nearest the bubble, and weaker at the containment wall, which is more remote.

The design specification for the resulting dynamic loads on the wetwell boundaries is summarized in Fig. 3B-11 of GESSAR-II. Below the rest-level of the pool surface, peak dynamic pressures of 21.8 psid and 10 psid are applied on the drywell and wetwell walls, respectively. Above the rest-level, the peak pressures on the walls decrease linearly with elevation to zero at the design breakthrough height of 18 ft above the rest-level. On the basemat, the peak pressure is 10 psid from the containment wall to a point half-way between the containment and drywell walls, and increases linearly from 10 to 21.8 psi from that point to the drywell wall. Consistent with experimental results, the dynamic pressures are assumed to rise from zero to the local peak value in 0.1 s, and drop back to zero in 0.5 s. Above the pool rest-level, the pressures are applied with a time delay consistent with a pool rise velocity of 40 ft/s. Vertical loads on structures attached to the walls are assumed to be transmitted to the walls.

The staff finds this load specification acceptable for the following reasons. The 21.8 psid on the drywell wall exceeds the dynamic pressure in the drywell itself during pool swell. Before breakthrough, that pressure is calculated as 20 psid by the conservative containment analytical model, and 16 psid by a best-estimate version of that model (see Sec. 3.2.1 above). Experiments show that the dynamic pressure on the containment wall is always less than half the pressure on the drywell wall (Fig. 3B-55, p. 3B-145/146 of GESSAR-II); hence the 10 psi on the containment wall is conservative. The distribution on the basemat is based on experimental observations that the peak pressure at the mid-point between the drywell and containment walls does not significantly differ from that on the containment wall (Sec. 3B.7, GESSAR-II). The pressure history at a given point is consistent with the PSTF data, and the delay time for points above the pool rest-elevation, although not necessarily precise, is certainly representative, based as it is on an average pool swell velocity of 40 ft/s.

3.2.4 Wetwell Pressurization During Froth Outflow

Following pool swell and breakthrough, the region of the wetwell above the top vent fills with froth. The air which is still being exhausted from the drywell tends to pressurize the wetwell and forces this froth out through the openings in the HCU floor. Since the froth has a relatively high density compared with air, the pressure required in the wetwell to drive the froth out through the HCU floor openings is much higher than that during pool swell, when only air is being displaced.

This pressurization of the wetwell between the time when the froth first reaches the openings in the HCU floor and the time of completion of air blowdown causes a pressure differential between the wetwell and the region above the HCU floor, and results in upward loads on the HCU floor itself and on the various structures which span the openings at the HCU floor level, including gratings.

The design specification for the wetwell pressurization, after the froth impact at the HCU level, which is discussed elsewhere, is 11 psid relative to the region above the HCU floor. This 11 psi was orginally computed with an analytical model[20] based on rather crude physical assumptions, but rendered usable by the grossly conservative nature of some key assumptions. A somewhat altered computation based on essentially the same model predicted a lower value (7.4 psid), and was shown to be some 3 to 3.5 psid conservative when benchmarked against all the PSTF 1/3 area-scaled tests without solid water impact on the roof (Sec. 3B0.3.2.35, GESSAR-II). The 11 psid is therefore quite a conservative value. Accordingly, the NRC staff finds that the 11 psid specification for the 238 Standard Plant acceptable.

3.2.5 Loads on Submerged Structures

Loads on submerged structures during the air bubble expansion are computed on the basis of the methodology developed for Mark II[21] containments and described in detail in Section 3BL.2.3 of GESSAR-II. The bubbles are assumed to form in phase, thus only a unit cell is considered with boundaries and pool surface represented by the method of images. The acceleration and velocity fields are computed on the basis of stationary spherical bubble dynamics, subject to mass flow from the drywell. Drywell pressure at top vent clearing is taken as the initial bubble pressure, the vent radius as the initial bubble radius. The acceleration and standard drag loads on cylindrical structure segments (no more than 2 ft long) are computed on the basis of the local acceleration and velocity at each segment center.

The acceleration volume is based on potential flow theory and the drag coefficient used is the standard steady flow, C_D. In the sample problem of Section 3BL.2.4 of GESSAR-II, a maximum drag coefficient of 1.2, corresponding to a relatively high Reynolds number, was used. While the loads thus computed are shown to bound sub-scale submerged structure data, a conservative multiplier of a factor of two is applied to the final load to account for the bubble motion and asymmetry not included in the theoretical analysis.

For the accelerating non-oscillating flows causing loads on cylindrical structures, the methodology is supported by both theory and experiments as cited in Reference 22. The staff, therefore, finds the procedure with the specific numerical values of acceleration volume and drag coefficient used as acceptable for structures of circular cross-section (cylindrical).

In Section 3BL.2.3 of GESSAR-II the same procedure is implied for noncylindrical structures with acceleration volumes based on potential theory presented in Tables 3BL-2 and 3BL-3 of GESSAR-II for some common shapes. No discussion of the drag coefficient is presented. The staff expressed concern about the application of this procedure to structure with sharp corners. The use of Mark I Acceptance Criteria[16] using a simple "equivalent cylinder" concept

was suggested as the procedure that bounds available data for both acceleration and standard drag. The response to the concern in Section 3B0.3.2.31(b.ii) of GESSAR-II accepts this suggestion. The staff therefore finds the methodology presented in 3BL.2.3 acceptable subject to the amendment of 3B0.3.2.31(b.ii).

3.2.6 Loads on Structures at the Pool Surface

Structures that have their lower surfaces either right at the pool surface or slightly submerged do not experience the pool swell impact loads of the structures above the initial pool surface, nor can the loads be adequately described by the LOCA Bubble Loads methodology discussed in Section 3.2.5 above. Section 3B.9 of GESSAR-II specifies the load as the sum of a bubble pressure load (21.8 psid on structures on the drywell wall and 10 psid on structures on the containment wall) and a drag load based on 40 ft/sec pool swell velocity.

When structures, such as ledges, are attached to the containment wall, the hydrodynamic flow field along the wall will be disturbed by the presence of the structure, resulting in localized loads on the containment wall. These local loads are specified in Section 3B.6.1.5 and Figure 3B-56 of GESSAR-II. Figure 3B-56 presents local pressure distributions on the wall due to two different protrusions, half-wedge and horizontal ledge. The pressure differentials shown correspond to a velocity of 40 ft/sec.

The bubble pressure load is considered very conservative because it assumes the entire pressure gradient to be taken across the structure. The issues associated with the local perturbation to the flow acceleration represented by the hydrodynamic mass concept are thus bounded by the ultra-conservative estimate of the pressure difference. The velocity of 40 ft/sec while not necessarily uniformly bounding the entire pool swell is adequately supported by empirical evidence as a conservative bound at the vertical positions (< 5 feet above the pool) of the structures especially near the drywell and containment walls.

The staff, therefore, finds the procedure for computing loads on structures at the pool surface during pool swell, described in Section 3B.9 of GESSAR-II to be acceptable.

With regard to the load specification in GESSAR-II of local wall pressures due to ledge-type protrusions, the staff finds it acceptable with the following limitations:

(1) If the local pool swell velocity, as specified in Section 3.2.1, above, is greater than 40 ft/sec, the drag pressures obtained by the GESSAR specification shall be multiplied by $(V/40)^2$, where V is the local pool velocity in ft/sec.

(2) If the frontal area of the structure is not fully immersed prior to pool swell, it will experience an impact force. This must be included in the specification.

For half-wedge protrusions the force history during impact shall be determined from Figure 3-3. The local velocity of impact (needed in Figure 3-3) shal be taken from the specification in Section 3.2.1,

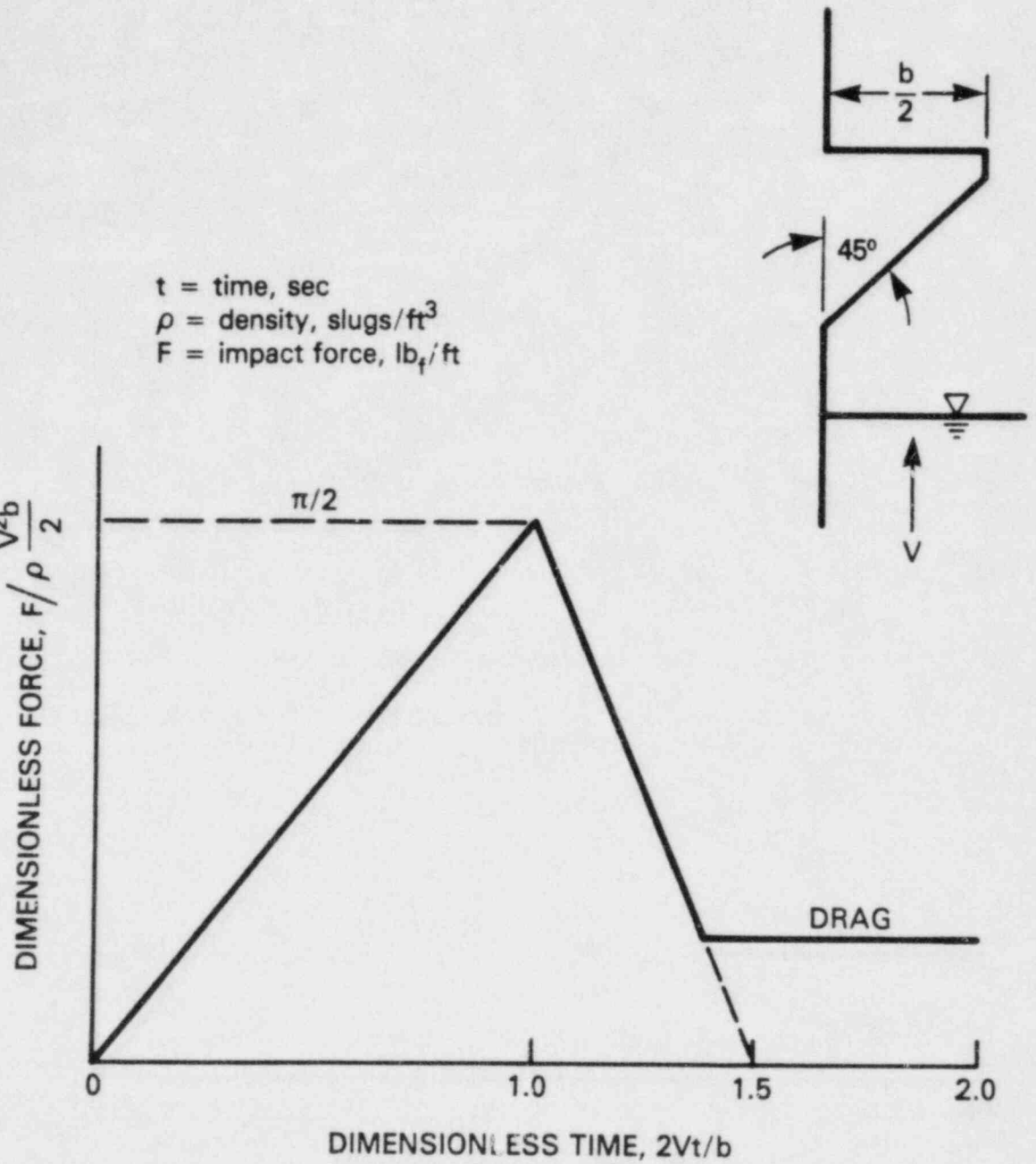

Figure 3-3 Impact Force (per unit length) on Wedge-Shaped Protrusions from the Containment Wall

corresponding to the height where the wedge is first fully submerged. If the lower portion of the wedge is initially submerged, the same impact history is applied except the abscissa is replaced by Vt/h, here h is the "unsubmerged height" of the wedge.

If the wedge angle is other than 45°, the following ratios can be used after obtaining the force history for a 45° wedge from Figure 3-3.

$$\frac{F_\beta}{F_{45}} = \left(\frac{\beta}{90-\beta}\right)^2 \cot \beta \qquad (3\text{-}2)$$

and

$$\frac{t_\beta}{t_{45}} = \cot \beta \qquad (3\text{-}3)$$

where β is the wedge angle. These ratios were derived from the analytical solutions in Reference 34.

For horizontal ledges the impact force shall be determined in the following manner:

(a) The force history will have a triangular shape as shown in Figure 3-4.

(b) Determine the hydrodynamic mass of impact (per unit area) for flat targets from Figure 6-8 of NEDE-13426P.[23] Use b (and not b/2) for target width.

(c) Calculate the impulse using the equation

$$I_p = \frac{M_H}{A} V * \frac{1}{(32.2)(144)} \qquad (3\text{-}4)$$

where

I_p = impulse per unit area, psi-sec

M_H/A = hydrodynamic mass per unit area, lbm/ft^2, from (b) above.

V = impact velocity, ft/sec, determined according to Section 3.2.1

(d) Calculate the pulse duration from the equation

$$\tau = .02 \frac{H}{V} \left(\frac{b}{2}\right) \qquad (3\text{-}5)$$

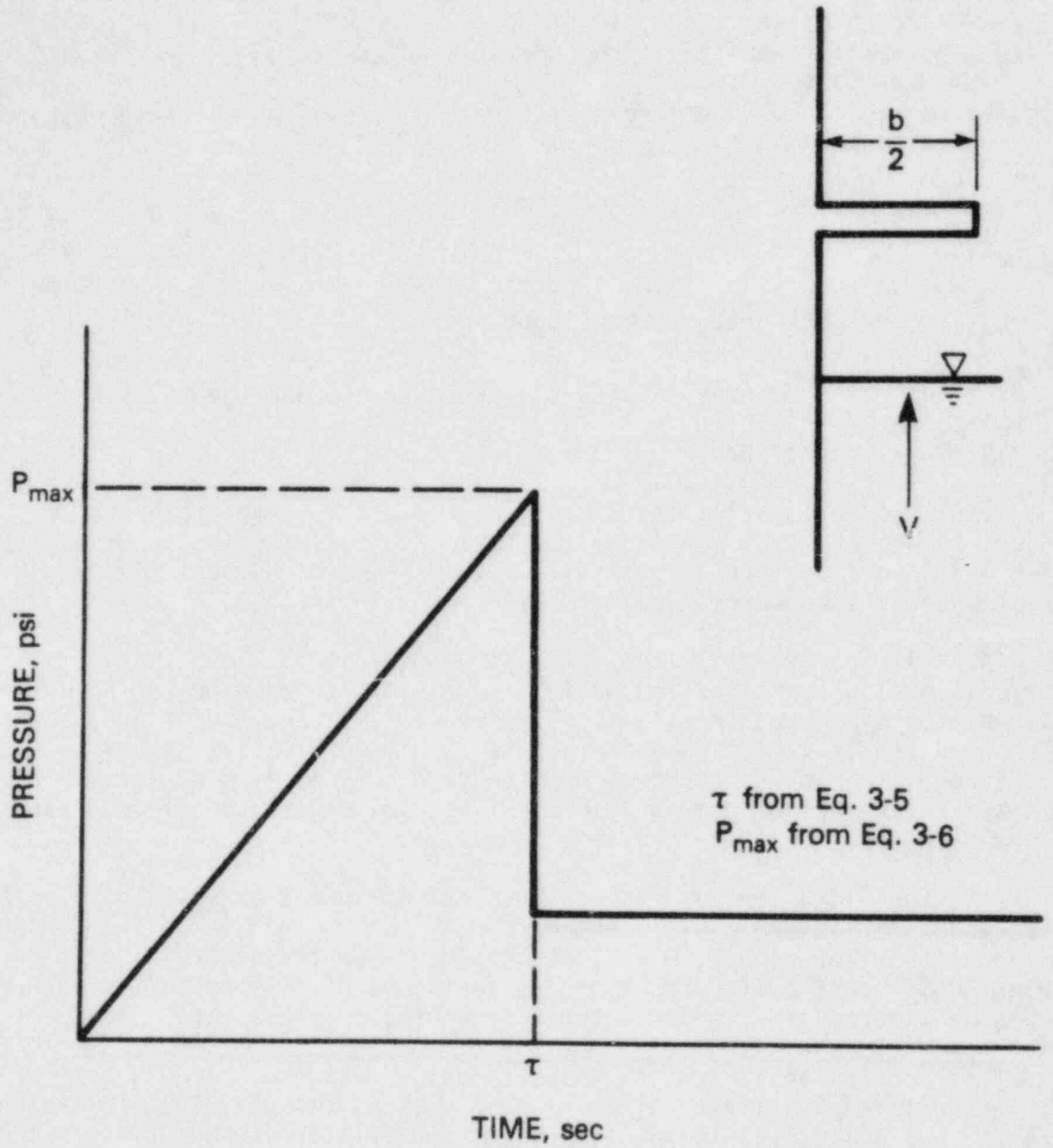

Figure 3-4 Impact Pressure on Horizontal Ledges Attached to Containment Wall

where:

τ = pulse duration, sec
H = height above the pool, feet
b/2 = width of the ledge, feet
V = impact velocity, ft/sec, determined according to Section 3.2.1

(e) The value of peak pressure amplitude, P_{MAX}, will be obtained using the following equation:

$$P_{MAX} = 2\ I_p/\tau \qquad (3\text{-}6)$$

where:

P_{MAX} = the peak pressure amplitude, psi.

3.2.7 Loads on Structures Between the Pool Surface and the HCU Floor

3.2.7.1 Bulk Impact Loads

As a result of pool swell, structures located above the containment pool are subject to impact loads. At lower elevations, i.e., from 0 to 18 feet above the initial pool surface, impact will occur in the bulk mode. By this we mean impact by an intact water ligament, as opposed to froth.

The GESSAR-II specification for small structures (i.e., less than 20 inches wide), is presented in Section 3B.10.1. It consists of a universal normalized force history, somewhat similar to a versed-sine shape, having a constant pulse duration of 7 milliseconds (Figure 3B-71, GESSAR-II). The maximum amplitude of this pulse (force/projected target area) is given as 115 psi for flat structures and 60 psi for pipes. These values are specified regardless of the local pool velocity or target size.

The basic specification for flat targets was derived from Test No. 5706/4[8] where a 20-inch square plate was impacted by the rising pool. The lower pressure amplitude for pipes (60 psi) was derived from the observation in Test Series 5805[23] that cylindrical targets were subjected to impact pressures that were approximately half of flat targets under comparable conditions.

The staff conclusion is that the specification, as described, is not applicable without additional limitations. The main reason for requiring limitations is that the pool velocity at impact, during PSTF Test 5706/4 was 21 ft/sec, whereas pool velocities as high as 50 ft/sec are possible.

The limitations imposed on the specification are discussed in Attachment 0 to the GESSAR-II, Sections 3B0.3.2.4, 5 and 33 (corresponding to Question/Response 4, 5 and 33).

In response to staff questions, GE conducted the following analysis. First, they noted that maximum stresses in uniformly loaded beams are proportional to the product of P_{max} and DLF, where P_{max} is the peak amplitude of the pressure pulse and DLF is the dynamic load factor. They then compared the stresses produced in the impacted structures using (1) the GESSAR-II specification and

(2) the NRC staff Mark II impact specification with one difference. The difference was that, whereas the Mark II pulse durations were based on flat-pool impact, in performing the above comparison, GE used experimentally observed pulse durations derived from Test Series 5805, corresponding roughly to Mark III pool curvature. These pulse durations were 6.8 msec for radial targets and 2 msec for circumferential. (Note that flat-pool impact results in the shortest pulse duration and highest stress.)

The results of these comparisons are best represented by plots of natural frequency vs. the width of the structure, as shown in Figures 3-5 through 3-7. These curves represent the locus of points where the two specifications, i.e., GESSAR-II and Mark II, result in equal stresses in the impacted structures. To the left of the curves, the GESSAR-II specification results in higher stresses, i.e., is conservative. The points on the graphs represent the specific structures located above the pool in the 238 Standard Plant. It is seen that, although this comparison has placed substantial constraints on the original GESSAR-II specification, the specific structures that are located above the Mark III pool are not overstressed above design.

The staff found this response acceptable, except for one particular concern. Since the pulse duration of 6.8 msec from Test Series 5805 was obtained with radial targets that spanned the pool annulus and were approximately 10 feet above the initial pool elevation, is this pulse duration appropriate (small enough) for shorter targets and for lower target elevations where the pool would be less curved? In response to this concern, GE demonstrated in Response 33 (Section 3B0.3.2.33 of GESSAR-II) that, for the specific targets above the Standard Plant pool, i.e., shortest target 4 feet long and closest distance above the pool of 6 feet, the 6.8 msec was still conservatively short.

The staff has reviewed Response 33 and finds it acceptable.

To summarize, the staff finds the GESSAR-II bulk impact specification acceptable provided:

(1) The impacted structures are in the "conservative" areas on plots of natural frequency vs. size. (Figures 3-5 through 3-7).

(2) The impacted structures are at least 4 feet in length.

(3) The impacted structures are not closer than 6 feet to the initial pool surface.

All structures above the containment pool in the GESSAR-II standard plant design satisfy limitations (1) through (3). In plant designs where some specific structures may not meet limitations (2) and/or (3), the pulse duration must be shortened with an appropriate adjustment to the pressure amplitude. The load specifications for these structures will be reviewed by the staff on a plant-unique basis.

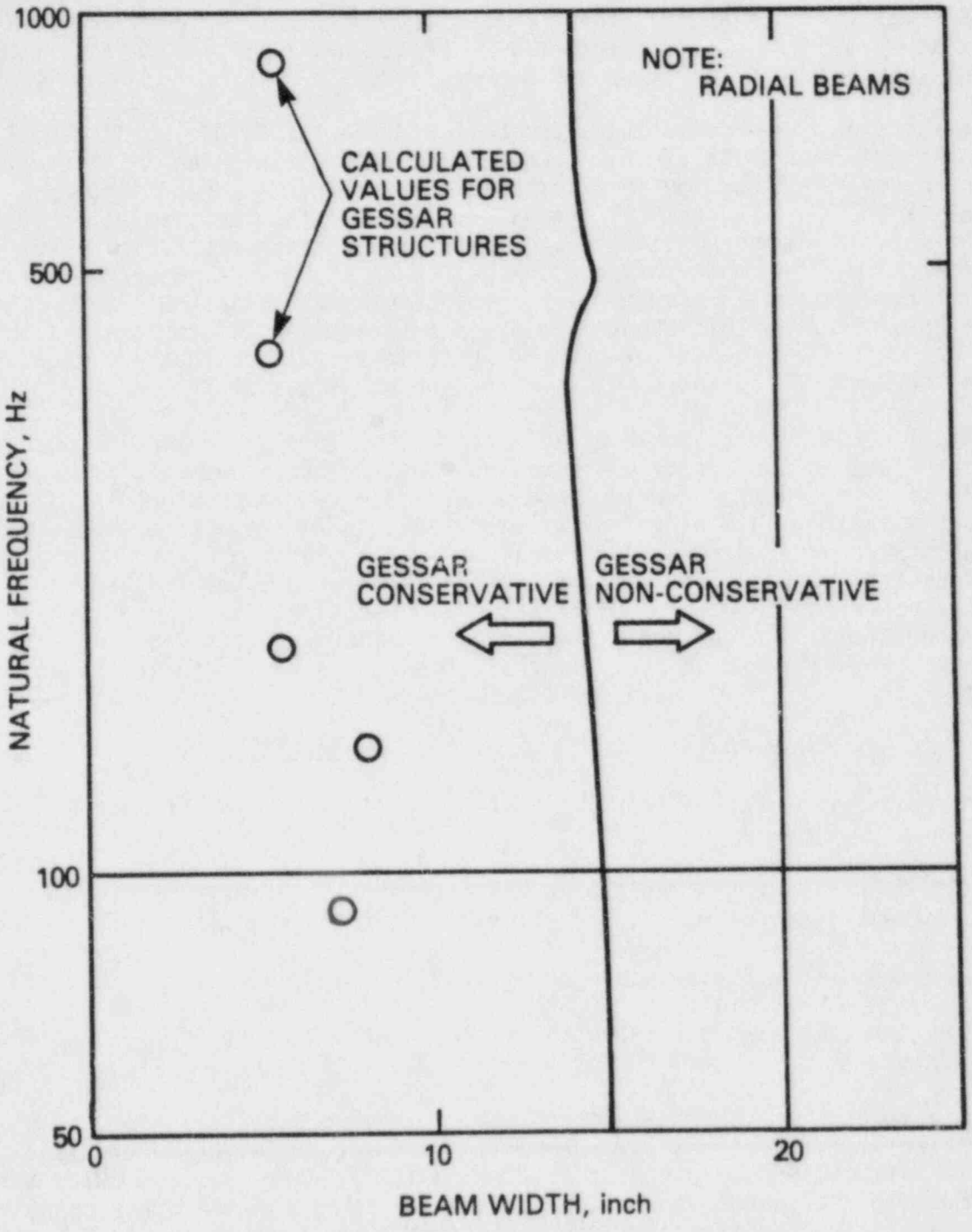

Figure 3-5 Limits on Applicability of GESSAR-II Bulk Impact Specification for Radial Beams

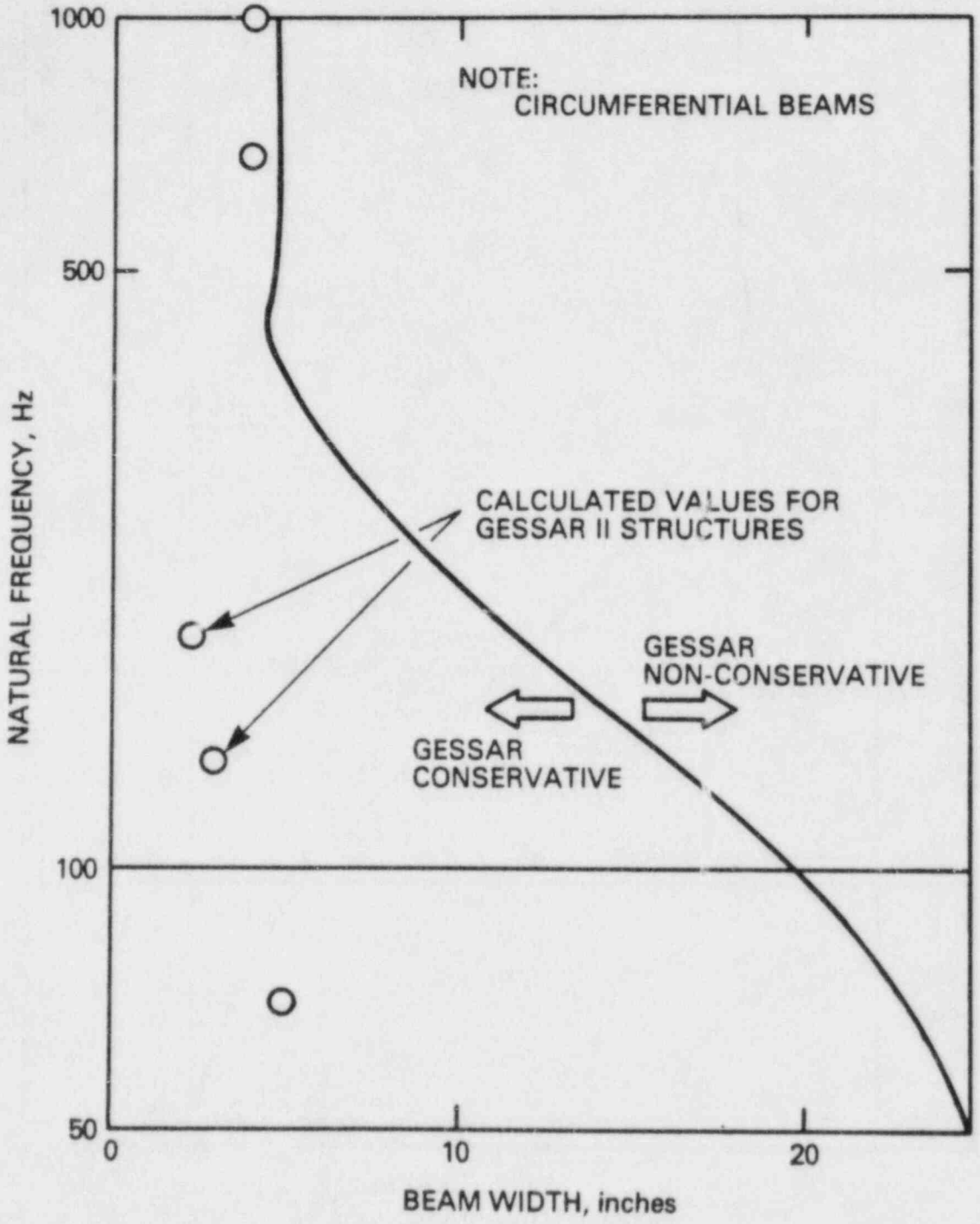

Figure 3-6 Limits on Applicability of GESSAR-II Bulk Impact Specification for Circumferential Beams

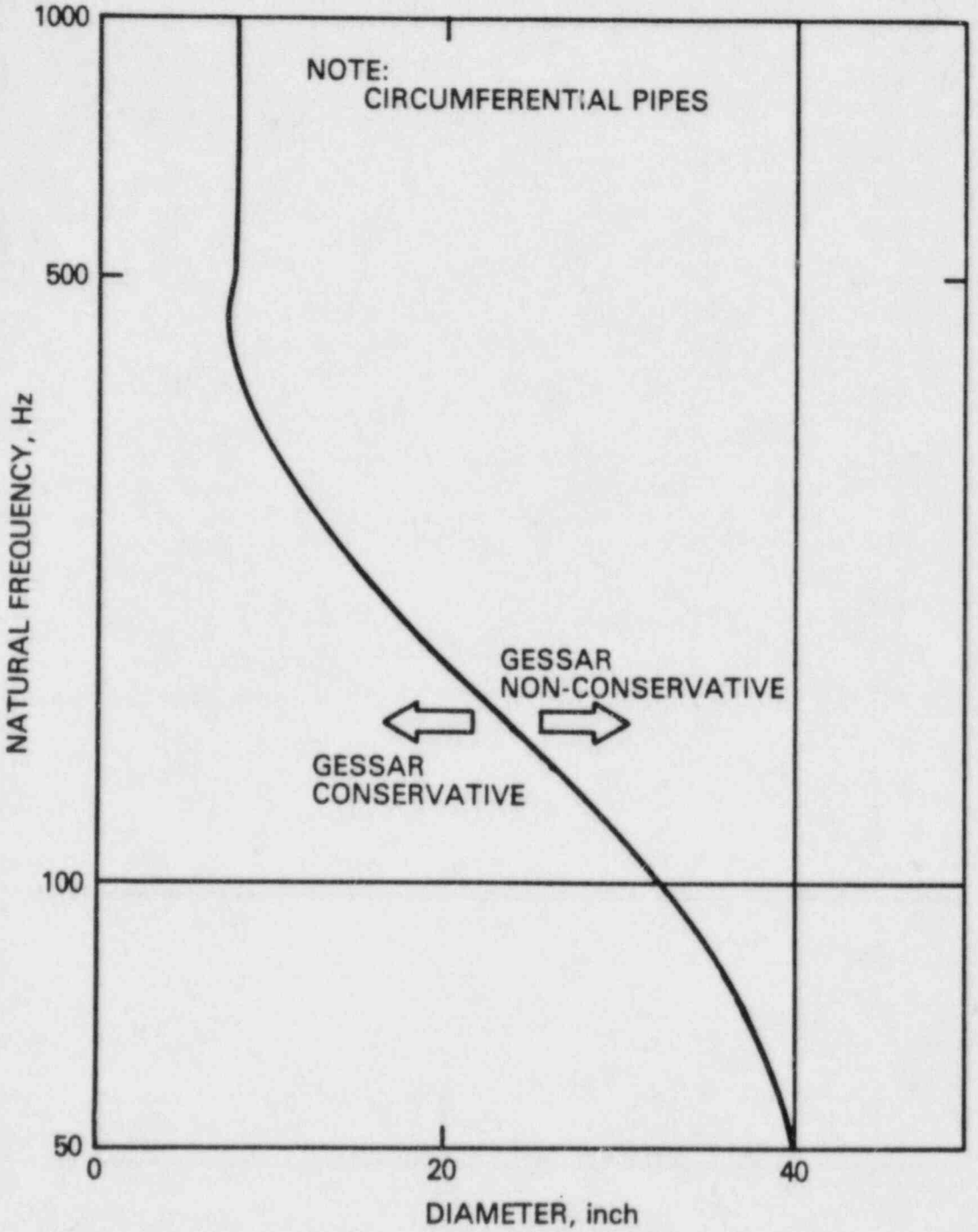

Figure 3-7 Limits on Applicability of GESSAR-II Bulk Impact Specification for Circumferential Pipes (Note: Standard Plant has none)

For structures less than 10 feet above the pool, the pressure amplitude may be reduced by

$$\frac{P}{P_{max}} = \frac{V^2}{V^2_{max}} = \frac{H^2}{100}\,(2.6 - 1.6\sqrt{\frac{H}{10}})^2 \qquad (3\text{-}7)$$

where P is the pressure amplitude at a structure H feet above the pool surface and P_{max} is the GE-specified pressure amplitude for bulk impact on small structures above the pool.

3.2.7.2 Froth Impact Loads

As the pool rises higher, the air bubbles that drive it will break through the surface, resulting in froth. This froth will impact on structures located at elevations higher than 19 feet above the initial pool surface. In addition to the so-called small structures, the froth will also impact on the bottom of the HCU floor (discussed later in Section 3.2.8.1).

The load specification in GESSAR-II (Section 3B.10.1) stipulates a triangular pressure pulse with a duration of 100 msec and a maximum amplitude of 15 psi. This specification is based on PSTF Test No. 5706/6[8] where a 20-inch square target was placed high above the pool where froth conditions were known to exist. A maximum area-averaged pressure of 5 psi was measured. In this particular facility, however, the walls of the pool did not extend all the way to the target. Consequently, as the froth was moving up, it was also spreading out laterally. GE estimated that this spreading may have reduced the density by a factor of 3. To account for this nonconservatism, the measured pressure of 5 psi was multiplied by 3, yielding the specification of 15 psi.

The staff has reviewed the GESSAR-II specification and finds it unacceptable. The basic reason is that the test was not conducted at prototypical Mark III flow conditions. The froth velocity at impact was 27 ft/sec, whereas froth velocities of 50 ft/sec are possible. Furthermore, it is difficult to demonstrate that froth density from Test 5706/6 (even using the factor of 3 multiplier) is really representative of froth conditions at 19 feet above Mark III pools. Consequently, the staff has formulated an independent acceptance criteria for froth impact.

The staff acceptance criteria is based on Modified Froude-scaled (or Moody-scaled) PSTF froth data that most closely represents the prototypical Mark III conditions. (This scaling analysis was described and reviewed in Section 3.2.1 above. The data used for this purpose came from the 1/3-scale PSTF Test Series 5801,[9] 5805[23] and 5806.[24] Only test runs with top-vent submergence of 5 feet were considered, as these give the closest three-dimensional simulation of the pool swell and breakthrough phenomena. (The GE 1/3-scale facility refers to scaling of the flow areas; the linear dimensions are really scaled as $1:\sqrt{3}$. The appropriate model submergence corresponding to this scale is 4.33 feet. No tests were run at this submergence and 5 feet is the closest available submergence.

Secondly, only tests that had the approximately correct scaled drywell pressurization rates (controlled by supply nozzle diameter) were considered. The test runs that satisfied these criteria are the following:

TEST/RUN	PRESSURIZING FLUID	TARGET LOCATION ABOVE POOL, FT.	TARGET GEOMETRY
5805/31	Steam	14	10" I-Beam
37	"	"	10" Pipe
43	"	"	20" Pipe
48	"	"	5" I-Beam
5801/5	"	17.3	PSTF Roof
9	"	"	"
15	"	"	"
5806/8	Air	17.8	"

Since all of the above tests were conducted in the same facility, with the same submergence and at the same driving conditions, it is expected that they all had the same froth conditions after breakthrough. The two parameters that were varied from test to test were the geometry of the impacted structure and the target height above the initial pool elevation.

The staff believes that for froth impact, target geometry plays only a secondary role. The froth is basically unaware of the target until the individual droplets actually impact and lose their momentum. The only mechanism that may affect their trajectories is the presence of air, which also has some vertical velocity. As air flows around the target, it exerts a lateral drag on the droplets. When this drag is sufficiently large, compared to the inertial force, some of the droplets may be diverted from the target. It is possible to estimate the fraction of the droplets that would miss the target. A substantial amount of technical data is available on the related problem of airframe icing. Much of this information has been collected and is published in a single document by the FAA[25]. This report presents correlations of "collection efficiency" for a large number of target geometries in terms of flow velocity, mean droplet diameter and target width. The froth in the PSTF tests was, of course, composed of water particles of various sizes. However, the smallest droplet that could be produced under the PSTF conditions is approximately 0.2 inches in diameter (obtained by balancing inertial and surface tension forces). The targets that were impacted in these tests ranged in size from a 5 inch I-beam to a continuous 6 foot span of the PSTF roof. For these conditions the FAA correlations indicate collection efficiencies ranging from 0.95 to 1.0. The low value of 0.95 is obtained if one assumes that all the froth is broken up into the smallest 0.2 inch diameter droplets (an unrealistic assumption). It is much more likely that only a small fraction of the water is in that droplet size range and a constant collection efficiency of 1.0 is applicable for all PSTF tests. Thus, the lateral deflection of droplets is negligible, and all PSTF structures, regardless of their geometry, should experience the same froth impact pressure, provided they are at the same height above the pool.

Since the specific target geometry is not an important parameter for froth impact, the only remaining variable for the test runs in the above table is target height above the initial pool surface. The measured impact pressures were plotted against the target height above the pool and a straight line was

fitted to the data. The resulting graph is shown in Figure 3-8. This graph represents the froth impact pressures in a 1:$\sqrt{3}$ scale model of the Mark III containment. The information had to be scaled up to prototypical Mark III conditions. Since the top-vent submergence is probably the most important dimension in characterizing bubble breakthrough and froth formation, this dimension was used as the basis for scaling up the data. The nominal full-scale submergence is 7.5 feet, whereas the PSTF data represented in Figure 3-8 had a submergence of 5 feet. Thus, the scale of the model was 5:7.5 or 1:1.5. (Note the lateral dimensions are scaled as 1:$\sqrt{3}$.) As stipulated by the Modified Froude Scaling, the froth pressures, as well as distances above the pool were scaled up to full size by multiplying both values by the scaling factor of 1.5. The resulting graph, representative of full-scale condition, is shown in Figure 3-9.

To arrive at an acceptance criteria for froth impact, it must be acknowledged that there are some uncertainties associated with the results in Figure 3-9. First, the model is not perfectly scaled geometrically. For example, the vent lengths, as well as the spacing between the vents in the PSTF facility, are full-scale rather than 1:1.5. The "Modified Froude Scaling" itself is an approximation containing conservative as well as nonconservative elements (see Section 3.2.1). The linear variation of froth impact pressure in Figure 3-9 is clearly an approximation of a more complex behavior. Froth impact itself is somewhat random and only approximately repeatable. To cover all these uncertainties, a margin of 3 psi was judged to be appropriate in arriving at the staff acceptance criteria. Its application is illustrated in Figure 3-9.

The other component of the froth impact specification is the pulse duration. The GESSAR-II stipulates a pulse duration of 100 msec, as determined from PSTF Test 5706/5.

The staff finds this pulse duration unacceptable since there is no assurance that the one specific (non-prototypical) test is representative of all possible pulse durations that may occur above the Mark III pool. Furthermore, the GESSAR-II specification makes no distinction between small or large targets.

The staff's acceptance criteria calls for a pulse duration that would maximize the dynamic load factor (DLF) for the structures impacted by froth. This implies that a range of pulse durations must be considered to ensure that the maximum DLF is identified. For structures that completely span the pool annulus, pulse durations shorter than 50 msec need not be considered.

The value of 50 msec was obtained by examination of pool curvature at incipient breakthrough. Figure 4-29 of NEDM-13407P,[9] which shows pool profiles corresponding to Test Run 5801/9, was used as the basis for this analysis, as mentioned earlier. Test Run 5801/9 can be considered a 1:1.5 scale-model simulation of Mark III pool swell. From the pool profiles and velocity, one can compute the total time required for the curved pool surface to sweep by a radial beam. When scaled up to full scale, a value equal to approximately 50 msec was obtained. This may be considered a lower limit for froth impact duration, as subsequent breakthrough can only enhance pool curvature and increase the pulse duration.

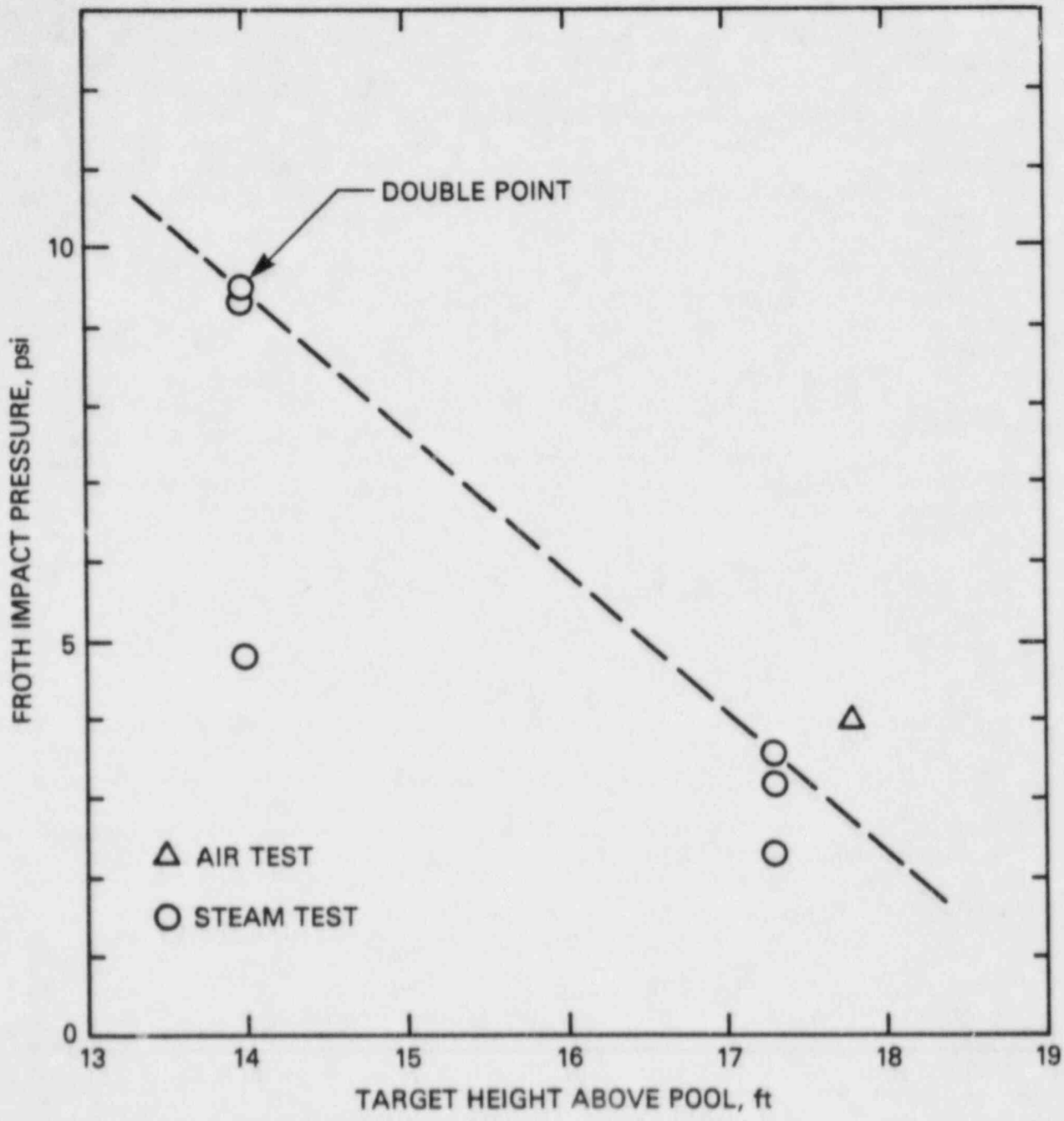

Figure 3-8 Measured Froth Impact Pressure from PSTF Tests
(5 foot submergence, 2.5 inch Diameter Nozzle)

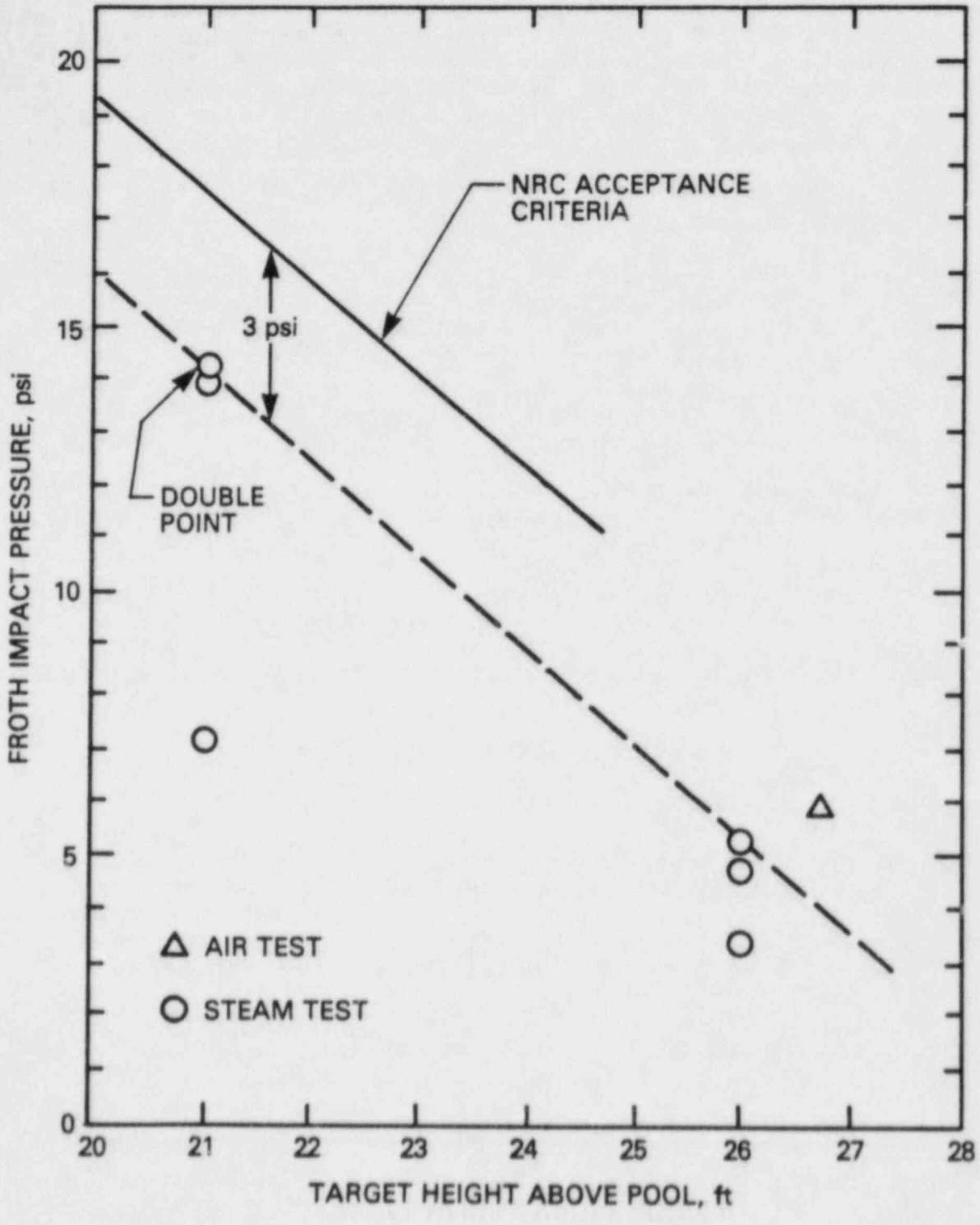

Figure 3-9 Froth Impact Measurements (from Figure 3-8) Scaled up to Full Size Using "Modified Froude Scaling"; Also Shown: NRC Acceptance Criteria

3.2.7.3 Transition Zone Impact Loads

Tne transition zone is defined as the region between 18 and 19 feet above the initial pool surface. The impact load specification for structures in this zone are given in Figures 3B-74, 3B-71, and 3B-73 of GESSAR-II. Basically, the transition zone impact loads are determined by linear interpolation of values between the bulk impact values and the froth impact values. The linear interpolation is considered acceptable for the transition zone; however, the bulk and froth impact must be consistent with Sections 3.2.7.1 and 3.2.7.2, respectively.

3.2.7.4 Liquid Drag Loads

Following bulk impact, the structures are subject to drag loads. These are specified in Section 3B.10.2 of GESSAR-II. The drag loads (average pressure differentials) for various structural geometries and a flow velocity of 40 ft/sec are presented in Figures 3B-19, 3B-72 and 3B-75.

The staff finds the GESSAR II specifications acceptable with the following limitations:

(1) If the local pool velocity, as specified in Section 3.2.1 above, is greater than 40 ft/sec, the pressure differential obtained by the GESSAR-II specification shall be multiplied by $(V/40)^2$, where V is the local velocity in ft/sec.

(2) If the shorter side ("b") of the plate in Figure 3B-75 of GESSAR-II is attached to the wall, the abscissa of the graph shall be 2a/b instead of a/b. (Also, the abscissa must start at 1.0 and not 0 as shown in Figure 3B-75).

3.2.8 Expansive Structures at the HCU Floor Elevation

3.2.8.1 Froth Impact Loads

The expansive structures at HCU floor elevation are subject to the froth impact as a result of pool swell. The GESSAR-II specification for froth impact (Section 3B.11) is a triangular pulse with a duration of 100 msec and a peak amplitude of 15 psi (same specification as for structures between the pool surface and the HCU floor). The basis for the GESSAR-II specification is Test Run 5706/6[3].

The staff finds the GESSAR-II specification unacceptable. The reasons are exactly the same as described earlier in Section 3.2.7.2.

Since froth impact is only slightly affected by the geometry of the structure, the same acceptance criteria that the staff has developed for froth on small structures between the pool and the HCU floor (see Figure 3-9) shall be used for expansive structures at the HCU floor elevation.

3.2.8.2 Froth Drag Loads

The pressurization of the wetwell during froth outflow via the openings at the HCU floor elevation (see Section 3.2.4) causes a period of steady upward loading on expansive structural members at the floor level.

An 11 psid pressure differential between the wetwell side and the containment side above the HCU floor is specified for these structures, lasting for 3 s (Section 3B.11, GESSAR-II). This specification is accepted by the NRC as conservative (see Section 3.2.4 above). On gratings, the 11 psi is to be applied on the entire grating, not just the solid portion (see Section 3B0.3.2.8, GESSAR-II).

The wetwell pressurization of 11 psi is quite conservative. As has already been discussed in Section 3.2.4, a computation based on a model which was rather crude, but whose shortcomings were compensated for by conservative assumptions, predicted 7.4 psi for the GESSAR 238 plant. This same model overpredicted the PSTF 1/3 area-scaled tests by some 3 to 3.5 psi on the average, thus suggesting that an adjusted best estimate for the wetwell pressurization might be in the neighborhood of 4 psi. However, given the crudeness of the computational model, and the fact that it was "tuned" on, and compared with, the PSTF tests where the wetwell pressurization conditions were significantly different from those expected in a full scale plant, the NRC considers it prudent to maintain the design value at 11 psi.

The froth drag load specification for gratings is conservative for another reason as well: the pressure which acts on a grating is actually lower than the bulk wetwell pressure when there is flow through the grating. This is due to the Bernoulli effect. If V is the approach velocity to the grating (that is, the velocity of the fluid before it enters the grating, somewhat upstream of it) then the pressure somewhat upstream of the grating will be below the wetwell pressure by $(1/2)\,pv^2$. If the pressure drop across the grating is defined as $k(1/2)pv^2$, where k is the grating loss coefficient based on the approach velocity and the pressure drop from just upstream of the grating to downstream of it, it follows that the pressure differential across the grating will be

$$\Delta P_G = \frac{k}{1+k}\,\Delta P \qquad (3\text{-}8)$$

where ΔP is the pressure differential between the wetwell and the region above the HCU floor.

The NRC finds Eq. (3-8) to be an acceptable alternative load definition for gratings at the HCU floor level, provided that the grating loss coefficient k is evaluated on a plant-specific basis, and provided the conservative value for Δp = 11 psi is used. Again, the pressure difference computed from Eq. (3-8) is to be applied on the entire grating, not just the solid portion.

3.2.9 Small Structures at and Above the HCU Floor Elevation

Small structures at the HCU floor elevation and higher (if above fully open or grated areas of the floor) are subject to froth impact. At the HCU floor elevation GESSAR-II specifies a triangular force history with a duration of

100 msec and a peak amplitude of 15 psi. Above the HCU floor, any structures in the line of sight of froth are subjected to a drag load calculated using the standard drag equation:

$$P = \frac{1}{2} C_D \rho V^2 \qquad (3\text{-}9)$$

where:

P = Drag pressure load, psid

C_D = drag coefficient, given for various geometries in Figure 3B-19 of GESSAR-II

ρ = froth density, taken at 18.8 lbm/ft^3

V = froth velocity, taken at 50 ft/sec at 19.5 feet above the pool and then decelerated to lower velocities by the action of gravity.

The staff finds these specifications unacceptable. The reason why the "small structure" specification at the HCU floor elevation is unacceptable is exactly the same as discussed previously in Section 3.2.7.2. For structures above the HCU floor, the drag specification has several deficiencies. First, the standard drag equation with the conventional C_D's is inappropriate for froth drag. (When one deals with froth, there is really no distinction between impact and drag. In both cases the load is caused by momentum transfer of individual particles of water as they impinge on the structure.) The main difficulty, however, is that the GESSAR-II specification underpredicts pressures when compared to values determined from test data in conjunction with the "Modified Froude-Scaled" Analysis. The comparison of the GESSAR-II specification with what the staff believes to be a realistic assessment of froth impact pressures is shown in Figure 3-10.

The NRC Acceptance Criteria stipulates that the same froth impact pressure (vs. elevation) used for small structures between the pool and the HCU floor (Figure 3-9) be also used for small structures at and above the HCU floor elevation. For flat structures higher than 26 feet and pipes higher than 28.5 feet above the initial pool surface the GESSAR-II specification is acceptable.

For structures above grated areas of the HCU floor, the pressures shown in Figure 3-10 may be multiplied by the ratio of grating open area to grating total area.

3.3 Loads During Fallback

During fallback the froth created after breakthrough falls back toward the pool bottom. All structures between the bottom vent and the HCU floor can experience loads as the mixture of air and water fall past the structure. Sections 3B.8.1.3, 3B.4.1.6 and 3B.6.1.7 of GESSAR-II specify for design purposes that the load on all those structures be based on a drag resulting from water flowing at 35 ft/sec which is the velocity resulting from a 20 ft free fall.

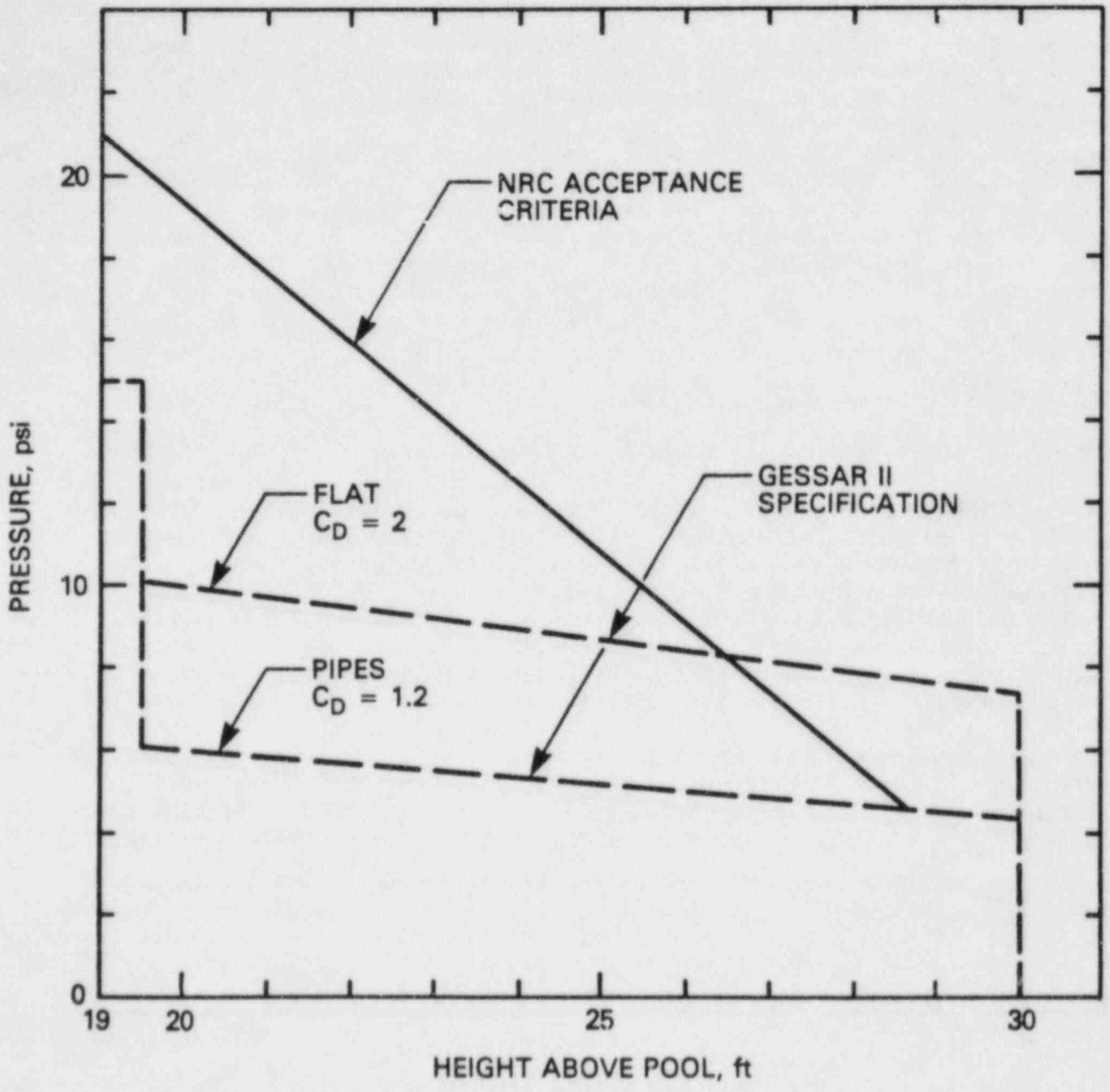

Figure 3-10 Comparison of NRC Acceptance Criteria with GESSAR-II for Froth Impact at and Above the HCU Floor

In the staff's judgment, the conservatisms associated with using the full water density and the upper bound of the velocity are sufficient to bound any of the forces that could result from the complicated process of fallback. The specification is therefore found acceptable.

3.4 Loads During Condensation Oscillation (CO)

Following the pool swell transient there is a period during which steam exits primarily from the top vents at mass fluxes from 10 to 25 lbm/sec/ft^2. During this period of high steam flow rate, the liquid-steam interface is located inside the suppression pool just beyond the top vent exit. Experiments indicate that the interface oscillates at frequencies ranging primarily from 3 to 20 Hz producing a cyclical loading on all submerged containment structures and boundaries due either to oscillations in flow or pressure, both of which decay in magnitude as a function of distance away from the top vent, or source. This CO phase persists for up to 1.5 minutes until the mass flux falls below the so-called chugging threshold level (i.e., 10 lbm/sec/ft^2). At this point, the relatively regular CO loads changes to the more stochastic, impulsive chugging phenomenon.

3.4.1 Loads on Submerged Boundaries

The design CO pressure loads for the submerged boundaries are specified in Sections 3B.4.1.5 (Drywell), 3B.5.1.9 (Weir Wall), 3B.6.1.9 (Containment) and 3B.7 (Basemat) of GESSAR-II. These loads were developed through a combination of scale model tests and analyses. The data base consists of measurements in three test facilities: the 1/9-area scale (Test Series 6003),[26] the 1/3-area scale (Test Series 5807),[27] and the full-scale (Test Series 5707)[28] Pressure Suppression Test Facilities (PSTF). The primary data base was obtained on the 1/3-scale PSTF while the 1/9-scale and full-scale data were used primarily for the confirmation of proposed scaling laws. In addition, the 1/9-scale PSTF was used to assess the importance of multiple-vent effects.

The most comprehensive set of tests was conducted in the 1/3-scale PSTF. These tests covered the full anticipated range of values of the several important parameters which influence CO loads (vent steam mass flux G, vent flow air content C_A, and bulk pool temperature T). Pressure measurements were made at numerous locations along the pool boundary: at the drywell wall, the containment wall, the basemat, and the weir wall. Using measurements from the 1/3-scale PSTF at the 2 ft. elevation on the containment wall, a regression analysis was performed to obtain empirical correlations for peak pressure amplitude (PPA) and CO frequency (f) of the form (GESSAR-3B0.3.2.1-31):

$$PPA_{1/3\ WALL} = C_1/G + C_2/(1 + C_A) + C_3T^2 + C_4T + C_5 \qquad (3\text{-}10)$$

and

$$f_{1/3} = C_6/G + C_7/(1+C_A) + C_8T + C_9 \qquad (3\text{-}11)$$

where C_1 through C_9 are the regression coefficients. These regression equations have been validated over the entire range of important parameters:

$$5 < G < 45 \text{ lbm/ft}^2\text{-sec}$$

$$0 < C_A < 0.16$$

$$90^\circ < T < 135^\circ F$$

To convert expressions shown as Eq. 3-10 and 3-11 to full scale, the following scaling laws are used for the peak pressure amplitude at the top vent and CO frequency.

$$PPA_{FS,\ VENT} = 0.8\ PPA_{1/3\ VENT} \tag{3-12}$$

and

$$f_{FS} = f_{1/3} * (d_{1/3}/d_{FS})^{\frac{1}{2}} \tag{3-13}$$

where d_{FS} and $d_{1/3}$ are the full-scale and 1/3-scale vent diameters. These scaling laws were derived by GE from an analysis based on first principles and confirmed by results from the three PSTF test series. Although we have some reservations concerning the analytical procedure, the final load specification can be justified entirely on the basis of experimental data as discussed below.

In order to use these scaling laws it is first necessary to determine the peak pressure amplitude at the top vent in the 1/3-scale PSTF. Because of the wide variability in pressure amplitude in the immediate vicinity of the top vent, source pressures are inferred from measurements at a remote location. A potential flow analysis (3B0.3.2.14-1) was performed to relate pressure at the 2-ft containment elevation to pressure at the top vent. This analysis yields the following attenuation relationship:

$$PPA_{1/3\ WALL} = 0.23 * PPA_{1/3\ VENT} \tag{3-14}$$

Combining equations 3-12 and 3-14, the following expression is obtained after the application of a 1.25 multiplier for conservation

$$PPA_{FS,\ VENT} = 5.5\ * \ PPA_{1/3,\ WALL} \tag{3-15}$$

Equations 3-13 and 3-15 are used to predict full-scale frequency and top vent PPA, respectively, from 1/3-scale PSTF test data. With the assumption that the functional dependence of frequency and PPA on G, C_A, and T is similar in all scales, Equations 3-13 and 3-15 then provide a means by which frequency and PPA in the 238 Standard Plant can be determined. Using these scaling relationships, the empirically determined functions of Equations 3-10 and 3-11, and the predictions of G, C_A, and T as functions of time during a DBA using the 238 Standard Plant Analysis[20] the CO forcing function is finally determined (GESSAR-II Subsection 3B.4.1.5).

$$P(\tau) = \frac{A(t)}{2}\ \{0.8 \text{ Sin } (2\pi\tau f(t)) + 0.3 \text{ Sin } (4\pi\tau f(t)) \tag{3-16}$$
$$+ 0.15 \text{ Sin } (6\pi\tau f(t)) + 0.2 \text{ Sin } (8\pi\tau f(t))\}$$

where

$P(\tau)$ = pressure amplitude (psid) for consecutive cycles beginning at time t = 3 sec and ending at T_{p_n}

$A(t)$ = peak-to-peak pressure amplitude variation with time (psid)

$$= 5.5\,[3.395 - 0.106t + 1.15 \log t - 7.987\,(\log t)^2 + 7.688\,(\log t)^3 - 1.344\,(\log t)^4]$$

$f(t)$ = fundamental frequency variation with time (Hz)

$$= 0.8\,[2.495 - 0.225\,t - 0.742 \log t + 10.514\,(\log t)^2 - 9.271\,(\log t)^3 + 3.208\,(\log t)^4]$$

t = time (sec), $3 \leq t \leq 30$, time from initiation of LOCA blowdown

τ = time increment for successive periods $T_{p_1} < \tau < T_{p_n}$

$T_{p_1} = \frac{1}{f(3)}$; where n is number of cycles between 3 and 30 sec

$$T_{p_n} = \frac{1}{f(3 + T_{p_1} + T_{p_2} + \ldots T_{p_{n-1}})} \qquad (3\text{-}17)$$

This forcing function attenuates as a function of distance away from the top vent in a manner predicted by the potential flow analysis. The distribution of loads thus determined is illustrated in Figure 3B-17 of GESSAR-II.

To account for the energy content of higher frequency components typically found in the PSTF data, three higher harmonics have been added to the load specification. To provide for additional conservatism, the design load was subjected to a 15% peak broadening.

The load specification described above relies largely upon data from the 1/3-scale PSTF. Confirmation of the 238 Standard Plant load specification was obtained by using both test results from the 1/9-scale and full-scale PSTFs, and a method of analysis termed the CO methodology. This refers to the procedure used to determine the load specification as described above. In this case, however, the analysis for predicting G, T, and C_A as a function of time uses the initial conditions for each test rather than the 238 Standard Plant DBA conditions. This results in a prediction of pressure amplitudes and frequency as a function of time during a particular test which can be directly compared to test measurements. Comparisons are made using peak pressure amplitudes (PPA), rms pressures (RMS), and amplified response spectra (ARS).* In

*The amplified response spectrum of a dynamic load represents the response of a single degree of freedom oscillator to this load. Such spectra are traditionally used to evaluate dynamic loading of structures, a notable application being earthquake analysis. The spectrum exhibits the excitation produced by the forcing function at different frequencies.

all scales, the predictions using the CO methodology generally exceed the measured values (3B0.3.2.13-13 to -94). More importantly, the load specification for the standard DBA bounded all measurements in which the break parameters (initial pool temperature, break size and relative humidity) were within the anticipated range for a standard plant.

In determining the CO load specification, it was assumed that multiple-vent effects were unimportant. This was confirmed by the 1/9-scale PSTF test results using 1, 2 and 3 rows of vents. These tests demonstrated that pressure magnitudes in the weir and suppression pool, characterized by average rms values, are lower in the multiple-cell configurations than in the single cell arrangement. Therefore, the omission of multiple-cell effects represents a slight conservatism.

In the course of the staff's review of this methodology, a number of concerns were identified regarding the adequacy of the load specification. In order to resolve these concerns, additional information was requested of the General Electric Co. The concerns which were raised and the responses obtained from GE are discussed individually below:

(1) The scaling analysis conducted by GE predicted that CO frequency would scale as the inverse of vent diameter. To provide some additional conservatism in this specification they used a scaling dependence of an inverse square root in the determination of the design load. To assess the accuracy of this prediction, GE compared the observed frequency in tests of all scales, to that which would be predicted using the CO methodology. This comparison is shown in Figure 3B.10(d)-5 of GESSAR II.

We were disturbed by two aspects of this comparison: first, all the full-scale measurements exceeded the predicted values, and second, the comparison consisted of only three full-scale data points. To resolve this concern, GE was able to demonstrate via their response to Question 3B.36 of GESSAR II that if the frequency of the four harmonic CO forcing functions was increased by 50% (a figure selected so as to bound the range of uncertainty), the predicted load is still bounded by the design load as confirmed by comparison of amplified response spectra (ARS). This was possible because of the 15% peak broadening which was incorporated into the initial load specification.

(2) Of all the test runs conducted in the full-scale PSTF, only two exhibited CO and were also properly instrumented for the analysis of CO. In order to compensate for the uncertainties associated with the small full-scale data base, GE provided added conservatisms such as the three added harmonics to boost the energy content of the load specification. In addition, despite the question raised in (1) above, the experiments on three scales provided some justification for the scaling laws. These two factors taken together were sufficient to convince the staff of the conservatism of the load specification.

(3) Because of the unique dependence of CO pressure amplitude and frequency on the various parameters, it seemed possible that the most severe loads might occur under conditions other than the standard DBA. For this reason, GE was asked to conduct a parametric study involving all relevant plant conditions and break sizes. By doing so, GE was able to demonstrate

via their response to Question 3B.37 of GESSAR-II that, with one exception, the standard DBA bounded all other possible accidents. This exception occurred during the initial phases of an SBA. It was further demonstrated, however, that the design load ARS exceeds the ARS of the SBA when considered over the entire period of CO except for frequencies below about 2 Hz, a range which GE states has no significance insofar as containment and equipment response is concerned.

(4) In response to a request for clarification regarding how the CO loads are developed (Question 3B.13 (C) of GESSAR-II), GE provided a number of comparisons between predicted and measured pressure responses. In some cases these comparisons revealed that the design loads did not always bound the measurements. In particular, exceedances at high frequency (above 20 Hz) were observed from full-scale tests, and at low frequency (below 3 Hz) during 1/3-scale tests. These potential nonconservatisms were addressed in a follow-up question (Question 3B.38 of GESSAR-II). GE was able to demonstrate that an excitation with frequency less than 3 Hz is not significant either for the containment or piping and equipment response. Further, GE was able to demonstrate that the exceedances at both high and low frequency could be bounded by other applied loading conditions (pool swell and chugging).

(5) Because the walls of the PSTFs are considerably more flexible than the walls of the 238 Standard Plant, there is the possibility that pressure amplitudes measured in the PSTFs might be influenced by fluid/structure interactions (FSI). If this were to result in a reduction in pressure amplitudes below that which would be observed in a rigid structure, then it would be necessary to compensate for this artifact when determining the design load.

At the request of the NRC staff,[29] the importance of FSI in the 1/9-scale and 1/3-scale PSTFs during CO was assessed by GE using coupled fluid-structure NASTRAN models with harmonic forcing functions imposed at the vent exits. The analyses yielded transfer functions relating pressure amplitude at the top vent to pressure amplitude on the containment wall for both rigid- and flexible-walled structures. The results of this analysis demonstrated that, although FSI effects are significant within the frequency range of interest, they tend to make the design load more conservative rather than less so, and therefore need not be considered.

This prediction was confirmed by comparing NASTRAN predicted transfer functions (south wall pressure/north wall pressure; see Figure B-1) to actual PSTF measurements. Although the trends predicted by the model were not evident in the experimental data, and despite enormous scatter in the data, it was clear that FSI plays little or no role in the test measurements. This was true for both the 1/3- and 1/9-scale PSTFs.

In view of the satisfactory resolution of the issues listed above, the staff finds the CO load specification to be acceptable. Although we continue to have some reservations concerning the correctness of the scaling laws proposed by GE, the design load contains sufficient conservatisms to compensate for these uncertainties.

3.4.2 Loads on Submerged Structures

The methodology for the calculation of condensation oscillation loads on submerged structures is presented in Section 3BL.2.6 of GESSAR-II. The methodology is fundamentally similar to that described in Section 3.2.5 for LOCA Bubble Loads. The major differences are:

(1) The oscillating steam condensation interface is represented by sources with their strength determined from Mark III 1/3-scale tests and with the frequency varied from 2 to 3.5 Hz.

(2) Only the acceleration forces are computed.

On the basis of concern expressed by the staff a justification for the source strength used is presented in Section 3BO.3.2.31(c.i) of GESSAR-II. The neglect of standard drag is justified on the basis of Mark I Acceptance Criteria[16] for all structures except the RHR test lines of 1.5 inch diameter. Standard drag will be calculated for those structures as in the Mark I procedure. The basis for this is presented in Section 3BO.3.2.31(c.ii) of GESSAR-II. The application of the loads to structures with sharp corners is subject to the same concerns that were expressed in Section 3.? 5 in connection with LOCA Bubble Loads. The use of an "effective cylinder" as in the Mark I Acceptance Criterion 2.14.4(2a)[16] is accepted as valid for Mark III in Section 3BO.3.2.31(c.iii) of GESSAR-II.

The 2 to 3.5 Hz frequency range of this load definition was chosen by GE because this range covers the primary frequency range of the CO phenomenon. This frequency range excludes the higher harmonics that were added to the wall boundary CO load definition (Section 3.4.1) for additional conservatism. To justify not adding any higher harmonics to the CO submerged structure load definition, GE provided an analysis[35] demonstrating that frequency components for submerged structures higher than 3.5 Hz are bounded by the pool swell submerged structure design load. The staff has reviewed this analysis and agrees with the GE conclusions. Thus, the 2 to 3.5 Hz frequency range is adequate and acceptable for use in the submerged structure load definition.

The staff finds the CO loading specification on submerged structures presented in Section 3BL.2.6 and 3BO.3.2.31(c) of GESSAR-II acceptable.

3.5 Loads During Chugging

When the steam flux through the top row of vents has fallen below about 10 $lb/ft^2/sec$, a transition from the relatively stable CO mode of steam condensation to the more erratic chugging mode is observed to occur. In this case, the steam-water interface does not remain attached to the top vent exit but intermittently collapses allowing suppression pool water to flood the vent and re-enter the weir annulus. An extended quiescent period then ensues until the gradual buildup of the drywell pressure forces the steam-water interface back into the pool, whereupon the cycle is repeated. These random, intermittent and highly impulsive motions create large pressure pulses within the top vent. These are transmitted to the suppression pool and weir annulus, thereby producing loads on both submerged boundaries and any structures as may be submerged within the pool.

3.5.1 Loads on the Top Vents

The loads on the top vents are specified in Section 3B.4.1.9.1 of GESSAR-II. The loads are of two types, a uniform pressure load which is to be applied to the inner cylindrical surface of the top vent as well as a total force acting vertically upward. The latter represents the imbalance in the inner pressure loading which is observed experimentally but is conservatively neglected when developing and applying the inner pressure loads. The two loads, which are applied concurrently, are specified in a dynamic fashion. The time dependence which is prescribed consists of a sequence of four triangular positive excursions from the zero load condition (relative to local hydrostatic). The amplitude, duration and interval between these pressure pulses varies with the first of these, in particular, exhibiting a roughly exponential decay. The overall duration of the pulse train is approximately 100 msec.*

Two values of peak pressure and force amplitude are prescribed depending on the intended design application. The higher of these (540 psid and 250 KIPS, respectively) are to be used for local design evaluation. That is, these higher loads would be applied to individual vents to determine, for example, the stresses in the vent lines. The lower values specified (214 psid and 91 KIPS, respectively) are used for global design evaluation. Thus, the load pulses defined with those lower amplitudes would be applied to all top vents simultaneously to evaluate, for example, piping and equipment response to chugging.

The basis for this load specification is the chugging data base selected from test runs 1 and 2 of the full-scale condensation test series 5707.[28] This data base consists of a total of 39 chugs.** The specified value of peak overpressure (540 psid) is equal to the highest pressure recorded within the top vent during these 39 chugs. The global value (214 psid) corresponds to the average of the 39 peak values. The specified value of peak force (250 KIPS) corresponds to the highest load deduced by spatial integration of all pressures (16) recorded inside the top vent for each of the 39 chugs. The global value is the average of the force computed for the 39 chugs.

The staff has reviewed the load specification and basis in detail and concludes that it represents a conservative loading suitable for the assessment of Mark III containment design and response to the chugging loads which would be experienced during a postulated LOCA. The load specification is therefore considered acceptable. The basis for the staff's conclusion is outlined below.

It was found during Test Series 5707 that the magnitude of the loads in the top vent was strongly influenced by pool temperature. The highest loads

---

*A prechug underpressure (half-sinewave) of amplitude 15 psi is also specified which approximately doubles the pulse duration.

**A total of 59 chug events were actually observed during these two test runs but 20 of these were excluded in developing the load specification. These occurred during the early stages of test 5707/1 and exhibited very low intensity pulses. It was speculated that this anomalous behaviour was due to the presence of non-prototypical concentrations of air in the steam. Accordingly, they were eliminated to provide added conservatism.

tended to occur at the lowest pool temperature. Although Test Runs 1 and 2 were conducted at temperatures well below that which is expected to occur during an actual LOCA, these runs were selected to provide the data base for the top vent chugging load definition. The staff estimates that this represents a conservative margin of about 100% for the mean pressure and 25% for the peak pressure.

A further conservatism in the specified pressure amplitude stems from the use of only the single highest pressure recorded during a particular chug from among all 16 pressure sensors to characterize the pressure for the entire vent. The staff estimates that this provides an additional margin of at least 15%.

The use of a triangular-shaped pressure and force pulse to represent the load transient is only an idealization. The actual traces differ significantly from these nominal forms. This difference also introduces a significant margin, as demonstrated by GE's response to Question 3B.18 of GESSAR-II. ARS comparison of the design vs. peak observed pressure signature indicates that the former exhibits significantly higher power (30-100% margin) over the entire frequency range of interest. The use of the mean value of all observed chugs for global design evaluation is reasonable given the experimentally demonstrated stochastic nature of the chug strength (3B0.3.2.17 of GESSAR-II). We do not expect all vents to experience the peak chug pulse simultaneously. Synchronous application of the mean chug strength at all vents represents, in our judgment, a reasonable but nevertheless conservative representation of the global loading likely to be experienced during a LOCA. Support for this conclusion stems from the 1/9-scale multivent test results[26] which show conclusively that the chugs in different rows of vents are not synchronized (3B0.3.2.16 of GESSAR-II).

In summary, the load specification represents a very conservative interpretation and application of data obtained under reasonably prototypical full-scale test conditions. The margins provided by this conservative definition are, in the staff's judgment, sufficient to bound any low probability, higher intensity loads that could be anticipated because of the stochastic nature of the chugging phenomenon.

3.5.2 Loads on Submerged Boundaries

3.5.2.1 Weir Annulus

Chugging loads on the weir annulus (weir wall, basemat and inside drywell wall) are defined in Section 3B.5.1.4 of GESSAR-II. The loading is qualitatively similar to the pressure pulse train prescribed for the top vent (Section 3.5.1) but with significantly lower amplitudes. The weir load also differs in that negative triangular pressure pulses are included in the pressure pulse train (Fig. 3B-46 of GESSAR-II). As was the case for the top vent pressure load, peak (43 psid) and mean (15 psid) pressure amplitudes are defined for use in either local or global design evaluation. In contrast to the top vent loading, the peak amplitudes vary spatially to reflect the experimentally observed attenuations. This spatial variation is shown in Figure 3B-50 of GESSAR-II. The highest amplitudes occur in the vicinity of the top vent and decaying to zero at the pool surface and to about 10% of the maximum at the basemat. In the circumferential direction, only the peak pressure is attenuated (to about 10% of maximum at a distance of 13 feet). No circumferential attenuation of the mean pressure amplitude is prescribed.

The basis for these loads is identical to that for the top vent loads (Section 3.5.1) since the weir annulus loads were also highest during the low pool temperature tests. Thus, the peak amplitude was taken equal to the highest pressure measured anywhere on the weir annulus during all chug events observed during Runs 1 and 2 of Test Series 5707.[28] The specified mean pressure amplitude represents the average of the individual peaks taken from the 39 selected chug events.

The staff has made a detailed review of the load specification and its basis and concludes that the specification generally provides a conservative representation of the loads which would be experienced by the weir annulus during the chugging phase of a postulated LOCA. Some potential non-conservatisms were identified. Their resolution, as well as the staff's basis for finding the load specification acceptable are enumerated below.

Generally speaking, the conservatisms cited in regard to the top vent load specification (Section 3.5.1) apply for this case as well. An additional conservatism relates to the spatial distribution which is employed. Figures 3B.41-1 through 4 of GESSAR-II which were prepared in response to the staff's Question 3B.41 show that the specified distributions would provide very substantial margin relative to the loads that would actually be experienced. The most significant conservatism, however, stems from the test facility configuration from which the data base was accumulated. As indicated in Appendix B, the full-scale PSTF represents a single sector of a Mark III containment wherein the planes of symmetry between two adjacent rows of vents are replaced by solid walls. It can be expected that the effect of such a simulation will be to maximize the boundary loads that will be observed since it corresponds to all vents chugging synchronously. Since the absence of synchronous chugging was demonstrated via the 1/9-scale multiple-vent tests,[26] and since the load specification calls for synchronous application of the loads, a substantial margin between design and actual loads can be anticipated.

The numerous conservatisms cited above provide confidence that the load specification is adequate to accommodate the single explicit nonconservatism which was identified during the staff's evaluation. We refer to the ARS comparison which was supplied by GE in response to the staff's Question 3B.18 of GESSAR-II (Figure 3B.18-3). This comparison between the design pressure signature and the pressure trace which gave rise to the peak observed pressure amplitude showed that the latter exhibits substantially higher power in the 20-30 Hz frequency range. The staff's concern regarding this exceedance was transmitted to GE via Question 3B.39 of GESSAR-II. Their response included the results of a structural evaluation of the weir wall which indicates that the frequency excursion does not affect weir wall integrity and that thermal stress is the bounding weir wall load condition. Based on these considerations, we find the proposed load specification to be acceptable.

3.5.2.2 Suppression Pool

The chugging loads on the suppression pool boundaries are defined in Section 3B.4.1.9.2 of GESSAR-II. In this case, a pressure signature consisting of a pre-chug expansion (half sine wave) followed by a chug spike (triangular positive pressure pulse) followed by a post-chug oscillation (damped sine wave) is specified (Figure 3B-27 of GESSAR-II). The peak amplitudes of the three segments of the wave form vary depending on design application (local vs

global), and location (spatial attenuation). The duration of the chug spike and the frequency of post-chug oscillation also vary according to boundary location. The specific values are given in Table 3B-4 and Figures 3B-28 through 3B-35 of GESSAR-II.

The basis for this load specification is the chugging data base derived during Test Runs 11 and 12 of the full-scale PSTF chugging test program (5707).[28] [These test runs correspond to high initial pool temperature during which the highest loads on the pool boundaries were found.] The peak values specified for design correspond to the highest value observed during the 113 chugging events which occurred during these tests while the specified mean values represent the average.

The staff has reviewed the specified loading and its basis and concludes that the design loads provide a conservative representation of the loads that can be expected to occur during the chugging phase of a postulated LOCA and is therefore acceptable. The staff's basis for its conclusion is given below.

The conservatisms cited in earlier sections (3.5.1 and 3.5.2.1) are also applicable here. The use of the high temperature results from Test Series 5707[28] is of particular significance. The pool temperature during the selected tests was well above that which would be expected during the entire LOCA blowdown (see Figure 3B.1(D)-3 of GESSAR-II). This implies margins on the order of 50% or more for both peak and mean values (see Figure 3B.1(D)-4 of GESSAR-II).

The margin provided by the idealized representation of the pressure spikes is even more substantial than for the top vent load. In terms of the power contained by the pressure wave form as reflected by its ARS, the margin varies from 100 to 200% for frequencies up to about 100 Hz (Figure 3B.18-2 of GESSAR-II).

The information supplied to the staff by GE also provides confirmation that the use of the mean values can be justified quantitatively. In response to the staff's Question 3B.16 of GESSAR-II, GE developed estimates of the excitation that would be produced on the Mark III containment when the peak chugging loads occurred at all vents but with the nonsynchronous behavior exhibited during the multiple vent tests.* This excitation was compared to that produced by the design global load. The latter was found to exceed the Monte Carlo results by a factor of at least two and as much as four throughout the frequency range of interest (see Figure 3B.16-5 of GESSAR-II).

In view of these considerations, the staff has concluded that the load specification is conservative and acceptable.

3.5.3 Fluid/Structure Effects During Chugging

The effects of FSI in the full-scale PSTF during chugging were assessed in two ways. First, a single degree-of-freedom model was used[29] in which the chugging forcing function is applied to a three-element system composed of the test facility mass, the mass of the surroundings, and the structural compliance. GE concluded from this model that FSI has about a 20% effect (nonconservative)

*Monte Carlo simulation was employed to develop chug intervals between vents.

on the pressure spike and a 10% effect (conservative) on the peak underpressure. These effects were deemed to be of limited value in view of concerns associated with the model.

In response to questions from the staff, GE prepared a second model employing a three-dimensional compressible fluid dynamic analysis of the full-scale PSTF suppression pool (3B0.3.2.24-1 to -12 of GESSAR-II). Results in the form of calculated responses to simulated chug forcing functions were subsequently compared with measured chug pressures. By this analysis, GE found that the effect of FSI on the measured chug pressures is generally small except on the drywell wall and that the effect of FSI is to make the load specification more conservative. They further demonstrated that the post-chug oscillation is a response of the test facility and is therefore unlikely to be found in the standard Mark III plant. Inclusion of the post-chug oscillation in the chug load specification may therefore be regarded as a source of conservatism.

The staff is satisfied with GE's assessment of FSI in the full-scale PSTF. It was demonstrated that FSI does influence the measurement of chugging pressures in the full-scale PSTF but since the effect is to amplify the measurements, there is no need to alter the load specification.

3.5.4 Loads on Submerged Structures

The methodology for the calculation of loads on submerged structures during chugging is presented in Section 3BL.2.8 of GESSAR-II. This methodology is based on a simplified superposition of acoustic pulses arriving at the structure. The pulses that could arrive within their own pulse-width are taken as simultaneous and in the same direction. The force is computed by applying, in effect, twice the total pulse pressure difference across the structure. The pulse strengths are based on experimental chugging data.

The staff expressed concern that the pulse strength chosen did not bound the highly stochastic data and could thus have a high probability of being exceeded at some vent during a LOCA. Because of the local nature of loads on submerged structures, no advantage could be taken of averaging source strengths over several vents. The concern was addressed in Section 3B0.3.2.31(d) of GESSAR-II, in a formal response to Question 3B.43. The essential conclusion of the above justification is that while the source strength chosen does not bound all the chugging data, the simplified formulation of the resulting force has a conservatism of at least a factor of 2.5. This factor holds for a 2 ft diameter cylindrical structure and is even larger for smaller structures. If one used this factor to increase the "effective" source strength, the calculated pressures bound all the chugs except for one chug at one pressure measurement location.

The staff feels that because of additional conservatisms associated with the procedures by which forces originating from different vents are summed, the issue of additional extrapolation of data to a low exceedance probability during a LOCA need not be considered. The specification is therefore found acceptable by the staff.

3.6 Loads During Drywell Depressurization

3.6.1 Drywell Wall

Following a LOCA, the Emergency Core Cooling System (ECCS) will be required to provide the necessary water to refill the reactor pressure vessel. The suppression pool water used by the ECCS will eventually cascade from the break into the drywell and begin condensing the steam. The condensation will cause a rapid depressurization of the drywell, thus drawing noncondensable gas from the containment free space via the drywell vacuum breakers. A conservative bounding end point calculation was performed for design purposes which assumed that the noncondensables did not return to the drywell through the vacuum relief system. The details of the calculation are presented in Attachment G of Appendix B to GESSAR-II.

The scenario chosen for the drywell negative pressure calculation begins with the air initially in the drywell being completely purged into the containment at the time of the steam condensation in the drywell. The maximum containment pressure, neglecting vacuum relief, is then calculated for the post-blowdown period assuming 100% relative humidity and a final containment temperature equal to the suppression pool temperature of 170°F. To evaluate the minimum drywell pressure at this time, it is assumed, in addition to the above assumptions, that all steam in the drywell is instantaneously condensed and that the ECCS flow out of the vessel is also at a temperature of 170°F. The negative pressure load across the drywell wall is then equal to the difference between the pressures of the containment and the drywell. The above calculation yielded a drywell-to-containment negative pressure differential of 21 psi. The staff has reviewed the calculation and finds it acceptable based on the conservative nature of the assumptions.

3.6.2 Weir Wall

The reflood phenomena described above also gives rise to inward acting impingement loads on the weir wall. The loads are a result of the drywell-to-containment negative pressure difference acting on the suppression pool water causing it to flow through the vents into the weir annulus. Eventually, the water will overflow into the drywell until the top row of drywell vents are cleared allowing direct communication between the containment and drywell volumes until the air flowing through the vents and the vacuum breakers equalizes the pressure difference prior to vent clearing, thus terminating the vent backflow transient.

To evaluate the weir wall loads during this transient, a simple steady-state flow analysis was performed to determine the flow velocities in the vent system. The details of the calculation can be found in Attachment J to Appendix 3B of GESSAR-II. The calculation described the pressure losses associated with three flow paths of the Mark III vent system utilizing the loss coefficients from Idel'Chik.[30] The simultaneous solution of these equations yielded vent velocities of the order of 40 feet/second assuming that the 21 psi differential existed between the drywell and containment. The impingement force on the weir wall is then obtained from a simple jet analysis which assumes that the force on the wall corresponds to a complete change of the horizontal momentum of the water flowing through the vents. A force of

12,800 lbf per vent, applied over the projected circular area of the vents, was calculated for the top vent and used to bound the forces corresponding to the lower vents. The staff has reviewed the above specification and finds it acceptable based on the conservatism inherent in the bounding calculation.

3.6.3 Structures Above the Weir Annulus

3.6.3.1 Weir Annulus Escape Velocity

Two velocities are of interest. One is the transient velocity of the water surface as it first rises from the weir annulus into the drywell. This velocity, which GESSAR-II has designated the jet front velocity, is of interest for determining impact loads on structures above the weir wall. After the initial entry of the jet into the drywell, the flow continues to accelerate until it reaches a steady-state velocity corresponding to the (constant) imposed pressure differential. This velocity is used to determine the drag loads on the structures.

The GESSAR-II specification for the jet front velocity is presented in Section 3B.5.1.5, with Figure 3B.52a showing its variation with height above the top of the weir wall. The jet front velocity was obtained by a simplified one-dimensional analysis. A constant pressure differential was imposed and the decelerating effects of gravity were included.

The staff has reviewed the analysis used for the jet front velocity and has concluded that, on the basis of conservative assumptions with regard to frictional losses and the imposed pressure differential, the resulting velocities are conservative (high) except very near the weir wall. Thus, the staff finds the specification (in Figure 3B-52a) acceptable, with the stipulation that V=4 ft/sec whenever the Figures shows V<4 ft/sec.

With regard to the steady-state velocity needed for drag computations, GESSAR-II stipulates the velocities presented in Figure 3B-52. The velocity at the entrance into the drywell, i.e., top of the weir wall, is 30 ft/sec. The flow is then decelerated by the effects of gravity until it comes to rest at 14 feet above the wall. This velocity was calculated using the drywell depressurization time-history shown in Figure 3B.51. This pressure transient, in turn, was calculated from a mass of energy balance of the drywell steam, vessel reflood break flow, vacuum breaker flow, and suppression pool flow over the weir wall. The calculation conservatively assumed thermodynamic equilibrium in the drywell as well as no heat transfer to the drywell wall, the vessel or the biological shield wall. In addition, no vent entrance or vent friction effects were included. Based on the conservative nature of the calculation, the staff finds the above specification acceptable.

3.6.3.2 Impact Loads

As the water slug rises from the weir annulus, it may impact on drywell structures in its path. The original GESSAR-II did not contain an impact specification, but in response to NRC Question 3B.30 (see GESSAR-II Section 3B.3.2.30) an impact specification was included in Revision 2. This revised specification (Section 3B.5.1.5 of GESSAR-II) corresponds to the Mark II acceptance criteria for impact[12], with one important exception. Whereas the Mark II acceptance criteria stimpulate a flat pool at impact, the present specification assumes a

curved pool with impact durations obtained from the PSTF tests: 6.8 msec for radial structures and 2.0 msec for circumferential. (Note that flat pool impact results in the shortest pulse durations and largest stresses in the impacted structures.)

Since the staff has accepted the basic Mark II impact methodology, the review focused on the acceptability of the pulse durations proposed in GESSAR-II. No quantitiative justification is offered for these pulse durations except for the statement that "...jet will have a curved surface due to the viscous drag of the drywell wall and the jet pressure gradient..." The staff is unable to accept this justification for the pulse duration. However, the staff concedes that the jet front will not be flat once it leaves the weir annulus. (If the pool were flat, the stresses due to impact could be several times greater than predicted by the GESSAR-II specification.)

The staff contends that the jet front will not be flat, basically because of the effects of gravity. Once the jet rises above the weir wall, gravity will induce a lateral velocity from the wall toward the center of the drywell. This problem could, of course, be analyzed numerically by any of the free-surface computer codes (e.g., FREESURF [32]), however, that seems to be unnecessary. The problem at hand has a similarity to the "dam break problem," which has already been worked out with these codes. The differences are: (1) in the problem at hand, water is not initially at rest but is being accelerated upward, and (2) the "dam" is not removed instantaneously but, rather, as if it were gradually lowered into the ground. The first difference, the effect of the acceleration, can be neglected because consideration of additional acceleration beyond the 32.2 ft/sec^2 can only enhance the lateral velocities. The second difference will be addressed below.

The lowest impacted structure above the weir annulus in the 238 Standard Plant is 0.25 feet above the weir wall. This is the location where flat pool impact is most likely to occur. Thus, the height of our hypothetical dam is 0.25 feet. From the jet front velocity in Figure 3B-52a of GESSAR-II, the velocity at this height is 4 ft/sec and its takes approximately 0.12 seconds to reach it. We are now interested in the jet front inclination at 0.12 sec after leaving the weir annulus. The profiles of the water surface for the dam problem, after breakage of the dam are available in nondimensional coordinates in the open literature (e.g., see Figure 7 in Ref. 26). As time progresses, the horizontal water surface initially upstream of the dam, assumes a progressively greater slope. We must now address the second difference between the dam breakage problem and the problem at hand: our dam "recedes" into ground in 0.12 sec instead of being removed instantaneously. To compensate for this difference, we chose to look at the water surface profile at 0.06 sec, which is half the time that would be appropriate if the wall were removed instantaneously. Using 0.06 seconds, in conjunction with the curves in Ref. 26, the jet front curvature at the time of impact results in a pulse duration of approximately 20 msec for structures that span the weir annulus. This is about 3 times greater than the pulse duration of 6.8 msec proposed by the GESSAR-II. However, the shape of the pressure pulse from this type of impact is expected to be quite different than the versed-sine shape in GESSAR-II.

The shape of the pressure pulse was estimated from the profile of the jet front at the time of impact. It was found to have a high impact pressure

initially, with a gradual decrease followed by an elongated tail. Thus, even though the total pulse duration is 20 msec, most of the impulse was absorbed in a much shorter time. In comparing the stresses that would result from application of this pulse and the GESSAR-II specification, it was found that below structural natural frequencies of 200 Hz, the GESSAR-II specification is conservative. Above 200 Hz, the stresses using the "dam break" jet fronts were somewhat higher. At natural frequencies greater than 500 Hz the stresses must be multiplied by a factor of 1.8. Between 200 and 500 Hz a linear interpolation of the multiplier is required.

For radial structures 1 foot and higher above the weir wall, an analysis similar to the one above, showed that the GESSAR-II specification overpredicted the stresses.

The above discussion applies only to structures with a radial orientation, since the surface inclination is in that direction. The Standard Plant also has numerous structures with circumferential orientation above the weir annulus. For impact on these structures, GESSAR-II stipulates a pulse duration of 2.0 msec (from PSTF data). The staff has compared this value against flat-pool pulse durations derived from Mark II acceptance criteria and found that, for the specific circumferential structures above the weir annulus in the 238 Standard Plant, the flat-pool pulse durations were greater than 2.0 msec.

The staff finds acceptable the GESSAR-II impact specification on structures above the weir wall, with the exception of radial structures within one foot of the top of weir wall. The stresses in these structures must be increased by a multiplier. This multiplier is 1.0 when the natural frequency of the structure is less than 200 Hz, 1.8 when the natural frequency is greater than 500 Hz with a linear ramp between these values.

For structures located between zero and 0.25 feet above the wier wall, flat pool impact should be considered (e.g., the acceptable criteria in Section 2.7 of Appendix A, NUREG-0661 is appropriate for flat pool impact). The velocity at impact for these structures shall be taken at 4 ft/sec. There are no structures that fall into this category in the standard plant design.

3.6.3.3 Drag Loads

Following jet front impact, the structures above the weir wall are subject to drag forces. The velocities associated with the drag forces (Figure 3B-52) may be considerably higher than what was used for impact because the flow continues to accelerate until it reaches a steady-state value (30 ft/sec at the top of the weir wall). The GESSAR-II specification for drag (Section 3B.5.1.5) uses the conventional drag formula with a constant drag coefficient of 1.2 for circular cylinders. Noncircular structures are handled by using the same drag coefficient in conjunction with an "equivalent" diameter circular cylinder. For I-beams, for example, the "equivalent" diameter is equal to $\sqrt{2}$ times the diameter of circle which circumscribes the cross-section of the I-beam.

The staff's comments on this specification are as follows: Although the drag coefficient on circular cylinders can exceed 1.2, this occurs at very low Reynolds numbers where drag would be negligible for any structures of practical

interest. Thus, $C_D = 1.2$ is acceptable for pipes. The use of "equivalent" diameter for noncylindrical structures is also acceptable since it overpredicts the actual drag by a small amount for I-beams, which are the only noncylindrical structures above the weir annulus in the Standard Plant.

The staff has concluded that the drag specification on structures above the weir wall is acceptable.

3.7 Other Primary Loads

3.7.1 Weir Wall Pressure Loads During High Vent Flow

Once the vents have been cleared of water, a relatively high flow rate of an air/stream mixture is established through the weir annulus and the vents. During this period the static pressure level in the weir annulus drops below the supply pressure which prevails inside the drywell, in general, and on the inner weir wall, in particular. This outward pressure differential is specified for design purposes to be 10 psid and to prevail for 30 seconds (Section 3B.5.1.3, GESSAR-II). The basis for this load specification is an analytical model developed by GE.[20]

The staff has reviewed the available information related to this load and conclude that the load specification is conservative and therefore acceptable. The basis for the staff's determination is as follows.

A very conservative intepretation of the 1/3-area scale test data base[9] indicates that the outward Δp likely to be experienced under prototypical DBA LOCA conditions will not exceed about 4 psi. The large margin (a factor of 2-1/2 or better) provided by the design specification is not surprising in view of the conservatisms employed by the analytical model (Appendix D). On the other hand, the static manner in which the load is applied degrades the margin substantially since the actual load is dynamic in character (a quasi-triangular spike with duration of about two seconds). However, since the worst possible combination of load duration and structure frequency imply a Dynamic Load Factor (DLF) not exceeding 2, the actual margin could not be reduced to less than 25%. It is the staff's judgment that this is adequate to account for any other uncertainties that may prevail (e.g., scaling inconsistencies in the 1/3-scale tests - see Section 3.2.1).

3.7.2 Asymmetric Loads During Pool Swell

An asymmetric load on the entire containment system is specified in Section 3B.6.1.3 of GESSAR-II. This is to account for the possibility of circumferentially non-uniform venting of the air/stream mixture from the drywell. The specification assumes that the dynamic pressure loads associated with initial bubble formation (Section 3.2.3) apply on 180 degrees of the system while the net dynamic load on the other 180 degrees is zero. As is the case for normal pool swell, this load is to be applied dynamically (Fig. 3B-11 of GESSAR-II).

The dynamic loading distribution is obviously conservative and therefore acceptable to the staff.

3.7.3 Thermal Loads

3.7.3.1 Suppression Pool Thermal Stratification

In the event of a postulated LOCA, the suppression pool water in the immediate vicinity of the vents is heated due to the energy release during the steam condensation portion of the transient. For the Mark III horizontal vent configuration, the majority of mass and energy is transferred to the pool through the top vents. Consequently, the upper portion of the suppression pool is heated more than the lower portion. Although turbulence and the large scale mixing induced by chugging tends to smooth out these gradients, experiments indicate that some thermal stratification will persist throughout the LOCA blowdowns. Structures which are exposed to this temperature gradient will experience thermal stresses due to non-uniform heating. A prime example of such a structure is the steel suppression pool liner with which Mark III plants are equipped.

The design temperature profile to be used for structural evaluation is specified in Section 3B.6.5 and its basis discussed in Attachment I of Appendix 3B of GESSAR-II. The profile is determined from

$$T_i = T_o + \varepsilon_i \, (\overline{T}-T_o)/\eta_i \qquad (3\text{-}18)$$

where T_i is the average water temperature in the ith horizontal layer or segment of the suppression pool, η_i is the height of this segment expressed as a fraction of overall pool depth, and ε_i the corresponding fraction of total blowdown energy Q.

The latter defines the bulk temperature $\overline{T}$ from

$$\overline{T} = T_o + Q/m_p c_p \qquad (3\text{-}19)$$

where m_p is the total water mass, c_p the specific heat and T_o the initial pool temperature. The values of η_i and ε_i are to be taken as follows:

i = 1 (uppermost segment)	η_i = 0.2	ε_i = 0.23
i = 2	0.2	0.23
i = 3	0.2	0.22
i = 4	0.2	0.20
i = 5 (lowest segment)	0.2	0.12

The basis for this energy deposition distribution is the temperature data recorded during the 2.5 inch venturi liquid blowdowns conducted during the 1/3-area scale test series 5807.[27] The thermal stratification observed under these conditions was the most severe both in terms of overall temperature difference (57°F) and gradient (about 7°F per foot). Note that for structural evaluation, the temperature gradient is the relevant parameter. The staff has reviewed this specification and the basis from which it was developed and concludes that the proposed temperature profile conservatively represents the

thermal environment which will be experienced by the Standard Mark III containment during all postulated LOCA events. The basis for the staff's conclusion is outline below.

It was found in Test Series 5807 that the degree of thermal stratification was strongly influenced by the blowdown mass/energy rate addition to the simulated drywell. The greatest stratification tended to occur at the higher rates. Over the range tested, the stratification varied from a low of 20°F to the maximum cited earlier (57°F). Since this result was obtained with a blowdown rate corresponding to about a 140% DBA*, use of this data to develop the design profile is clearly conservative for a DBA LOCA provided the applicability of the 1/3-area scale data for full scale can be demonstrated. This concern and its resolution will be discussed next. Finally, the suitability of this same profile for other postulated LOCAs (IBA, SBA) is examined.

The concern relating to scale arises due to the possibility of nonprototypical pool mixing caused by the distorted geometry scaling (i.e., shortened horizontal pool length). In response to the staff's question concerning this issue (see Attachment O of GESSAR-II, Question/Response 3B.28), a numerical analysis was performed by GE to provide additional insight and justification. The study utilized the RELAP4/MOD5 thermal hydraulics computer code. The code was applied first to the 1/3-area scale Test Run 5807/22 to verify the RELAP code could adequately predict the PSTF results. Reasonable agreement between the results and the PSTF data was achieved with the agreement improving with time. Then to investigate and confirm that the RELAP model could be scaled up, the model was applied to the full scale test 5707/1. In a similar manner, the PSTF data was again reasonably well predicted by the model. The next step in the study consisted of running a hypothetical full-scale PSTF case having a blowdown flow rate and energy flux three times that of the 1/3-area scale test 5807/22 in order to simulate a prototypical full-scale PSTF case. A comparison of these two simulations having prototypical blowdown energy addition per pool mass was then made to assess the effect of the distorted geometry on the stratification. The results indicated that the 1/3-scale distorted geometry stratification is similar to the full-scale thermal stratification with the 1/3-area scale having greater stratification than prototypical at later times in the transient.

Experimental confirmation for this trend of increasing stratification with decreasing scale is provided qualitatively by a comparison of the 1/9-area scale test results[26] with the 1/3-area scale results. Although data scatter prevents making quantitative statement, it is clear from a careful examination of the test results that the stratification in 1/9 scale is no less and probably greater than any observed in 1/3 scale particularly in terms of temperature gradient. Since this result was obtained with a relatively low blowdown flow rate (2.5-inch venturi steam vs. 2.5-inch liquid and 3.0-inch steam in the 1/3-area scale tests), it would appear that the inverse trend of stratification with scale is sufficiently strong to overcome the opposing trend with blowdown

---

*As noted in Reference 9, simulation of a BWR/6 recirculation line break requires use of a 2-1/8-in. venturi. In the worst case test discussed here a 2-1/2-in. venturi was used so that in terms of break size the blowdown rate is $(2.5/2.125)^2 = 1.4$ times greater than prototypical.

flow rate. Accordingly, it is concluded that the analytically derived trend is correct and that the use of the energy deposition distribution derived from 1/3-area scale provides a conservative representation for the DBA LOCA.

To justify the use of the same temperature profile for a long-term LOCA (SBA, IBA), GE performed an additional RELAP calculation in which a prototype Mark III IBA was simulated (also Question/Response 3B.28). The simulation was performed using standard licensing assumptions but without the effect of vent interactions during chugging and RHR operation. Both of these effects contribute to mixing in the suppression pool so that their neglect can be considered a significant conservatism. The results showed that the maximum stratification in this case was bounded by the specified temperature profile. The staff therefore concludes that the specification is applicable and acceptable for all postulated LOCA events.

3.7.3.2 Top Vent Temperature Cycling

During the chugging portion of the condensation transient, the vicinity of the top vent experiences a cyclic temperature variation brought about by the fluctuating steam-water interface. The top vent cycle fluid temperature time-history and its area of application were derived from the full-scale Test Series 5705 and are discussed in Section 3B.4.6 of GESSAR-II.

The shape of the cycling fluid temperature history as shown in Figure 3B-39 of GESSAR-II is derived from a statistical analysis of the response of a temperature sensor located 1 foot into the pool along the top vent centerline for the 185 temperature cycles observed in full-scale Tests 1 through 6. The relative time durations of the plateaus obtained in this manner were then conservatively adjusted by doubling the amount of time the structures are exposed to the steam temperatures. The profile cycles from a maximum temperature of 230°F to a minimum temperature of 100°F over the period equal to the chugging period which randomly varies from 1 to 5 seconds. The maximum temperature of 230°F is the maximum steam temperature entering the pool during chugging in the full-scale Test Series 5707, whereas, the minimum temperature of 100°F corresponds to the minimum vent temperature observed during chugging for runs having an initial pool temperature of 70°F. The design methodology specifies that this ΔT amplitude should be reduced due to bulk pool temperature increases during the transient. Therefore, the bulk temperature, which is a conservatively low estimate of the temperature in the vicinity of the vents, is used as the lower fluid temperature in the thermal cycling specification. This specification is applied to all areas where cyclic conditions are expected.

The areas of application of the cycling temperature profile as derived from the full-scale Test Series 5707 are the following:

1. A 4-foot horizontal band on the weir wall and inside drywell

2. The upper inside vent surface (top vent only)

3. An area of the outside drywell wall just above each top vent as shown in Figure 3B-39 of GESSAR-II.

The areas of application as shown in Figure 3B-39 were determined from a series of level conductivity probes located in the weir annulus, top vent and pool and bound all observations of steam-water interface travel in both the full-scale (Test Series 5707)[28] and 1/3 area-scale (Test Series 5807)[27] test series.

Additional information concerning both the cycling fluid temperature history and its area of application can be found in Attachment O to Appendix 3B of GESSAR-II. More specifically, the information is contained in Responses 3.B.25 through 3.B.27 to the staff's questions concerning the above methodology. Based upon the prototypical nature of the full-scale chugging transient coupled with the conservatisms associated with the specification of the load, the staff finds the above methodology acceptable.

3.7.4 Intermediate (IBAs) and Small Break Accidents (SBAs)

In general, the magnitude of dynamic loading conditions associated with a LOCA decrease with decreasing break size because of the lower drywell pressurization rates. The only LOCA-related hydrodynamic loads from an IBA or SBA that are equal in magnitude to those loads assocated with a design-basis accident (DBA) are CO and chugging loads. The duration and timing of those loads for IBAs or SBAs, as well as combining them with other phenomena (e.g., the IBA is examined in conjunction with actuation of the Automatic Depressurization System) is different from the DBA case. These features are defined in a series of loading charts such as those cited above (Figures 3B-36, 44, and 65 for IBA; Figures 3B-37, 43, and 66 for SBA of GESSAR-II).

The staff has reviewed the information described above and concludes that the loads which are prescribed for IBAs and SBAs are acceptable. The basis for this conclusion is enumerated below.

The conditions that govern the load characteristics of CO and chugging loads were detailed in Sections 3.4 and 3.5, respectively, of this report. For IBAs and SBAs, the range of parameters that control the load characteristics of CO and chugging phenomena are within the parameter ranges used by GE to arrive at the load definitions for these loads. Therefore, we conclude that the magnitude of CO and chugging loads for IBAs and SBAs will be equal to or less than the magnitude of the loads following a DBA.

The timing and duration of CO and chugging loads during IBAs and SBAs are dependent on the mass and energy release from the break in the primary system. We conclude that the release rates have been conservatively calculated by GE and that the duration and timing of these loads are acceptable.

The combination of IBA and SBA LOCA-related hydrodynamic loads with other phenomena has been performed by GE using acceptable procedures, i.e., single-failure criteria, system characteristics (e.g., ADS actuation), and 10 CFR Part 50 requirements (e.g., seismic accelerations).

3.8 Secondary Loads

3.8.1 Sonic Wave

Immediately following the postulated instantaneous rupture of a large primary system pipe, a sonic wave front may be created at the break location and propagate through the drywell to the vent system. This phenomenon is neglected on the basis that the finite opening time of a real break coupled with the rapid attenuation with distance and short duration produces an insignificant loading in the drywell. The staff concurs with this assessment and concludes that the sonic wave load may be considered negligible.

3.8.2 Compressive Wave

The rapid compression of the drywell air could result in a compressive wave in the weir annulus water. The wave if produced would then travel down the weir annulus, through the vents, and through the pool to the containment wall. This phenomenon is not included in the Mark III containment design on the basis that the approximately 20 psi/sec pressure rise rate in the drywell is not sufficiently rapid to generate a significant compressive wave in the water. In addition, even if a wave were generated, the subsequent attenuation of the wave as it crosses the 18.5 feet wide suppression pool would lead to insignificant containment wall loads. It is also concluded in Section 3B.8.1.6 of GESSAR-II from an examination of applicable PSTF data that compression wave loads on structures in the suppression pool are significantly smaller than loads caused by the water jet for structures close to the drywell and therefore they are not included as design loads. Based on these considerations, the staff concludes that compression waves may be considered negligible.

3.8.3 Water Jet Loads During Vent Clearing

During the initial phase of pool swell, water in the weir annulus is expelled through the vents into the suppression pool. The resulting water jets and their induced flowfield could potentially produce loads on submerged structures in the vicinity of the vents.

Significant loads on submerged structures due to the initial water jets are confined to regions either directly within or very near the jet paths. A conservative estimate based on experimental data[31] yields a zone of influence within which these loads could be significant. Section 3B0.3.2.31(a) of GESSAR-II shows that for Mark III plants only small portions of the S/RV quenchers lie within these zones of influence and that at these locations the loads are bounded by the subsequent air bubble loads. Therefore, no water jet load is specified. The staff finds this acceptable.

3.8.4 Fallback Loads on Containment Boundaries

The staff has examined the potential for "water hammer" type loads during the fallback of the suppression pool. Such loads could occur if the water slug remained intact during this phase. All available experimental evidence accumulated during the Mark I and Mark II containment loads programs, however, suggest that the fallback process consists of a relatively gradual settling of the pool water as the remaining air "percolates" upward. Careful examination

of pool boundary pressures from the Mark III PSTF confirms the absence of any large overpressures during the fall back phase. The staff concludes that fallback loads on the containment boundaries, if they occur at all, are small and need not be considered for design evaluation.

3.8.5 Impact Loads During Fallback

For the same reasons discussed in Section 3.8.4 above, intact water slug impact on any structures between the bottom vent and the HCU floor is not expected to occur during fallback. Some potential for froth type impact does exist. However, as indicated in Section 3.3, the drag loads which are specified by the GESSAR-II methodology, because of the conservatisms which are employed, represent the bounding design load. Thus, froth type impact loads need not be considered in the Mark III containment design evaluation.

3.8.6 Post-Pool Swell Waves

Following the pool swell process, the surface of the suppression pool assumes an agitated state consisting of pool wave action. Visual observations of PSTF tests indicate that these waves have peak-to-peak amplitudes of less than two feet. Since these wave heights do not generate significant containment loading conditions, the staff considers a separate wave load specification unnecessary.

3.8.7 Asymmetric Chugging Loads

The methodology of GESSAR-II does not include the specification of an asymmetric chugging load to account for the possibility that either chugs of unequal strength occur on opposite sides of the containment or that they occur in a nonsynchronous manner. The staff via its Question 3B.42 requested justification for the absence of such a loading on the containment and GE's response to these requests have satisfied the staff that it is justified. The basis for this conclusion is as follows.

GE's approach to eliminate the concern identified above was to generate, by means of Monte Carlo simulation, a realistic but nevertheless conservative estimate of an asymmetric chugging load on an actual Mark III containment. In generating these simulations, random variation of both the time of chug occurrence at the various vents, as well as chug amplitude, were employed. For the former, time windows taken from the 1/9-scale multivent tests were employed. For chug amplitude, only values of peak pressure ranging from mean to maximum observed were utilized. The sensitivity of the results to choice of time window was examined and the worst case value (80 ms) was employed in the simulations.

The results of these simulations were displayed as the ARS of the x and y overturning moments acting on the containment and compared with that corresponding to the asymmetric pool swell loads (Figures 3B.42.1 and 3B.42.2 of GESSAR-II). The results demonstrated unequivocally that the pool swell asymmetric load represents the bounding design load. This is true even if the chugging excitation is combined with the excitation induced by a single SRV actuation and seismic loading (see Figures 3B.42.1 and 3B.42.2).

Thus, the asymmetric chugging load is considered a secondary load since it is bounded by another design load and need not be considered in the Mark III containment design.

4 CONCLUSIONS AND IMPLEMENTATION OF GUIDELINES

The staff and its consultants have reviewed the Mark III containment LOCA-related hydrodynamic loads criteria contained in Appendix 3B of GESSAR-II and conclude that, with a few exceptions as noted, these load specifications provide conservative loading conditions. The staff's acceptance criteria for LOCA-related hydrodynamic loads are contained in Appendix C of this report.

The loads definitions presented in this report were based on the physical characteristics of the standard GESSAR-238 Mark III containment design detailed in the GESSAR-II document. However, the conservative assumptions used in developing these loads definitions and the minor deviations from the standard design seen by the staff to date should make the loads definition acceptance criteria contained in Appendix C applicable to all Mark III plants. Each applicant using the Mark III containment design, however, will be required to justify the use of the staff's acceptance criteria if deviations from the standard design exist. These loads definitions are to be applied in the response analyses of containment structures and components. These analyses need not be performed if it can be shown to the staff that a previously analyzed Mark III plant has sufficient similiarity in plant characteristics to make the analyses performed for that plant design applicable to the Mark III plant design under consideration.

The staff will review each applicant's use of the NRC acceptance criteria for applicability to their plant design. Mark III applicants for a construction permit need only furnish a commitment to use the staff's acceptance criteria in the design of their containment. Mark III applicants for an operating license will be required to show how the NRC acceptance criteria were applied and to justify any deviations taken. For both CP and OL applicants, the information required shall be submitted in a timely manner to allow for the evaluation to be included in the plant's Safety Evaluation Report, or supplements thereto.

The staff is reviewing, separately from the generic B-10 review, concerns raised by Mr. J. Humphrey regarding the Mark III containment design, which include concerns related to LOCA-related hydrodynamic loads. The staff does not anticipate that the ultimate resolution of the Humphrey concerns will require any modifications to the generic load definition contained herein. This review is being handled on a plant-unique basis and the final results will be plant unique only, not generic.

5. REFERENCES

1. General Electric Co. (GE), NEDM-10848, "Mark III Confirmatory Test Progress Report," April 1973.*

2. ---, NEDM-10976, "Mark III Analytical Investigation of Small-Scale Test Progress Report," August 1973.

3. ---, NEDO-11314-08, "Information Report for Mark III Dynamic Loading Conditions," July 1975.

4. ---, NEDE-21078-P, "Test Results Employed by General Electric for Boiling Water Reactor Containment and Vertical Vent Loads," October 1975.*

5. U.S. Nuclear Regulatory Commission, NUREG-75/110 "Safety Evaluation Report Related to the Preliminary Design of the GESSAR 238 Nuclear Island Standard Design," Section 6.2.1, December 1975.

6. ---, Supplement 1 of NUREG-75/110, "Safety Evaluation Report Related to the Preliminary Design of the GESSAR 238 Nuclear Island Standard Design," Section 6.2.1, September 1976.

7. ---, NUREG-0802, "Safety/Relief Valve Quencher Loads: Evaluation for BWR Mark II and III Containments," October 1982.

8. General Electric Co., Supplement 1 of NEDO-20550, "Fifth Quarterly Progress Report Mark III Confirmatory Test Program," July 1974.*

9. ---, NEDO-13407-P, "Mark III Confirmatory Test Program 1/3-Scale Three Vent Tests (Test Series 5801 through 5804)," May 1975.*

10. ---, NEDE-24648-P, "Mark III Confirmatory Test Program 1/9-Area Scale Multivent Pool Swell Tests - Test Series 6002," September 1979.*

11. G. Maise (Brookhaven National Laboratory), letter to R. L. Tedesco (NRC), containing a report prepared by P. W. Huber and A. A. Sonin entitled, "Review of General Electric's Data Base for Predicting Mark III Pool Swell," March 25, 1977.

12. A. A. Sonin (Massachusetts Institute of Technology (MIT)), Presentation contained in the minutes of the ACRS Fluid/Hydraulic Dynamic Effects Subcommitte meeting held on September 24, 1981.

13. A. A. Sonin (MIT), Presentation contained in the minutes of the ACRS Fluid/Hydraulic Dynamic Effects Subcommittee meeting held on January 22, 1982.

14. General Electric Co., NEDM-13377, "Mark III Confirmatory Test Program Phase 1 - Large-Scale Demonstration Tests - Test Series 5701 through 5703, October 1974.*

15. N. G. Ruggieri and A. A. Sonin (MIT), NUREG/CR-1444, "Investigation of Distorted-Geometry Simulation of Pool Dynamics in Horizontal Vent BWR Containments," April 1980.

16. U.S. Nuclear Regulatory Commission, NUREG-0661, "Safety Evaluation Report - Mark I Containment Long-Term Program," July 1980.

17. ---, NUREG-0487, "Mark II Containment Lead Plant Program Load Evaluation Report and Acceptance Criteria," November 1978.

18. F. J. Moody, "Scale Modeling Thermo-Hydraulic Phenomena in Nuclear Containments, "Proceedings of ANS/ASME/NRC International Topical Meeting on Nuclear Reactor Thermo-Hydraulics, NUREG/CP-0014, Vol. 1, October 5-8, 1980.

19. General Electric Co., 22A7007, "General Electric Standard Safety Analysis Report" (GESSAR-II), Attachment B of Section 3B0.3.2.32, February 25, 1982.

20. ---, NEDO-20533 and Supplement 1, "The General Electric Mark III Pressure Suppression Containment System Analytical Model," June 1974 and August 1975, respectively.

21. ---, NEDE-21471, "Analytical Model for Estimating Drag Forces on Rigid Submerged Structures caused by LOCA and Safety/Relief Valve Ramshead Air Discharges," September 1977.

22. U.S. Nuclear Regulatory Commission, Supplement 1 to NUREG-0487, "Mark II Containment Lead Plant Program Load Evaluation and Acceptance Criteria," September 1980.

23. General Electric Co., NEDE-13426-P, "Mark III Confirmatory Test Program 1/3-Scale Pool Swell Impact Tests - Test Series 5805, August 1975.*

24. ---, NEDE-13435-P, "Mark III Confirmatory Test Program 1/3-Scale Three Vent Air Test - Test Series 5806," October 1975.*

25. Bowden, D.T., et. al., "Engineering Summary of Airframe Icing Technical Data," Federal Aviation Agency, Technical Report FAA ADS-4, December 1963.

26. General Electric Co., NEDE-24720-P, "Mark III Confirmatory Test Program - 1/9 Area Scale Condensation and Stratification Phenomena - Test Series 6003," November 1979.*

27. ---, NEDE-21596-P, "Mark III Confirmatory Test Program 1/3-Scale Condensation and Stratification Phenomena - Test Series 5807, May 1977.*

28. ---, NEDE-21853-P, "Mark III Confirmatory Test Program Full Scale Condensation and Stratification Phenomena - Test Series 5707," August 1978.*

29. L. S. Rubenstein (NRC), letter to R. Buchholz (GE), "First Round of Questions on the Mark III LOCA-Related Pool Dynamic Load Criteria," November 19, 1980.

30. I.E. Idel'Chik, "Handbook of Hydraulic Resistance, Coefficients of Local Resistance and of Friction," 1960.

31. General Electric Co., NEDE-21606-P, "Mark III One-Third Area Scale Submerged Structure Tests," October 1977.*

32. F. J. Moody and W. C. Reynolds, "Liquid Surface Motion Induced by Acceleration and External Pressure," J. of Basis Engineering, Trans. ASME, September 1972.

33. General Electric Co., 22A7007, "General Electric Standard Safety Analysis Report" (GESSAR-II), Appendix 3B through Amendment 1, February 25, 1982.

34. H. Wagner, "Uber Stoss - und Gleitvorgage an der Oberflache von Flussigkeiten, "Zietschrift fur Angewandte Mathematik und Mechanik, Vol. 12, No. 4, August 1932.

35. H. C. Pfefferlen (GE), letter to Secretary of the Commission (NRC), "Input to Request for Public Comment on Draft NUREG-0978 - Technical Evaluation Report on Mark III LOCA-Related Hydrodynamic Load Definition," May 25, 1984.

*This document is not publicly available because it contains proprietary information.

Appendix A

Containment/Drywell Pressure Transient During a DBA

Appendix A

Containment/Drywell Pressure Transient During a DBA

1 DESCRIPTION OF DBA EVENT

For the standard BWR 6/Mark III containment design, the assumed sudden double-ended rupture of a main steam line between the reactor vessel and the flow limiter would result in the maximum flow rate of primary system fluid and energy to the drywell. This would, in turn, result in the maximum positive drywell differential pressure. The sequence of events immediately following the rupture of a main steam line between the reactor vessel and the flow limiter has been determined. The flow in both sides of the break will accelerate to the maximum allowed by the critical flow considerations. In the side adjacent to the reactor vessel, the flow will correspond to critical flow in the steam line break area. Blowdown through the other side of the break will occur because the steam lines are all interconnected at a point upstream of the turbine by the bypass header. This interconnection allows primary system fluid to flow from the three unbroken steam lines, through the header and back into the drywell via the broken line. Flow will be limited by critical flow in the steam line flow restrictor. The total effective flow area is given in Figure A-1.

The reactor blowdown rate is calculated using the following assumptions:

(a) The vessel depressurization flow rates are calculated using Moody's critical flow model.[A1] During the first second of blowdown, the flow consists of saturated steam. Immediately following the break, the total steam flow rate leaving the vessel would exceed the steam generation rate in the core, causing the initial depressurization of the reactor pressure vessel (RPV). Void formation in the reactor vessel water causes a rapid rise in the water level, and it is conservatively assumed that the water level reaches the vessel steam nozzles one second after the break occurs. The water level rise time of one second is the minimum that could occur under any reactor operating condition. From that time on, a two-phase mixture would be discharged from the break.

(b) The main steam isolation valves (MSIVs) are assumed to start closing at 0.5 second after the accident and be fully closed in the maximum time of five seconds following closure initiation. By assuming slow closure of these valves, a large effective break area is maintained for a longer period of time. The peak drywell pressure occurs before the reduction in effective break area and is, therefore, insensitive to any additional delay in closure of the isolation valves.

(c) The reactor is assumed to be at 102% of rated power.

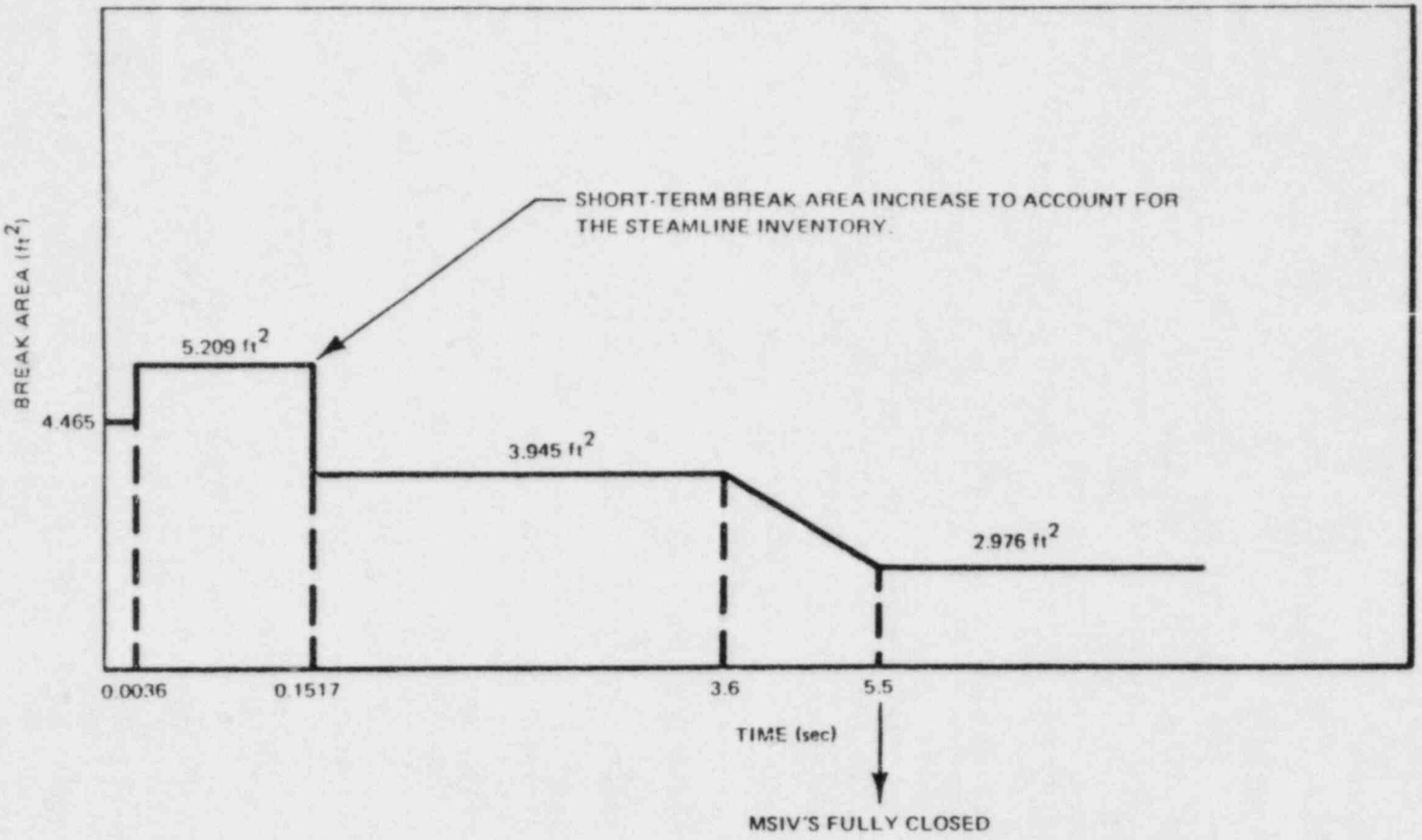

Figure A-1. Effective Blowdown Area for the Main Steamline Break

(d) Reactor power generation is assumed to cease at the time of accident initiation because of void formation in the core region. Scram also would occur in less than one second from receipt of the high drywell pressure signal. The difference between the shutdown times is negligible.

(e) A complete loss of offsite power is assumed to occur simultaneously with the pipe break. This condition results in the loss of power conversion system equipment and also requires that all vital systems for long-term cooling be supported by onsite power supplies.

(f) The core decay heat and the sensible heat released in cooling the fuel to initial average coolant temperature are included in the RPV depressurization calculation. The rate of energy release is calculated using a conservatively high heat transfer coefficient throughout the depressurization period. The resulting high energy release rate causes the RPV to maintain nearly rated pressure for approximately 20 seconds. The high RPV pressure increases the calculated blowdown flow rate, which is again conservative for analysis purposes. The sensible energy of the fuel stored at temperatures below the initial average coolant temperature is released to the vessel fluid along with the stored energy in the vessel and internals as vessel fluid temperatures decrease during the remainder of the transient calculation.

The pressure response of the containment during the blowdown period of the accident is analyzed using the following assumptions:

(a) Thermodynamic equilibrium exists in the drywell and containment. Since highly turbulent conditions are expected due to the blowdown flow, the analysis assumes complete mixing.

(b) The fluid flowing through the drywell-to-suppression pool vents is formed from a homogeneous mixture of the fluid in the drywell. The use of this assumption results in complete carryover of the drywell air and a high positive flow rate of liquid droplets, which conservatively maximizes vent pressure losses.

(c) The fluid flow in the drywell-to-suppression pool vents is assumed compressible except for the liquid phase.

(d) Heat sinks are neglected inside the containment. In reality, condensation of some steam on the drywell and containment surfaces would be expected to occur.

2 SHORT-TERM ACCIDENT RESPONSE

Figure A-2 shows the pressure responses of the drywell and suppression chamber during the primary system blowdown phase of the steam line break accident (LOCA) and Figure A-3 shows the drywell differential pressure response using the GE Pressure Suppression Containment System Analytical Model.[A2, A3]

The peak differential pressure occurs shortly after the vent-clearing transient. As the blowdown proceeds, the primary system pressure and fluid inventory will decrease, resulting in reduced break flow rates. As a consequence, the flow rate in the vent system and the differential pressure between the drywell and suppression chamber begin to decrease.

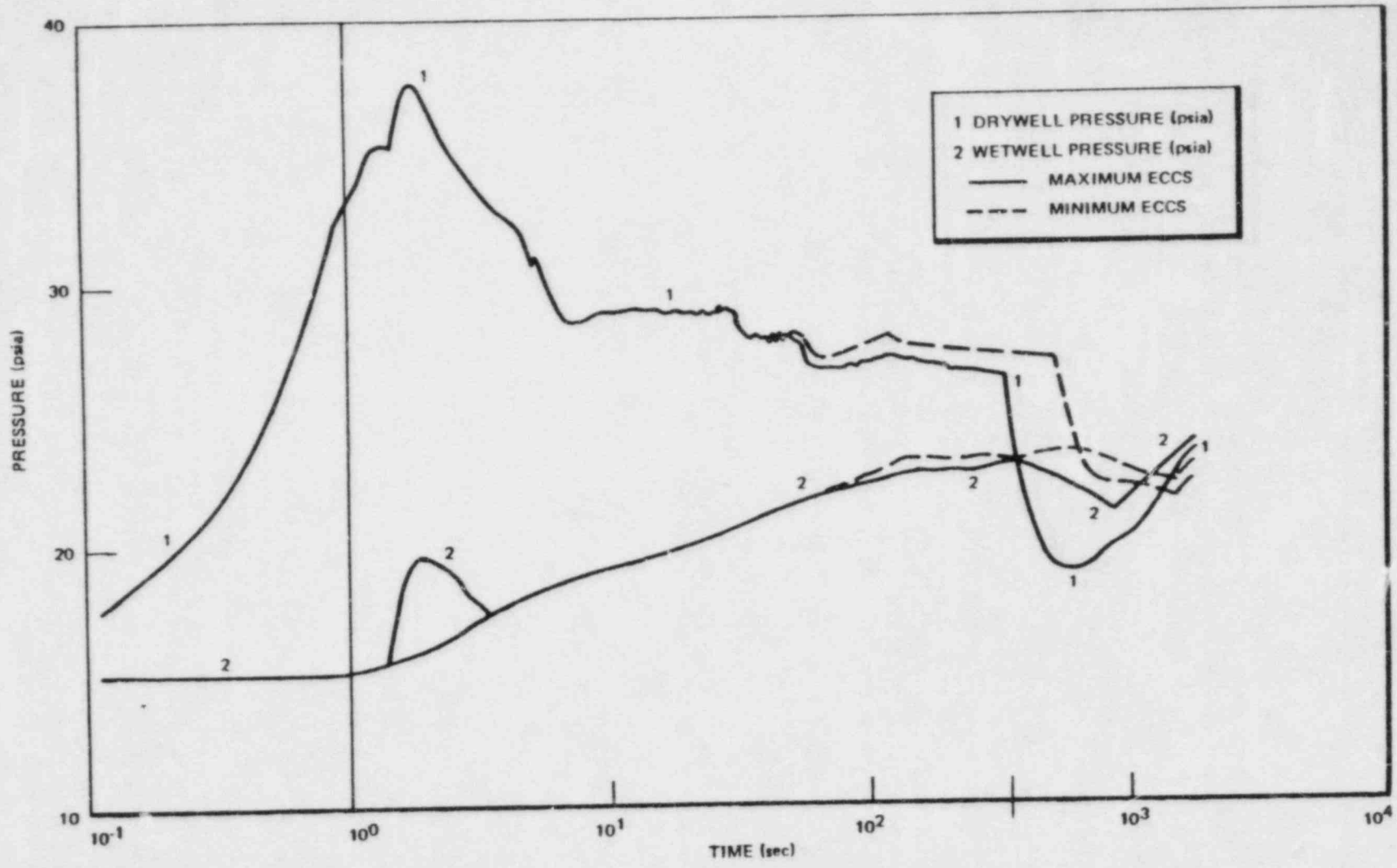

Figure A-2. Mk III Short-Term Pressure Following a Main Steamline Break

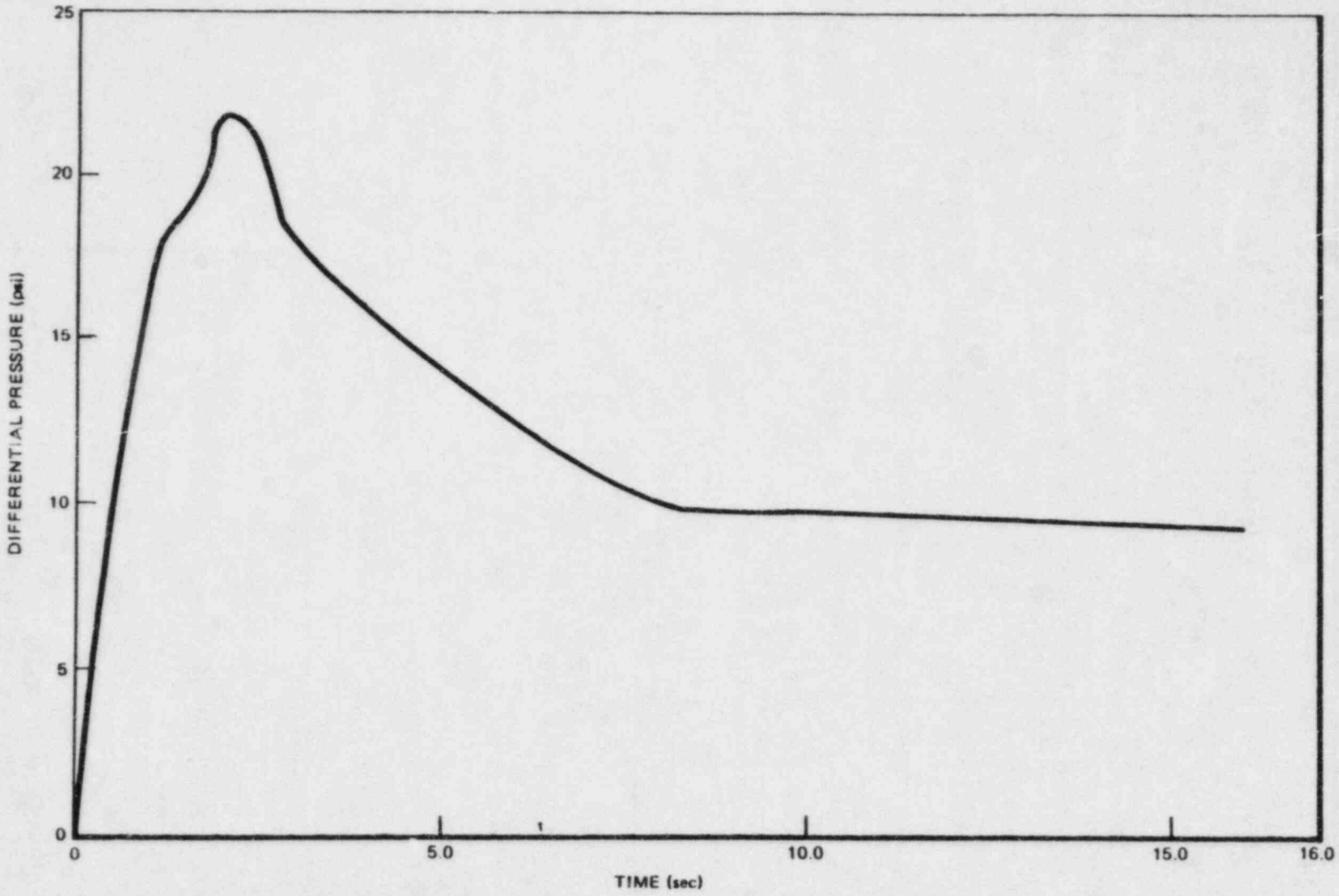

Figure A-3. Short-Term Drywell Differential Pressure Following a Main Steamline Break

After the primary system pressure has dropped to the drywell pressure, the blowdown will be over. At this time, the drywell will contain saturated steam, and the drywell and containment pressures will stabilize. The pressure difference corresponds to the hydrostatic pressure of vent submergence.

The drywell and suppression pool will remain in this equilibrium condition until the reactor vessel refloods. During this period, the emergency core cooling pumps will be injecting cooling water from the suppression pool into the reactor. This injection of water will eventually flood the reactor vessel to the level of the steamline nozzles and the ECCS flow will spill into the drywell. The water spillage will condense the steam in the drywell and thus reduce the drywell pressure. As soon as the drywell pressure drops below the containment pressure, the drywell vacuum breakers will open, and noncondensible gases from the containment will flow back into the drywell until the pressures in the two regions equalize.

3 DESCRIPTION OF DRYWELL PRESSURE TRANSIENT ANALYTICAL MODELS

The pressure reponse of the standard Mark III containment drywell and containment is calculated by General Electric (GE) using the GE Pressure Suppression Containment System Analytical Model[A2, A3] and the results are confirmed by the NRC staff using the CONTEMPT-LT/028A[A4] computer code. Both models use similar assumptions in calculating the pressure of the drywell atmosphere and the flow of water/air/steam through the horizontal vents and a general description of the assumptions used, which apply to both models, is contained below.

The overall approach to the simulation of the Mark III drywell transient is to assume the drywell to be a single-pressure system whose total energy and mass of air, vapor, and water are known at all times from an integration of the various flows across the system boundary. Equations giving the rate of change of total drywell energy, water inventory, and air inventory are solved with finite time step techniques. Once the thermodynamic condition of the drywell constituents is known (i.e., whether the water phase is saturated or superheated) the drywell temperature and pressure may be calculated. Although the vent clearing transient is a three-dimensional event, the analytical models assume one-dimensional flow. Multidimensional vent effects are approximated, however. The major assumptions used to develop the multinode modeling of the horizontal vent clearing transient are:

(a) Incompressible transient flow of a pure liquid

(b) Adiabatic conditions

(c) One-dimensional conservation equations for each node

(d) Vents clear as plugs

(e) Multidimensional vent effects are represented by irreversible loss terms.

The final vent clearing equations solved are dependent on the wetwell and drywell vapor region pressures.

Once the increasing drywell pressure has accelerated enough water from the vent system to clear the first row of vents, the process of air/steam flow through the vents will begin. Similarly as the second and third vents are cleared of water, flow of drywell atmosphere will flow through these vents.

The overall approach to the analytical simulation of the containment response is to continuously integrate the air, water vapor, and liquid in both the drywell and containment. Thus, at any time during the transient, the pressure at both ends of the vent system are known and the vent flow that will occur as a result of this pressure difference can be calculated. This flow rate is then used to advance (over a very small time step) the integration of drywell and containment inventories. The containment airspace is divided by the HCU floor into two modes with a simulated flow restriction in the GE analytical model, whereas the CONTEMPT-LT/28 code models this airspace as one node. The GE approach is more realistic, and conservative, since the short-term pressure differential in the containment (Fig. A-2) due to the HCU floor flow restriction leads to higher peak drywell pressures by delaying the vent clearing process.

A comparison of the results between GE's analytical model and CONTEMPT-LT/28[A4] for the short-term pressure transient for a typical Mark III plant (Grand Gulf 1&2) design is provided in Figure A-4. Table A-1 contains a comparison of the vent clearing times using the two models. As can be seen from Figure A-4, the GE analytical model predicts a peak drywell pressure of 22 psig for Grand Gulf while a CONTEMPT-LT/28 run, using the same mass and energy release rates from the reactor vessel, predicts a peak pressure of 18.5 psig inside the drywell. The higher pressure prediction of the GE model is in large part due to the slower vent clearing times calculated by their vent clearing model (approximately 0.1 seconds slower than the CONTEMPT-28 calculation -see Table A-1), which is mainly a result of the two node modeling of the containment in the GE approach, as discussed earlier.

Another conservatism in the GE model has to do with the change in the state of the break effluent which is described below.

Immediately following a steam line break, the blowdown flow will be saturated reactor steam. The rapid reactor vessel depressurization associated with steam blowdown will cause the reactor water level to rise and the level is conservatively assumed to reach the elevation of the main steam line nozzles one second after the break. This will result in the blowdown flow changing from steam to a two-phase mixture of steam and water. Prior to the two-phase flow at one second, the reactor steam creates a superheated condition in the drywell atmosphere. Immediately following the two-phase flow, the decompressing reactor steam and liquid will remain in the saturated state and at typical drywell pressures the liquid will decompress to approximately 40% steam by weight. At the time this two-phase blowdown starts, the drywell is full of superheated steam and noncondensible gases at calculated tempertures approaching 330°F. If instantaneous and complete mixing between these gases and the two-phase blowdown is assumed, as the CONTEMPT-28 code does, then there will be a drywell pressure decrease of up to 2 psig when two-phase flow begins. The GE model conservatively modifies this phenomenon by assuming that the decompressed reactor liquid does not contribute to the drywell thermodynamic transient when calculating the drywell pressure. However, in order to maintain conservation of mass and energy, the blowdown liquid is continuously monitored

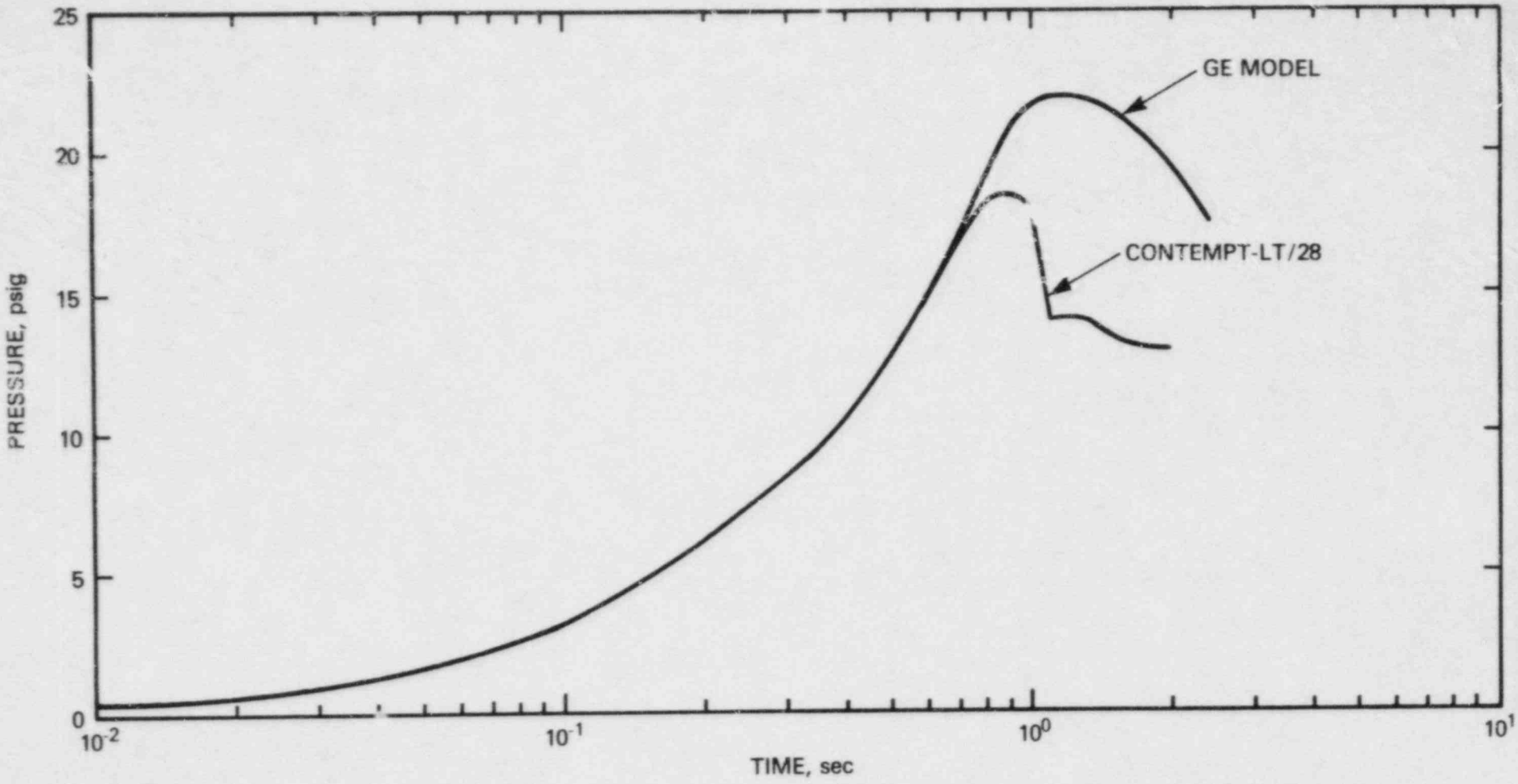

Figure A-4. Mark III Drywell Pressure Transient Comparison between GE and NRC Models

Table A-1 Typical Mark III vent clearing times

Model	Time of full vent clearing		
	Top Vent	Middle Vent	Bottom Vent
GE Model	0.86 seconds	1.08 seconds	1.44 seconds
CONTEMPT-28	0.77 seconds	0.96 seconds	1.27 seconds

and is used when calculating the drywell density for the vent flow model. This monitored mass also allows for a subsequent return to the assumption of homogenous mixing in the drywell following the peak calculated drywell pressure.

Based on the drywell pressure transient comparison between the GE analytical model and the CONTEMPT-LT/28 code, the staff concludes that the design drywell/containment pressure transient used in the formulation of the hydrodynamic load definitions is acceptable.

REFERENCES FOR APPENDIX A

A1. General Electric Co., Topical Report APED-4827, "Maximum Two-Phase Vessel Blowdown from Pipes," 1965.

A2. ---, NEDO-20533, "The General Electric Mark III Pressure Suppression Containment Analytical Model," June 1974.

A3. ---, NEDO-20533-1, "The General Electric Mark III Pressure Suppression Containment Analytical Model," Supplement 1, September 1975.

A4. EG&G Idaho, Inc., NUREG/CR-0255, "CONTEMPT-LT-028, A Computer Program for Predicting Containment Pressure-Temperature Response to a Loss-of-Coolant Accident," April 1979.

Appendix B

Description of Test Program

Appendix B

Description of Test Program

1 INTRODUCTION

The data base for Mark III containment LOCA-related hydrodynamic loads was obtained at the Pressure Suppression Test Facility (PSTF) constructed by General Electric (GE) in San Jose, California. The objective of the test program conducted at the PSTF was to evaluate pool dynamic effects on the Mark III containment geometry due to a LOCA.

2 TEST FACILITY DESCRIPTION

Figure B-1 is a schematic view of the PSTF. The nominal volumetric scale factor for the facility is 1:130. In brief, the PSTF consists of a 160 ft^3 electrically heated steam generator or pressurizer vessel connected to a 2365 ft^3 drywell by an 8-in. blowdown ine, which includes a critical flow venturi, rupture disc assembly, and 8-in. gate valve. The blowdown line is connected to a 10.357-in. riser inside the pressurizer, which allows blowdowns from the top of the vessel (the riser tube is removed when liquid blowdowns are desired) and to a 10-in. riser inside the drywell, which allows blowdown flow to be injected at the top of the drywell. The pressurizer can be charged with air or saturated water. The drywell is a cylindrical vessel having a 10-ft diameter and a 26-ft height, with a 6-ft diameter vent duct, which enters the suppression pool building and is connected to the vent test section. In the full-scale chugging tests (Test Series 5707), B1, B2, B3 the drywell was augmented with the 2000 ft^3 Temporary Tall Test Tank used in Mark II experiments. The suppression pool building simulates both the pool and wetwell air space. The 213 blowdowns completed in the PSTF between 1973 and 1980 were done in three differently sized suppression pool segments, a full-scale model (Fig. B-1), a one-third area scale model, and a one-ninth area scale model. The three different configurations are shown in Figure B-2.

The full-scale model vent systems simulated the weir annulus and a single column of horizontal vents of the Mark III containment. Three full-scale 27.5 in. i.d. horizontal vents with 4.5 ft spacing between the vent centerlines were used. The vents had full-scale lengths of 5 ft. The pool in the full-scale model represented an 8 degree sector of the Mark III suppression pool with full-scale depth and surface area. The baffles that formed the sides of the 8 degree pool sector extended only a few feet beyond the normal water level.

The one-third area scale pool segment used full-scale submergence and vent lengths with the annulus area, vent area, and pool surface area scaled by one-third. As in the full-scale model, the one-third area scale pool segment model contained a single column of horizontal vents and represented an 8 degree

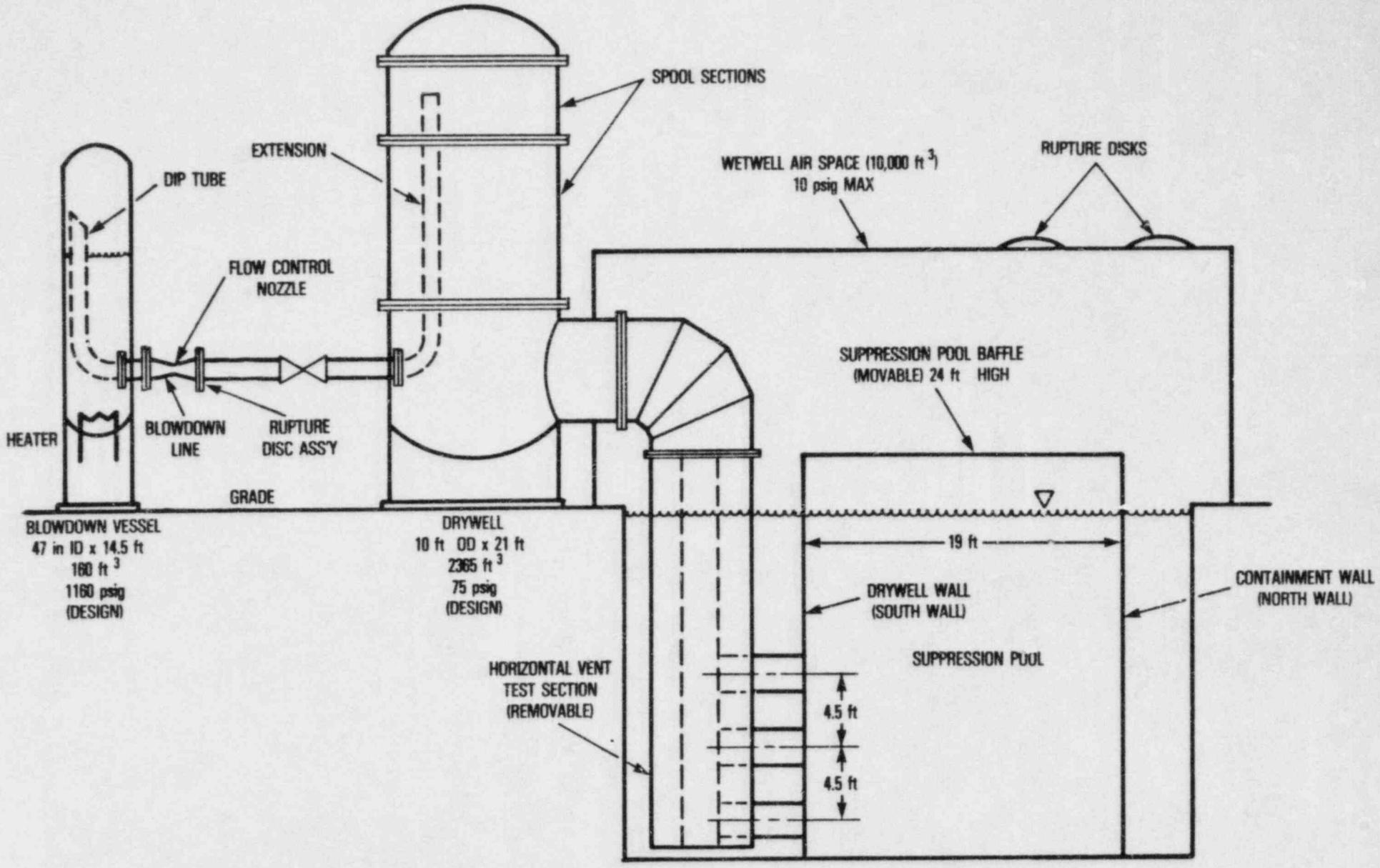

Figure B-1. Pressure Suppression Test Facility Schematic (Full Scale)

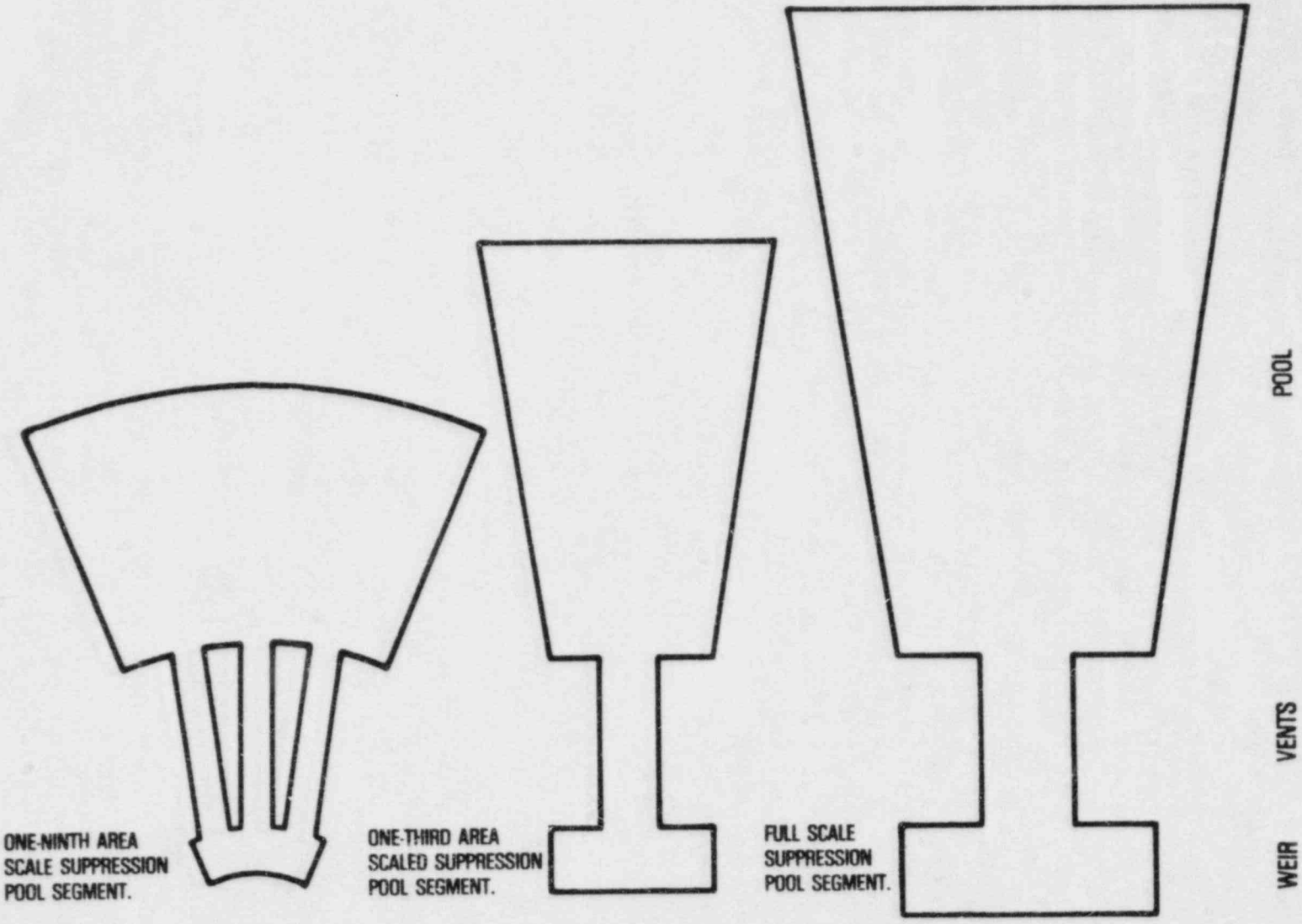

Figure B-2. PSTF Suppression Pool Segments

sector of the Mark III suppression pool. Unlike the full-scale model, the baffles that formed the sides of the 8 degree sector in the one-third area scaled segment extended all the way up to the PSTF roof to allow evaluation of pool swell phenomena.

The one-ninth area scale pool segment model consisted of a 24 degree segment of the prototype weir annulus and suppression pool with the annulus, vent and pool surface areas reduced by a factor of one-ninth from the full-scale model. The one-ninth scale model contained three columns of horizontal vents with full-scale vertical spacing between the vents and full-scale vent lengths. The radial spacing of the vents within the suppression pool is proportional to scale. Due to the non-geometric scaling of the vent length, the radial vent spacing within the weir annulus is less than that which is proportional to scale.

More detailed information on the PSTF test facility including test procedures and instrumentation arrangements can be found in References B3 (for the full-scale model), B4 (for the one-third scale model), and B8 (for the one-ninth scale model).

3 PSTF TEST RESULTS

The PSTF was used to gather data on a spectrum of hydrodynamic phenomena for load definition purposes. Test Series 5701-5703,[B1] 5705-5706[B2] and 5707[B3] were performed with the full-scale PSTF arrangement. Test Series 5801-5804,[B4] 5805,[B5] 5806[B6] and 5807[B7] were performed with the one-third area scale PSTF arrangment; and Test Series 6002[B8] and 6003[B9] were performed with the one-ninth area scale PSTF arrangement. The principal variables for these runs were pressure vessel blowdown rate (achieved by varying blowdown line flow restrictor diameter) and horizontal vent initial submergence.

Test Series 5701-5703 were begun in November 1973 and were the first tests run at the PSTF. Test Series 5701 consisted of 21 steam blowdown runs with the top two of the three horizontal vents in the full-scale test section plugged. With this configuration, the vent area open to flow represented the scaled area of the Mark III design with the nominal scale factor of 1:130. Test Series 5702 consisted of 17 steam blowdown runs with the top vent plugged. Test Series 5703 included three steam blowdown runs with all three full-size vents open to flow. The results of these tests were used to obtain vent clearing and condensation effectiveness data.

Test Series 5705-6, performed in 1974, consisted of four and seven air blowdown runs, respectively, with the top vent plugged. The primary objective of 5705 was scoping the pool swell effects and was used by GE to derive their design pool swell velocity of 40 ft/sec. Test Series 5706 also provided data on pool swell and was used by GE to develop the pool swell solid water impact and froth impact specifications for structures over the pool.

Performed in 1977, Test Series 5707 consisted of 22 steam blowdowns with all three full-size vents open. Chugging phenomena, pool swell and thermal stratification were investigated and the parametric effects were evaluated during this test series. The primary emphasis was placed on chugging phenomena, and the resulting vent system, pool boundary, and submerged structure loads. The

principal variable was initial pool temperature. The Mark III chugging load definition is based on the results of Test Series 5707.

The first series of tests using the one-third area scaled version of the PSTF (Test Series 5801-5804) was performed in 1974. Primary emphasis during this phase was on the interaction of pool swell with flow restrictions above the suppression pool surface. Other areas of interest were vent clearing, drywell pressurization and jet forces on pool walls. Data from these experiments were also used by GE to justify the froth impact load definition. The principal variables for these tests were steam generator blowdown rate (varied by changing blowdown line restrictor diameter), horizontal vent initial submergence and pool roof opening ratio.

Test Series 5801 consisted of 19 steam blowdown runs with a matrix of test conditions intended to provide data to evaluate the pressure drop due to the flow of two-phase air/water mixture through a restriction above the suppression pool. Since it was expected that the pressure drop would be a strong function of mixture density, efforts were made to measure the void fraction of the flow as it passed through the restriction.

Test Series 5802 consisted of three steam blowdown runs intended to generate pool swell maps and provide two-phase flow through the roof to supplement the matrix of Test Series 5801. Test Series 5803 consisted of two liquid blowdown runs to gather preliminary saturated liquid critical flow data and to compare the transient response of simulated recirculation line breaks with steam line breaks. Test Series 5804 consisted of five steam blowdown runs to fill out the 5801 test matrix and to provide test repeatability data.

Test Series 5805 was conducted in 1975 and consisted of 51 steam blowdowns with the intention of providing additional data on impact loads on structures above the initial pool surface. Conducted in the same year, Test Series 5806 consisted of 12 air blowdowns. Primary emphasis during Test Series 5806 was to obtain pool velocity and slug thickness values to use with the one-third area scale steam test values from Test Series 5805. This information was used to investigate the influence of vent flow composition on the effects associated with the pool swell phenomenon.

Test Series 5807 was performed in late 1976 and consisted of 20 steam and liquid blowdowns. Test objectives were to: (1) examine the effects of initial suppression pool temperature, blowdown flow rate, and blowdown type (saturated liquid vs. saturated vapor) on suppression pool thermal stratification; and (2) investigate condensation phenomena and associated loads. This test series is the basis for GE's condensation oscillation load definition.

The one-ninth area scale tests, Test Series 6002 and 6003; were conducted in 1978 and 1979 to investigate the multicell effects on hydrodynamic phenomena.

Test Series 6002 consisted of 14 steam blowdowns and was separated into two phases. For Phase 1, the suppression pool and weir annulus were divided by partitions to provide separate one- and two-cell sections. Both sections were supplied steam simultaneously from the drywell during a blowdown transient. Break size and vent submergence were varied during this phase to study the

influence of these factors on hydrodynamic phenomena. For Phase 2, the partitions were removed to provide a three-cell configuration, and a test program comparable to Phase 1 was carried out. The objective of Test Series 6002 was to demonstrate that single-cell pool swell results are conservative relative to multicell results and to evaluate the effects of cell interaction on pool surface shape, pool surface displacement, water slug thickness, velocity and wall loads.

Test Series 6003 was divided into two phases similar to 6002 and 12 steam blowdown runs were performed. The primary objectives of Test Series 6003 were to: (1) confirm that single-cell loads due to condensation are conservative when compared to multicell test data; (2) study vent interaction and its effects during the condensation phases of the LOCA transient; and (3) evaluate the multicell effects on pool thermal stratification.

REFERENCES FOR APPENDIX B

B1. General Electric Co., NEDO-13377, "Mark III Confirmatory Test Program Phase 1 - Large-Scale Demonstration Tests," October 1974. (Proprietary Report).

B2. ---, NEDO-20550, "Fifth Quarterly Progress Report: Mark III Confirmatory Test Program," July 1974.

B3. ---, NEDO-21853, "Mark III Confirmatory Test Program - Full Scale Condensation and Stratification Phenomena - Test Series 5707," August 1978.

B4. ---, NEDO-13407, "Mark III Confirmatory Test Program 1/3-Scale Three Vent Tests (Test Series 5801 through 5804)," June 1975.

B5. ---, NEDO-13426, "Mark III Confirmatory Test Program 1/3-Scale Pool Swell Impact Tests - Test Series 5805," August 1975.

B6. ---, NEDO-13435, "Mark III Confirmatory Test Program 1/3-Scale Three Vent Air Tests - Test Series 5806," October 1975.

B7. ---, NEDE-21596, "Mark III Confirmatory Test Program 1/3-Scale Condensation and Stratification Phenomena - Test Series 5807," March 1977.

B8. ---, NEDO-24648, "Mark III Confirmatory Test Program 1/9-Area Scale Multivent Pool Swell Tests - Test Series 6002," May 1979.

B9. ---, NEDO-24720, "Mark III Confirmatory Test Program 1/9-Area Scale Condensation and Stratification Phenomena - Test Series 6003," November 1979.

Appendix C

NRC Acceptance Criteria for LOCA-Related Mark III Containment Pool Dynamic Loads

Appendix C

NRC Acceptance Criteria for LOCA-Related
Mark III Containment Pool Dynamic Loads

The following acceptance criteria were developed from the staff's review of Appendix 3B of GESSAR-II 238 Nuclear Island (GESSAR) and the supporting analytical and experimental programs as referenced therein. The staff has determined that the procedures described in the GESSAR document are acceptable for evaluation of the Mark III containment response to LOCA-related pool dynamic loads with the following exceptions, modifications, qualifications and/or clarifications:

1 POOL SWELL LOADS

1.1 Pool Swell Velocity

The water slug velocity V to be used for the determination of slug drag loads, as well as slug impact loads as prescribed in 1.2, 1.3 and 1.5 below, shall be determined from the relation:

$$V = 5\,H\,(2.6 - 0.506\,\sqrt{H}); \qquad H < 10 \text{ ft, and} \qquad \text{(C-1)}$$

$$V = 50 \text{ ft/sec} \qquad H \geq 10 \text{ ft}$$

In these relations, V is the slug velocity in feet per second (fps), H denotes the height (in feet) above the initial pool surface.

1.2 Pool Swell Loads on Structures Attached to the Containment Walls

The GESSAR-II specification for these loads is given in Section 3B.6.1.5. It is based on steady drag at a flow velocity of 40 ft/sec. This specification should be modified as described below;

(1) If the local pool swell velocity, as specified in Section 1.1 above, is greater than 40 ft/sec, the drag pressures obtained by the GESSAR specification shall be multiplied $(V/40)^2$, where V is the local pool velocity in ft/sec.

(2) If the frontal area of the structure is not immersed prior to pool swell, it will experience an impact force. This must be included in the specification.

For half-wedge protrusions the force history during impact shall be determined from Figure C-1. The local velocity of impact (needed in Figure C-1) shall be taken from the specification in Section 1.1, corresponding to the height where the wedge is first fully submerged. If the lower portion of the wedge is initially submerged, the same impact history

is applied except the abscissa is replaced by Vt/h, where h is the "unsubmerged height" of the wedge.

If the wedge angle is other than 45°, the following ratios can be used after obtaining the force history for a 45° wedge from Figure C-1.

$$\frac{F_\beta}{F_{45}} = \left(\frac{\beta}{90-\beta}\right)^2 \cot \beta \qquad \text{(C-2)}$$

$$\frac{t_\beta}{t_{45}} = \cot \beta \qquad \text{(C-3)}$$

Where β is the wedge angle.

For horizontal ledges the impact force shall be determined in the following manner:

(a) The force history will have a triangular shape as shown in Figure C-2.

(b) Determine the hydrodynamic mass of impact (per unit area) for flat targets from Figure 6-8 of NEDE-13426. Use b (and not b/2) for target width.

(c) Calculate the impulse using the equation

$$I_p = \frac{M_H}{A} V * \frac{1}{(32.2)(144)} \qquad \text{(C-4)}$$

where:

I_p = impulse per unit area, psi-sec

$\frac{M_H}{A}$ = hydrodynamic mass per unit area, lbm/ft^2, from (b) above.

V = impact velocity, ft/sec, determined according to Section 1.1.

(d) Calculate the pulse duration from the equation

$$\tau = 0.02 \frac{H}{V} \left(\frac{b}{2}\right) \qquad \text{(C-5)}$$

where:

τ = pulse duration, sec
H = height above the pool, feet
b/2 = width of the ledge, feet
V = impact velocity, ft/sec, determined according to Section 1.1

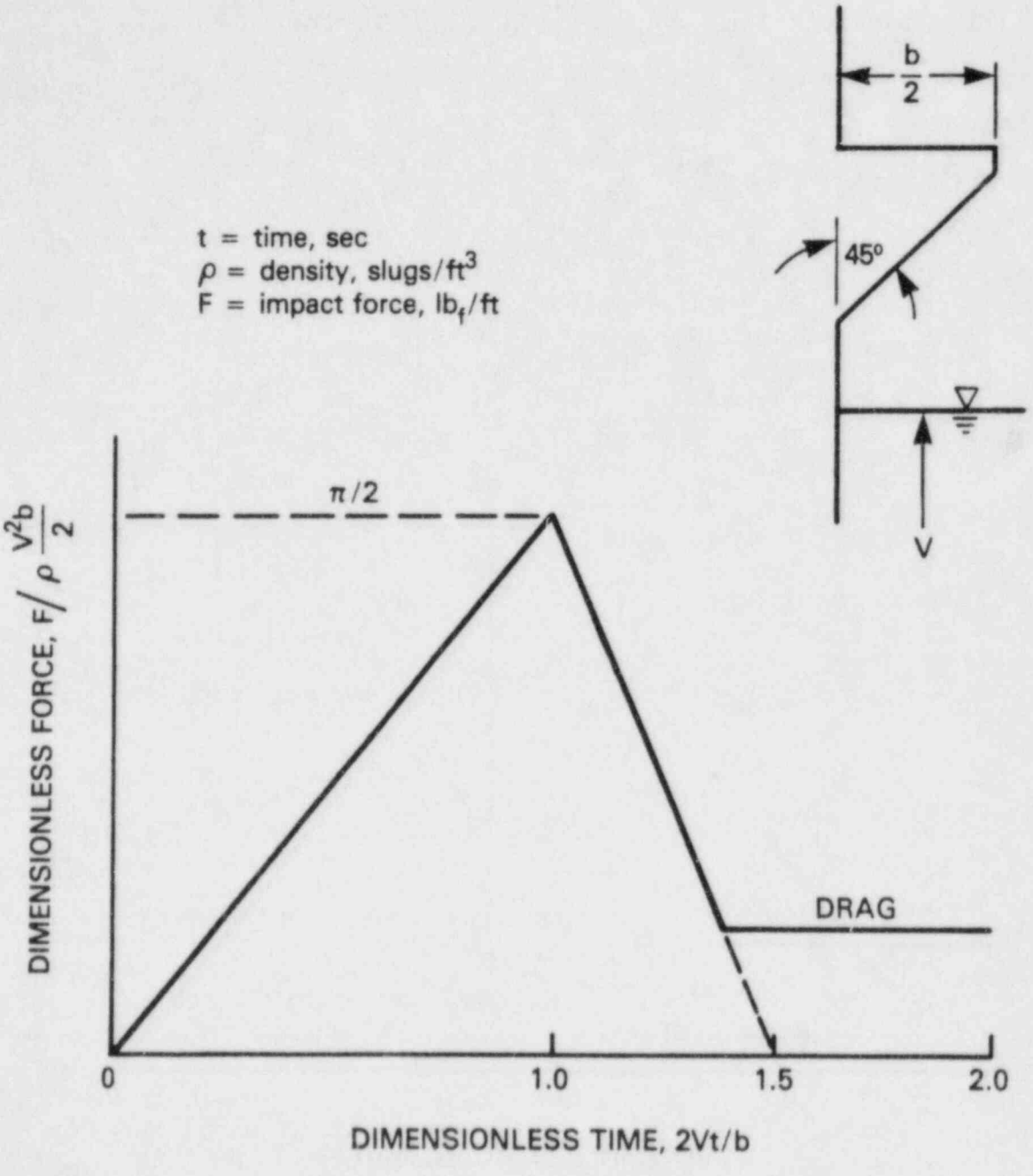

Figure C-1 Impact force (per unit length) on Wedge-Shaped Protrusions from the Containment Wall

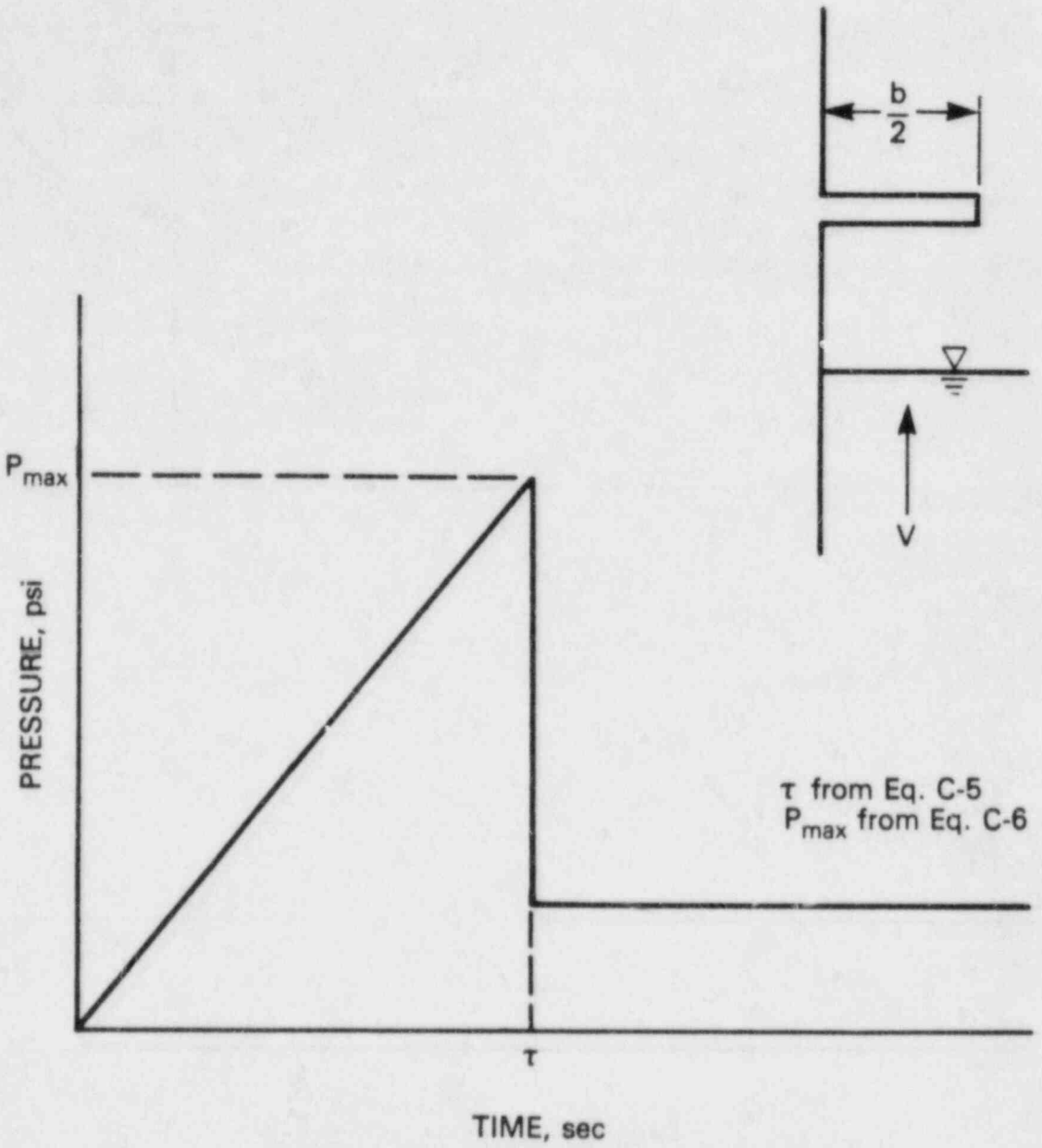

Figure C-2 Impact Pressure on Horizontal Ledges Attached to Containment Wall

(e) The value of P_{max} will be obtained using the following equation:

$$P_{max} = 2\ I_p/\tau \qquad \text{(C-6)}$$

where:

P_{max} = the peak pressure amplitude, psi.

1.3 Bulk Impact Loads on Small Structures

"Small structures," in the present context, are defined as beams and pipes with lateral dimensions no larger than 20 inches. For these structures the bulk impact specification, as described in Section 3B.10.11 of GESSAR-II, is acceptable with the specific limitations discussed in Section 3B0.3.2.33 of Attachment 0 (Question/Response 3B.33).

These limitations are:

(1) Targets must have combinations of widths and natural frequencies such that Figures 3B.33-1, 2, 3 and 4 indicate them to be in the "GESSAR conservative" region with respect to the V = 50 ft/sec pool velocity curve.

(2) There are no structures smaller than 4 feet long.

(3) There are no structures closer than 6 feet above the pool.

All structures above the containment pool in GESSAR-II standard plant design satisfy limitations (1) through (3). In plant designs where some specific structures may not meet limitations (2) and/or (3), the pulse duration must be shortened with an appropriate adjustment to the pressure amplitude. The load specifications for these structures will be reviewed by the staff on a plant unique basis.

For structures less than 10 feet above the pool, the peak pressure amplitude may be reduced by

$$\frac{P}{P_{max}} = \frac{V^2}{V^2_{max}} = \frac{H^2}{100}\left(2.6 - 1.6\sqrt{\frac{H}{10}}\right)^2 \qquad \text{(C-7)}$$

where P is the pressure amplitude at a structure H feet above the pool surface and P_{max} is the GE-specified pressure amplitude for bulk impact on small structures above the pool.

1.4 Froth Impact Loads

The froth impact specification is applicable between an elevation of 19 feet above the pool and the HCU floor. Over open or grated areas of the HCU floor this specification extends to an elevation of 26 feet for flat structures and 28.5 feet for pipes. Between these elevations and 30 feet the froth drag specification in GESSAR-II, Section 3B.12 is applicable.

The forcing function for froth impact shall be an isosceles triangle with a maximum pressure amplitude given in Figure C-3. The pulse duration shall be chosen such as to give a maximum DLF with a triangular pulse. For elongated structures that span the annulus of the wetwell, pulse durations shorter than 50 msec need not be considered.

For structures above grated areas at the HCU floor the pressures from Figure C-3 may be multiplied by the ratio of grating open area to grating total area.

1.5 Drag Loads

The GESSAR-II specification for drag loads on small structures, as described in Section 3B.10.2, is acceptable with the following limitation. If the local pool velocity, as specified in Section 1.1 above is greater than 40 ft/sec, the drag forces obtained by the GESSAR-II specification shall be multiplied by $(V/40)^2$, where V is the local velocity in ft/sec.

If Figure 3B-75 in GESSAR-II is used for drag loads on plates and if the shorter side (b) is attached to a wall, the abscissa of the graph becomes 2a/b instead of a/b.

2.0 LOADS ON SUBMERGED STRUCTURES

The procedures for the computation of loads on submerged structures as described in Sections 3.B.8 to 3.B.8.1.7 and Attachment L of GESSAR are acceptable subject to the limitations and/or modifications of Section 3.B.0.3.2.31 of Attachment 0. In particular, the computation of acceleration loads on non-cylindrical structures and the evaluation of standard drag for CO loads must be based on the Mark I Acceptance Criteria (NUREG-0661) as described in the responses to questions 3.B.31(b.ii), (c.ii) and (c.iii) in Attachment 0.

3.0 IMPACT LOADS ON STRUCTURES ABOVE THE WEIR ANNULUS

The staff finds acceptable the GESSAR-II impact specification on structures above the weir wall, with the exception of radial structures within one foot of the top of weir wall. The stresses in these structures must be increased by a multiplier. This multiplier is 1.0 when the natural frequency of the structure is less than 200 Hz, 1.8 when the natural frequency is greater than 500 Hz with a linear ramp between these values.

For structures located between zero and 0.25 feet above the weir wall, flat pool impact should be considered (e.g., the acceptance criteria in Section 2.7 of Appendix A, NUREG-0661 is appropriate for flat pool impact). The velocity at impact for these structures shall be taken at 4 ft/sec.

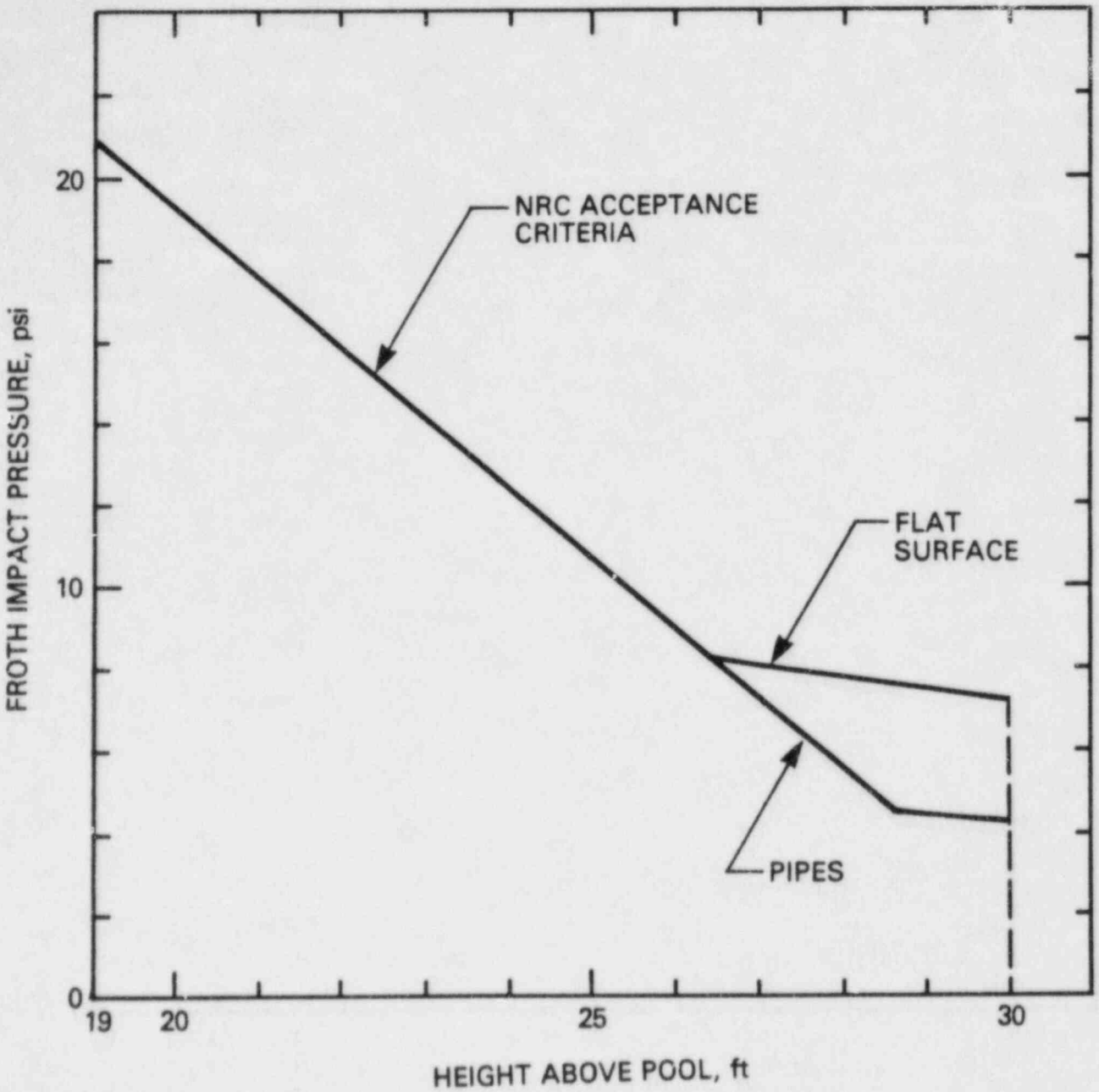

Figure C-3 NRC Acceptance Criteria for Froth Impact: Peak Amplitude of Pressure Pulse

NRC FORM 335 (2.84) NRCM 1102, 3201, 3202

U.S. NUCLEAR REGULATORY COMMISSION

BIBLIOGRAPHIC DATA SHEET

SEE INSTRUCTIONS ON THE REVERSE

1. REPORT NUMBER (Assigned by TIDC, add Vol. No., if any)

NUREG-0978

2. TITLE AND SUBTITLE

Mark III LOCA-Related Hydrodynamic Load Definition
Generic Technical Activity B-10 - Final Report

3. LEAVE BLANK

4. DATE REPORT COMPLETED

MONTH	YEAR
August	1984

5. AUTHOR(S)

M.B. Fields, J.A. Kudrick

6. DATE REPORT ISSUED

MONTH	YEAR
August	1984

7. PERFORMING ORGANIZATION NAME AND MAILING ADDRESS (Include Zip Code)

Division of Systems Integration
Office of Nuclear Reactor Regulation
U.S. Nuclear Regulatory Commission
Washington, D.C. 20555

8. PROJECT/TASK/WORK UNIT NUMBER

9. FIN OR GRANT NUMBER

10. SPONSORING ORGANIZATION NAME AND MAILING ADDRESS (Include Zip Code)

Same as 7. above.

11a. TYPE OF REPORT

Technical

b. PERIOD COVERED (Inclusive dates)

12. SUPPLEMENTARY NOTES

13. ABSTRACT (200 words or less)

This report, prepared by the staff of the Office of Nuclear Reactor Regulation and its consultants at the Brookhaven National Laboratory, provides a discussion of LOCA-related suppression pool hydrodynamic loads in boiling water reactor (BWR) facilities with the Mark III pressure-suppression containment design. Its issuance completes NRC Generic Technical Activity B-10, "Behavior of BWR Mark III Containment."

On the basis of certain large-scale tests conducted between 1973 and 1979, the General Electric Company developed LOCA-related hydrodynamic load definitions for use in the design of the standard Mark III containment. The staff and its consultants have reviewed these load definitions and their bases and conclude that, with a few specified changes, the proposed load definitions provide conservative loading conditions.

The staff approved acceptance criteria for LOCA-related hydrodynamic loads are provided in Appendix C of this report.

14. DOCUMENT ANALYSIS - a. KEYWORDS/DESCRIPTORS

Mark III containment
LOCA-related hydrodynamic loads
Task Action Plan B-10

b. IDENTIFIERS/OPEN-ENDED TERMS

15. AVAILABILITY STATEMENT

Unlimited

16. SECURITY CLASSIFICATION

(This page)
Unclassified
(This report)
Unclassified

17. NUMBER OF PAGES

18. PRICE